

**Mechanistic insight into PIN1 regulation on
MYC: A new interaction pattern &
the association with the nuclear pore**

By Yulong Su

A DISSERTATION

Presented to the Department of Molecular and Medical Genetics

and the Oregon Health and Sciences University

School of Medicine

in partial fulfillment of the requirement for the degree of

Doctor of Philosophy

Approved by the Oral Examination Committee

July 2017

Table of Contents

Table of Contents	ii
List of Figures and Tables	iv
List of Abbreviations	v
Acknowledgements.....	1
Chapter One : Introduction	1
Preface.....	2
The potent transcription factor MYC	3
The molecular timer PIN1	21
Many facets of transcription at the nuclear periphery	38
Chapter Two : Pre-Anchoring of PIN1 to Unphosphorylated MYC in a Fuzzy Complex Regulates MYC Activity	50
Abstract:	52
Introduction:.....	53
Results:.....	58
Discussion:	82
Chapter Three : PIN1 regulates the spatial distribution of transcriptionally active MYC at the nuclear pore	88
Abstract:	89
Introduction:.....	90
Results:.....	93
Discussion:	121

Table of Contents

Supplemental Figures.....	126
Acknowledgements.....	133
Chapter Four : Summary and Discussion.....	134
A novel motif of MYC that primes PIN1 binding.....	135
PIN1 regulates the subnuclear localization of MYC.....	138
Chapter Five : Materials and Methods.....	148
Plasmids and siRNA.....	149
Cell-lines and Transfection.....	150
Antibodies.....	151
Western Blotting.....	152
RT-PCR analysis.....	152
qRT-PCR analysis.....	153
Cyclohexamide half-life.....	153
Coimmunoprecipitation.....	154
Colony Formation Assay.....	154
FISH Assay.....	155
Luciferase Assay.....	155
ChIP-seq analysis.....	156
Proximity Ligation Assay and Immunofluorescence.....	157
Appendix.....	159
Contribution to Figures:.....	159
References.....	160

List of Figures and Tables

Figure 1.1: Structural organization of MYC (Lüscher and Vervoorts, 2012).	4
Figure 1.2: Site-specific transcriptional activation of target genes through the MYC network (Poole and van Riggelen, 2017).....	8
Figure 1.3: Schematic showing the mitogenic regulation of c-Myc protein stability (Helander et al., 2015).....	19
Figure 1.4: Schematic of the structure of Pin1 showing the regulatory posttranslational modification sites (Lu and Hunter, 2014).....	24
Figure 1.5: PIN1 regulating network in cell cycle (Lin et al., 2015).....	29
Figure 1.6: PIN1 mediated MYC isomerization depends on the phosphorylation status (modified from Helander et al., 2015).	37
Figure 1.7: Nuclear periphery and gene expression (Mekhail and Moazed, 2010).	42
Figure 1.8: Schematic of the nuclear pore complex (NPC) (Strambio-De-Castillia et al., 2010).....	44
Figure 2.1: Phosphorylation and Conserved Patterns in c-Myc.....	61
Figure 2.2: Evaluation of c-Myc1–88-Pin1 Affinities by Surface Plasmon Resonance.	62
Figure 2.3: NMR Analysis of c-Myc1–88 Per-Residue Interactions with Pin1 and Its Subdomains.....	67
Figure 2.4: NMR Relaxation Analysis of c-Myc1–88 Binding to Pin1.	68
Figure 2.5: NMR Mapping of Pin1 Interactions with c-Myc1–88 and pSer62-c-Myc1–88.....	72
Figure 2.6: Increased PP2A-B56 α activity reduces c-Myc protein levels.	76
Figure 2.7: Mutations in MB0 Decrease Pin1 Affinity and Regulate c-Myc activity.	81
Figure 3.1: pS62 MYC associates with the nuclear pore basket.	97
Figure 3.2: Ser62 phosphorylation is important for MYC association with the NPC.	100
Figure 3.3: PIN1 promotes MYC association with the NPC.....	105
Figure 3.4: PIN1 promotes the formation of TPR-MYC-GCN5 axis.....	108
Figure 3.5: PIN1 is critical for mitogen induced MYC association with the NPC.	113
Figure 3.6: PIN1 promotes MYC binding to the nuclear peripheral targets.	117
Figure 3.7: Pin1 knockout mice exhibit defects in wound healing.....	120
Figure 4.1: PIN1 regulates MYC translocation to the nucleolus.	144
Figure 4.2: PIN1 is the upstream of USP36 in the MYC degradation pathway..	144
Figure 4.3: PIN1 promotes MYC driven pre-rRNA synthesis.....	145
Figure 4.4: PIN1 mediated dynamic MYC localization in the nucleus.....	147
Table 5.1: Primer sequences.....	149

List of Abbreviations

List of Abbreviations

Ad	Adenovirus
AP1	Activator Protein 1
ARF	ADP Ribosylation Factor
CDK9	Cyclin dependent kinase 9
ChIP	Chromatin Immunoprecipitation
c-Myc	Cellular Myc
DMEM	Dulbecco's Modified Eagle's Medium
Dox	Doxycycline
ERK	Extracellular Receptor Kinase
FBS	Fetal Bovine Serum
GLS	Glutaminase
GSK3 β	Glycogen Synthase Kinase 3 β
HAT	Histone acetyltransferase
HDAC	Histone deacetylase
HLH	Helix Loop Helix
JNK	Jun N-terminal Kinase
IL	Interleukin
L-Myc	Lung Myc
LAD	Lamina associated domain
LAS	Lamina associated structure

List of Abbreviations

MB0	Myc Box 0
MB1	Myc Box I
MB2	Myc Box II
MNT	Max binding protein
MYC	c-Myc
NLS	Nuclear Localization Signal
N-Myc	Neuronal Myc
NPC	Nuclear Pore Complex
Nup	Nucleoporin
P	Phosphorylation
p53	Tumor Protein 53
PI3K	Phosphoinositide-3-Kinase
Pin1	Prolyl Isomerase 1
PP2A	Protein Phosphatase 2A
RB	Retinoblastoma
S62	Serine 62
SAPK	Stress Activated Pathway Kinase
SCF	Skp/Cullin/F-box
shRNA	Short Hairpin RNA
siRNA	small interfering RNA
SV40	Simian Virus 40
T58	Threonine 58

List of Abbreviations

TAD	Transactivation Domain
TCF	T Cell Specific Factor
TGF β	Transforming Growth Factor β
TPR	Translocated Protein Region
WNT	Wingless
WT	Wildtype
β -gal	β -Galactosidase

Acknowledgements

Acknowledgements

Foremost, I would like to thank Dr. Rosalie Sears as my mentor, who cultivated, encouraged, and urged me, whose enthusiasm for science, for life, always shines in front of me. I surely lack the talent to do experiments swiftly, but Rosie taught me what matters is the willingness to spend effort, to take risks, to focus on the subject as long as it fits the good purpose. It is not easy to pursue Ph.D., even harder for an international student as me. Thank you Rosie, for being so patient and supportive.

I also need to thank my committee members, Drs. Soren Impey, Matt Thayer, Susan Olson, and David Qian. Soren is my co-mentor, whose lab I spent most of my two years in learning and practicing ChIP, DIP, RNA sequencing technologies, and also where I had my first laughs and tears in graduate school for library making is truly beautiful and torturing. Matt is my committee chair, and gave me deep insights into nuclear structure. If Rosie is a type of mentor that seems to be “too” optimistic, then Matt is a perfect balance by emphasizing the importance of critical thinking. I thank Susan for being so approachable, even outside of science. Being around with Susan makes one fulfilled with hope and kindness. I thank David for not only your scientific advice, but also for the care of students.

Acknowledgements

Additionally, I want to thank Carl Pelz, Drs. Mushui Dai, Xiaoxin Sun, Xiaolin Nan and Gail Mandel for collaborations and advice on experiments.

Next, I want to thank all the Sears lab members for creating such a warm atmosphere for doing research. I want to specially thank Karyn Taylor, our lab manager, for helping on both lab and life affairs. You are always in such a good mood, chatting with you in the middle of the day will simply refuel our energy. Thank you for your sympathy and kind heart. Tyler Risom, Nick Kandinsky, Ellen Langer, Brittney Peterson, Ellen Langer, Jason Link, Meghan Joly, and Keith Early, thank you for lighting the lab up with you humorous personalities.

Juan Liang, a former postdoc fellow in our lab, whom I learned most of my bench skills from, Xiaoyan Wang, who helped me a lot on the experiments and on life, Collin Daniel, who gave me many advice and endured many of awkward jokes, own my many thanks as wise seniors, as supportive colleague, and most importantly as close friends. Thank you for being around no matter good or bad times.

My friends in Portland, Kang Wang, Bin Li, Yuhan Wang, Weinan Sun, Haijiao Zhang, and Qiuchen Cui, memories with you are truly cherishable. I cannot thank enough for the unconditional help and support. Kang has been a friend since I arrived in Portland, thank you for being my friend for so long, for not judging me when I made mistakes, for your praise when I made progress.

Acknowledgements

I need to thank my parents for their endless support. Although I have not made it home for so long, but the connection with you through phone or video is the most fundamental resource to give me strength to carry on. Mom and Dad, I want to try my best to make you proud. Lastly, I want to thank my future wife, who seems to always play an important role in the last paragraph of acknowledgements, thank you for being so patient on showing up, I just hope you won't miss me in the end.

"Life is about connecting with people to bring the best of each other."

-- Dr. Arlene Sharpe

Introduction

Chapter One :

Introduction

Introduction

Preface

The transcription factor MYC has been studied for decades as one of the most potent cancer drivers. Recent advances in next generation sequencing and molecular biology have uncovered a broad impact of MYC and its partners on the genome under both physiological and cancerous settings. This thesis investigates the interaction between MYC and PIN1, a previously identified regulator of MYC, with focus on the biophysical features, subnuclear localization, as well as the functional consequences. Such understanding potentiates more clinical utility of MYC by providing new biomarkers of MYC activity and novel strategies to inhibit MYC oncogenic functions.

The studies are organized in the following outline: In Chapter 1, I delve into the background of MYC and PIN1 and their roles in cancer biology. In Chapter 2, which was published in *Structure* 2015, I characterize a novel MYC motif that PIN1 recognizes, and how it impacts MYC activity. In Chapter 3, which is close to submission for publication, I address how PIN1 mediated nuclear distribution of MYC is important for MYC driven transcription. Finally, in Chapter 4, I connect all the threads and provide thoughts on future directions of this research.

The potent transcription factor MYC

Background of MYC

MYC (or c-MYC) was discovered as a cellular homologue of the avian retroviral proto-oncogene v-MYC that causes MYeloCytomatosis (leukemia and sarcoma) (Vennstrom et al., 1982). Since then, intensive studies have revealed its role in cell growth, transformation, tumor ignition and progression, covering virtually every aspect of cancer hallmarks (Hanahan and Weinberg, 2000). MYC functions as a transcriptional factor, with a unique ability to bind a wide range of gene targets, resulting in both transcriptional activation and repression (Kress et al., 2015). To target MYC for cancer therapeutics, it is critical to understand the mechanisms regulating MYC's activity and target gene selection.

MYC as a transcription factor

MYC belongs to a basic helix-loop-helix transcription factor family that also includes N-MYC, and L-MYC, which were discovered in neuroblastomas and small cell lung carcinomas, respectively (Brodeur et al., 1984; Nau, 1985). Similar to other transcriptional factors, the MYC proteins are modular. MYC carries a loosely defined transcriptional activation domain (TAD) at its N-terminus, followed by a canonical nuclear localization signal (NLS) at amino acids 300-328, and a

Introduction

carboxy-terminal basic helix-loop-helix leucine zipper (bHLH-LZ) DNA binding domain that forms a heterodimer with MAX, another bHLH-LZ protein, to bind the E-box consensus DNA sequence (CACGTG and other derivatives) (Figure 1) (Blackwell et al., 1990; Kato et al., 1990; Landschulz et al., 1988; Luscher and Eisenman, 1990). The MYC-MAX heterodimer, upon binding to DNA, can both activate and repress gene expression, controlling a wide range of cell behaviors.

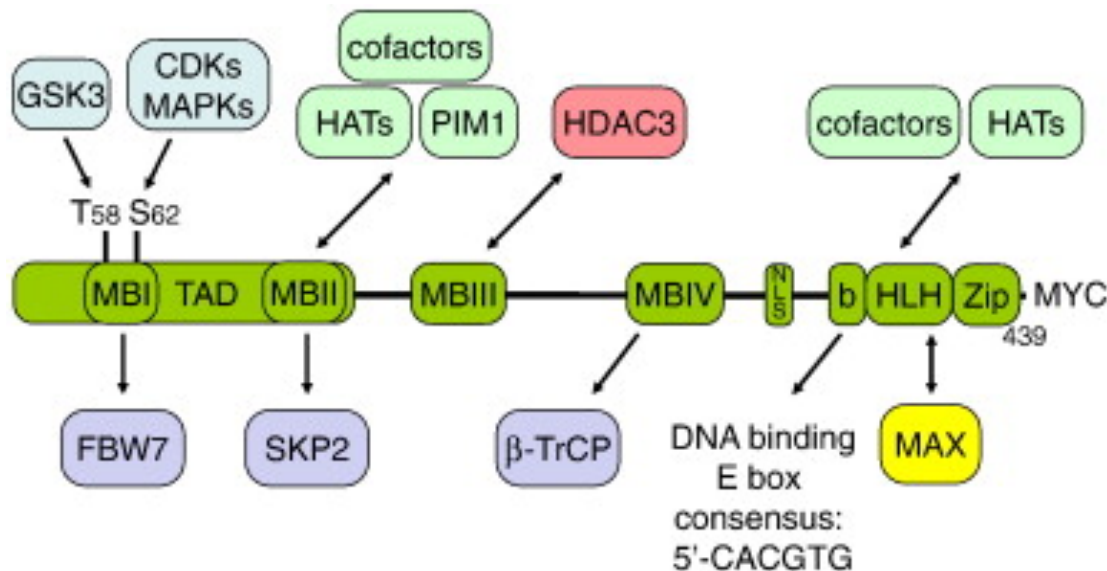


Figure 1.1: Structural organization of MYC (Lüscher and Vervoorts, 2012).

The domain structure of MYC. MB, conserved MYC boxes; TAD, transactivation domain; NLS, nuclear localization sequence; b, basic region; HLH, helix-loop-helix domain; Zip, leucine zipper region. Threonine 58 and serine 62 are indicated as two key phosphorylation sites. Interactions with cofactors and with E3 ubiquitin ligases are indicated with arrows. Not all the cofactors are mentioned specifically. Copy permission was obtained from *Gene*.

MYC regulation on site-specific target genes

While it is not known precisely how MYC-MAX transactivates site-specific target genes, one proposed model is through recruitments with chromatin-modifying co-

Introduction

factors. Many of these interactions are mediated through the N-terminal TAD and the associated Transactivation/ Transformation - Association Protein (TRRAP) (McMahon et al., 1998, 2000). TRRAP serves as a scaffold to recruit the histone acetyl transferases (HATs) GCN5 and Tip60 (Frank, 2003), as well as the chromatin remodeler SWI/SNF complex (Fuchs et al., 2001). These histone modifiers loosen the nucleosomes and maintain openness by histone acetylation (an active histone marker) at the local chromatin, allowing the access of RNA Polymerase II (Pol II) to the promoter, which stimulates transcription activation (Ciurciu et al., 2006; Kenneth et al., 2007). As a TRRAP-independent transactivation mechanism, MYC can directly recruit the HAT co-factors p300/CBP to its TAD or C-terminus, though the exact interaction sites may differ on different target promoters (Faiola et al., 2005; Vervoorts et al., 2003). Interestingly, in addition to modifying histone residues, CBP and GCN5 have been shown to acetylate MYC, affecting MYC's turnover, indicating that these enzymes not only conduct but also regulate MYC's activity (Faiola et al., 2005; Zhang et al., 2005). Besides histone acetylation, MYC-MAX can also recruit lysine-specific histone demethylases (KDMs) to activate target genes. For example, the central region (amino acids 99-300) of N-MYC interacts with KDM4B. Upon recruitment to E-Box containing targets genes, KDM4B specifically demethylates lysine 9 of histone 3 (H3K9), removing the repressive chromatin marker H3K9me2/me3, thereby contributing to gene activation (Das et al., 2014; Yang et al., 2015).

Introduction

Tracking with *MYC* mRNA levels, *MYC* protein levels are maintained at very low levels in quiescent cells and upon mitogenic stimulation protein levels increase, peaking by four hours post-stimulation and then declining to ~30% of peak level (Sears 2004). Control of *MYC* expression at the post-translational level is managed in large part through protein stability and turnover of *MYC* protein via multi-ubiquitination and degradation by the 26S proteasome (Flinn et al. 1998; Gross-Mesilaty et al. 1998; Salghetti et al. 1999). Many proteins that are degraded by ubiquitination and the 26S proteasome are marked by phosphorylation (Hoyt 1997; Krek 1998; Karin and Ben-Neriah 2000). *MYC* is no exception as T58 phosphorylation of *MYC* signals the SCF^{Fbw7} ubiquitin ligase machinery to multi-ubiquitinate *MYC* marking it for degradation by the 26S proteasome (Welcker et al. 2004; Yada et al. 2004). Interestingly, T58 phosphorylation of *MYC* is dependent upon a set of hierarchical reversible phosphorylation events on T58 and S62 (Henriksson et al. 1993; Lutterbach and Hann 1994; Pulverer et al. 1994). The hierarchical phosphorylation events on T58 and S62 are discussed in more detail below.

MYC-mediated, site-specific gene repression is also critical for *MYC*-driven tumor initiation and maintenance. The most studied mechanism underlying *MYC*-MAX controlled gene repression is through the interaction with MIZ-1. There are currently two mechanisms to explain *MYC*-MAX-MIZ1-driven repression. The first is a site-specific model, whereby at the initiator element (INR) MIZ1 binding sites,

Introduction

MYC-MAX-MIZ1 represses gene transcription by disrupting recruitment of co-activators such as CBP/p300, as well as by recruiting co-repressors such as histone deacetylases (HDACs) (Herold, 2002; Staller, 2001; Wanzel, 2008; Wu, 2003). The second model is based on the genomic binding sites of MYC and MIZ1, whereby at the E-box elements, the transcriptional outcome is determined by the MYC/MIZ1 ratio: a MYC/MIZ1 ratio higher than 1 leads to activation; MYC/MIZ1 close to or less than 1 leads to repression (Walz et al., 2014). The repression on MYC's canonical gene targets can also be achieved by the dimerization of MAX with other bHLH-LZ factors, such as the MXD family and MNT. Competing with MYC-MAX at the same E-box binding site, MAX-MXD recruits HDAC1 and HDAC3 to reduce local histone acetylation levels, resulting in more condensed chromatin and gene repression (Ayer et al., 1993, 1995; Larsson et al., 1994). Thus, the HATs recruited by MYC-MAX and HDACs recruited by MAX-MXD can be viewed as a switch to adjust the “opening” and “closing” of local chromatin, leading to transcription activation and repression respectively (Figure 1.2).

Introduction

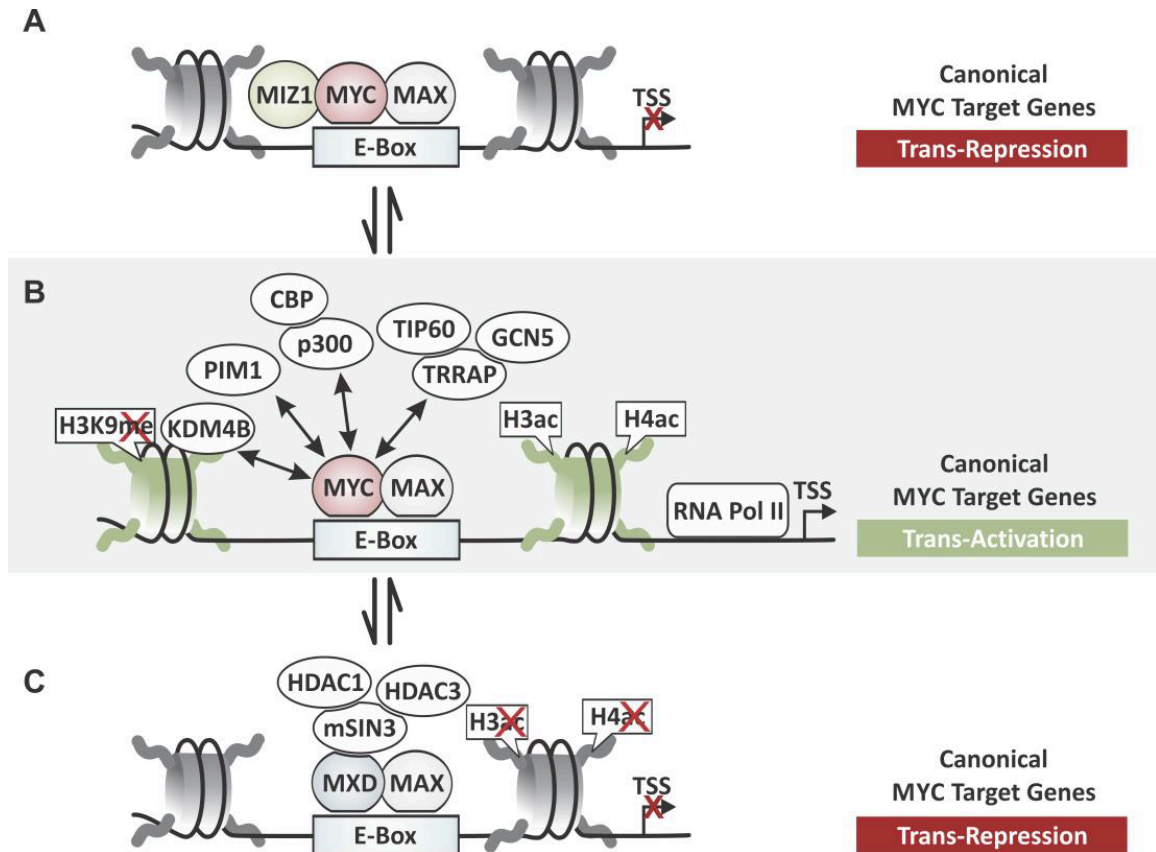


Figure 1.2: Site-specific transcriptional activation of target genes through the MYC network (Poole and van Riggelen, 2017).

(A) MIZ-1 can be recruited to form a trimeric complex with MYC-MAX to repress gene transcription; (B) MYC-MAX heterodimer binds E-box sequences to transactivate canonical target genes through recruitment of chromatin modifying co-factors. The KDM4 demethylase removes the inactive histone 3 lysine 9 trimethylation (H3K9me3) mark for activation. PIM1 kinase phosphorylates nucleosomes at histone 3 serine 10 (H3S10ph) locally for activation and phosphorylates MYC itself to enhance protein stability. TIP60 and GCN5 via TRRAP and p300/CBP act as histone acetyltransferases (HATs) to increase acetylation of histone H3 and H4 (H3ac and H4ac) in the vicinity of the binding site, allowing RNA Polymerase II (RNA Pol II) machinery to bind the core promoter. (C) MXD-MAX heterodimer competes with MYC-MAX for E-box binding, and repress canonical target genes through recruitment of HDACs (HDAC1 and HDAC3) via scaffolding protein SIN3 Transcription Regulator Family Member A (mSIN3), resulting in local deacetylation of histone H3 and H4. TSS: Transcription start site. Copy permission was obtained from *Genes*.

Introduction

MYC regulation of global transcription

In addition to modulating the local chromatin features at canonical gene promoters, MYC is also thought to facilitate global transcription elongation via recruitment of the Positive Transcription Elongation Factor b (pTEFb). pTEFb releases RNA Pol II from pausing by phosphorylating Ser2 in the heptad repeat of the Pol II carboxyl terminal domain (Pol II CTD). By doing so, it has been suggested that MYC can amplify essentially all actively transcribed genes, and consistent with this idea, MYC is found with Pol II at active gene promoters (Lin et al., 2012a; Rahl et al., 2010). However, considering that MYC itself and many site-specific target genes of MYC are potent drivers of cell proliferation and biosynthesis of macromolecules (this will be discussed in the **MYC and metabolism** section), the observed global RNA amplification described in (Lin et al., 2012a) might be a secondary effect of MYC-induced increase in cellular biomass. In support of this notion, if the cells are already in a proliferating state where global RNA amplification is not as prevalent as cells transitioning from quiescence to proliferation, ectopic expression of MYC leads to both activation and repression of certain groups of genes (Kress et al., 2015; Sabò et al., 2014).

Appealing as the general amplifier model is, how MYC regulates chromatin and transcription will be much more complicated based on knowledge of protein-chromatin and chromatin-chromatin interactions. At the molecular level, assuming the general effect of MYC on transcription is through promoting Pol II

Introduction

release from pause, the extent to which MYC does so is probably heavily dependent on the context: local chromatin organization or connection between cis-regulatory elements, histone modifications, accessibility of co-factors, MYC posttranslational modifications and associated conformational dynamics in MYC's transactivation domain (discussed below in **MYC regulation of specific gene target** section). Moreover, many of these factors may affect one another, for example, the chromatin organization may limit MYC and its factors to bind to DNA, and binding of MYC may initiate recruitments of chromatin modifiers to change the chromatin structure. Lastly, the discussed scenarios are mostly snapshots of a series of rapidly changing yet organized events to which we currently know little of. Nonetheless, an integration of the site-specific effect of MYC on local chromatin/genes and its broad approach to the genome helps to explain MYC's wide-ranging effects on cell fate determination, tumor initiation, and tumor progression.

MYC-regulated cell functions

MYC and the cell cycle

One of the earliest discovered functions of MYC was to promote cell cycle progression. MYC depletion in Rat1 cells leads to slower cell growth with an elongated G1 phase (Mateyak et al., 1999). Consistently, antisense oligonucleotides against MYC prevent human lymphoid and myeloid cells from S-

Introduction

phase entry (Heikkila et al., 1987; Wickstrom et al., 1988). The critical role of MYC in G1 progression and G1/S transition is demonstrated through MYC's coordinated regulation on CDKs and cyclins. MYC has been shown to directly bind and activate the transcription of CDK4 and its partner cyclin D during early G1 (Bouchard, 2001; Mateyak et al., 1999). Although it's unclear whether CDK2 is a direct target of MYC, cyclin E is induced by MYC that upon binding to CDK2, leads to CDK2 activation during late G1 (Qi et al., 2007; Yap et al., 2011). MYC also activates CDKs through antagonizing the CDK inhibitor p27. As a target of MIZ1, p27 expression is repressed by MYC through the MYC-MIZ1 interaction (illustrated previously); alternatively, MYC induced miR-221/222 recognize p27 mRNA and promotes its degradation (Chandramohan et al., 2004; Li, 2003). In addition to the above mechanisms, MYC can also induce the E3 ubiquitin ligase SKP2, which promotes proteasome-mediated degradation of p27 (Bretones et al., 2011).

MYC and metabolism

To compensate for the energy and biomass needs of the dividing cells, MYC also plays a driving role in energy production and cell mass accumulation. MYC's role in cell growth control is conserved across species. In *Drosophila*, the cells of the wing imaginal disc are smaller upon dMYC deletion and larger with dMYC overexpression (Johnston et al., 1999). In mouse, inducible deletion of MYC in T lymphocytes prevents the T-cell receptor-stimulated growth response (Wang et

Introduction

al., 2011a). Overexpression of MYC in B lymphocytes leads to cell growth that can be uncoupled from an increase in cell number (Schuhmacher, 1999). MYC promotes cell size increase or cell growth through manipulating key regulators in the metabolism of glucose and glutamine, the two major ATP and carbon sources. For most genes in the glycolytic pathway, MYC binds the consensus E boxes (CACGTG) of the promoters to activate their transcription. For example, MYC upregulates the expression of LDHA, which converts pyruvate generated from glycolysis into lactate (Qing et al., 2010; Shim et al., 1997). In this manner, MYC stimulates aerobic glycolysis, or the Warburg effect, which is a strategy taken by rapidly growing tumors cells to generate macromolecules as byproducts of ATP production. In addition to the ability to induce glycolytic genes, MYC also controls glutamine metabolism. In growing cells, glutaminase (GLS) converts glutamin to glutamate that is metabolized in the TCA cycle to provide ATP and carbon skeleton for protein and nucleotide synthesis, and is therefore viewed as one of the rate-limiting enzymes for glutamine metabolism. At the transcription level, MYC can moderately induce the mRNA level of GLS (Wise et al., 2008); post-transcriptionally, MYC can maintain the high expression level of GLS by repressing miR23a and miR23b, microRNAs that inhibit GLS synthesis (Gao et al., 2009).

MYC and Apoptosis

Introduction

Although MYC is well recognized for its predominant role in cell proliferation, deregulated MYC can also induce programmed cell death, or apoptosis, a process shared by certain other oncogenes such as E1A and E2F1 (Lowe et al., 2004). Oncogene-induced apoptosis is thought to provide a built-in failsafe for the cell to prevent uncontrolled proliferation under inappropriate conditions. The ability of MYC to trigger apoptosis in response to growth stress has been demonstrated in multiple studies. In the case of interleukin 3 (IL-3)-dependent myeloid progenitor cells, withdrawal of IL-3 leads to growth arrest accompanied by quenching of MYC expression. Enforced MYC expression drives apoptosis in this IL-3 deprived cells, which is attenuated by re-supply of IL-3. However, IL-3 cannot protect the cells from MYC-driven apoptosis when the cells are grown in high density, another growth-stress factor (Askew DS et al., 1991). MYC-induced apoptosis has also been observed in Rat1a cell lines or primary rat embryo fibroblasts that are grown in serum-free media (Evan, 1992). The level of MYC required to trigger apoptosis, however, varies between cell types: transformed cells are either resistant or tend to require more MYC expression to induce apoptosis, reflecting the disrupted failsafe to keep the cancer cells in check for proliferation. Further, cancer cells, due to their metabolic addiction to MYC are also driven to apoptosis upon acute loss of MYC expression.

MYC triggers or sensitizes cells to apoptosis through both p53-dependent and p53-independent mechanisms. MYC induces the expression of Arf, which in turn

Introduction

stabilizes p53 through inhibition of MDM2 (Eischen CM et al., 1999). It is worth noting that MYC overexpression is often associated with DNA damage and genomic instability, which triggers ATM-mediated p53 activation (Pauklin S et al., 2005; Pusapati RV et al., 2006; Reimann, 2007). Conversely, in multiple mouse models, inhibition of the p53 pathway accelerates tumorigenesis driven by MYC (Alt et al., 2003; Bouchard, 2007; Eischen CM et al., 1999; Finch, 2006; Jacobs, 1999; Schmitt CA et al., 1999). MYC also amplifies apoptotic pathways via altering the balance of pro- and anti- apoptotic members of the Bcl-2 family. MYC can directly bind to the promoter and induce RNA expression of the pro-apoptotic regulator Bax (Cao X et al., 2008; Dansen TB et al., 2006; Eischen et al., 2001a; Jiang X et al., 2007), the oligodimerization of which permeabilizes the mitochondria membrane, resulting in cytochrome *c* release that triggers a downstream apoptotic signaling cascade. In the absence of apoptotic signals, the function of Bax is blocked by anti-apoptotic Bcl-2 family members, such as Bcl-2 and Bcl-X_L. MYC overexpression suppresses the RNA and protein of Bcl-2, which releases Bax from inhibition to activate apoptosis (Bissonnette et al., 1992; Eischen, 2001). Many of the MYC-driven apoptosis processes associated with the changes in Bcl-2 family activity are in cell systems with inactivation of the Arf/p53 pathway, indicating that MYC's influence on cell-intrinsic apoptosis can be p53-independent (Eischen et al., 2001b; Maclean et al., 2003).

MYC and cell morphology

Introduction

Deregulated MYC not only favors unlimited cell growth during tumorigenesis, as apoptotic machinery is commonly bypassed, but it also changes cell morphology and motility such as epithelial-mesenchymal transition (EMT), a feature associated with increased metastasis during tumor progression. The connection of MYC to EMT and metastasis was indicated through its regulation of miR-9, a microRNA that targets E-cadherin, which is an epithelial marker and adheres cells to its surrounding matrix (Ma et al., 2010). Apart from indirect regulation, MYC has also been shown to directly facilitate cellular TGF- β signaling through binding to and activating the expression of *SNAIL*, which encodes SNAIL, the key transcription factor that promotes EMT (Proestling et al., 2015; Smith et al., 2008). MYC may also promote metastasis beyond the process of EMT, as depletion of MYC via siRNA disrupts cell migration, invasion, and metastasis of MDA-231 breast cancer cells *in vivo*, which are already highly metastatic states and not associated with EMT (Wolfer et al., 2010). In support of this idea, MYC can also upregulate OPN, an integrin-binding ligand that stimulates the migration and invasion of cancer cells (Martinez et al., 2010). In addition to promoting the early stages of cancer metastasis (cell migration and invasion), MYC has also been shown to promote the seeding of metastatic cancer cells in cooperation with other components of the RAS pathway (Podsypanina et al., 2008; Rapp et al., 2009), providing rationales for targeting MYC even for patients with advanced tumor stages.

Regulation of MYC expression

Since MYC is a master regulator of crucial cell behaviors such as proliferation, metabolism, motility, and apoptosis, its expression level must be under tight control for cells to function normally. In non-transformed cells, MYC expression is regulated transcriptionally (target of other transcription factor), post-transcriptionally (mRNA stability), and post-translationally (protein stability) (Jones and Cole, 1987; Kelly et al., 1983a; Luscher and Eisenman, 1990; Sears et al., 1999). Conversely, overexpression of MYC due to disruption of one or several of these regulations contributes to malignant transformation of many human cancers (reviewed in (Dang, 2012; Meyer and Penn, 2008)).

Transcriptional control of MYC

In normal tissues, the abundance of MYC mRNA is usually kept at basal levels as a result of low transcriptional activity and rapid turnover. Hyper activation of MYC transcription in malignant cells can be attributed to chromosomal translocations and gene amplifications. In Burkitt's lymphoma, overexpression of the *MYC* gene is caused by a balanced translocation that juxtaposes *MYC* to one of the actively transcribed immunoglobulin genes in B cells (Dalla-Favera et al., 1982; Taub et al., 1982). The causal effect of this translocation event is demonstrated in the *Eu-myc* mouse model, in which the *Myc* gene driven by IgH enhancer invariably leads to B cell lymphoma (Harris et al., 1988). MYC is also

Introduction

frequently translocated in multiple myelomas and transcriptionally overexpressed (Shou et al., 2000), probably through similar mechanisms due to the vicinity of translocated MYC loci to an upstream cluster of active enhancers (a “super enhancer”) (Hnisz et al., 2013). In contrast to chromosomal translocations in hematopoietic malignancies, in various solid tumors, increases in *MYC* gene expression are associated with gene amplification, including neuroblastoma, small cell lung cancer, breast cancer, and colorectal cancer (Beroukhim et al., 2010). In addition to these mechanisms involving alterations of DNA elements, aberrant upstream signaling could also cause the upregulation of MYC transcription. In T cell leukemia, deregulated NOTCH signaling leads to transcriptional activation of MYC (Palomero et al., 2006; Sharma et al., 2006; Weng et al., 2006); in human colon carcinoma, MYC is activated by enhanced TCF activity due to a deregulated WNT pathway (He et al., 1998).

The stability of mRNA is another factor contributing to MYC transcript abundance. MYC mRNA is rapidly turned over with a half-life around 10mins in the steady-state of cells (Dani et al., 1984; Herrick and Ross, 1994). This is, at least in part, due to control of the 3' untranslated regions (UTR). The 3'UTR of MYC can be bound by RNA binding protein HuR and microRNA Let-7, which triggers degradation of MYC transcripts through the process of miRNA-induced silencing (Kim et al., 2009; Sampson et al., 2007). Consistent with its negative role in MYC mRNA stability, deletion of 3'UTR elevates MYC expression (Brewer and Ross,

Introduction

1988). The expression of MYC is also regulated at the translational level through its 5'UTR-mediated translational initiation (Stoneley et al., 1998). A C-T point mutation in the 5'UTR is reported to be associated with enhanced MYC translation in multiple myeloma (Chappell et al., 2000).

Post-translational modification of MYC

In addition to transcriptional control, fine-tuned MYC expression also occurs at the post-translational level, affecting its protein stability. MYC post-translational modifications include two specific and conserved residues across all MYC family members. Serine 62 (S62) phosphorylation stabilizes MYC and Threonine 58 (T58) phosphorylation promotes proteasome-mediated degradation of MYC. Following growth stimulation, multiple RAS downstream kinases (MEK/ERK and PI3K/AKT) play a dual role in phosphorylating MYC (Lutterbach and Hann, 1994; Sears et al., 1999, 2000). ERK phosphorylates MYC on S62, while AKT inhibits GSK3b that phosphorylates T58 (Cross et al., 1995). With growth signal withdrawal, ERK and AKT activity decreases, suppressing additional S62 phosphorylation and unlocking GSK3b from inhibition. GSK3b then phosphorylates T58 (Lutterbach and Hann, 1994; Pulverer et al., 1994). The dual-phosphorylated form of MYC is catalyzed by PIN1 at Proline 63 from *cis* to *trans*. In *trans*, MYC is dephosphorylated by PP2A at S62, and undergoes Fbw7-mediated proteasome degradation (Alvarez et al., 1991) (Figure 1.3).

Introduction

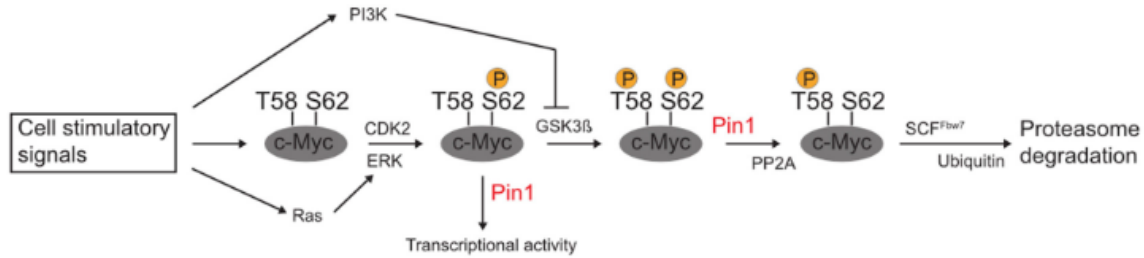


Figure 1.3: Schematic showing the mitogenic regulation of c-Myc protein stability (Helander et al., 2015).

In response to mitogen stimulation, RAS activation turns on the RAF/MEK/ERK and PI3K/AKT pathways. ERK and CDK2 can phosphorylate MYC on S62 and simultaneously, PI3K/AKT inhibit GSK3 β phosphorylation of T58, keeping MYC in a stable form early in G1. Late in G1, RAS activity decreases and GSK3 β phosphorylates MYC on T58, destabilizing MYC by allowing SCF^{Fbw7} to recognize and multi-ubiquitinate c-Myc marking it for degradation via the 26S proteasome. Copy permission was obtained from *Structure*.

Post-translational modification seems to not only control MYC degradation but also its activity. For instance, mutation of Serine 62 to Alanine (S62A), which completely abolishes the phosphorylation potential of S62, reduced MYC activity in a transactivation assay, even though stability of this mutant is often higher than wild-type MYC. Additionally, both T58A (Threonine 58 mutated to Alanine, which has constitutively high phosphorylation at S62 and no phosphorylation at T58) and S62A, but not WT MYC can drive tumorigenesis in mouse mammary models, but these models exhibit different phenotypes, indicating different MYC activities associated with different mutations (Wang et al., 2011b). Lastly, in the case of PIN1, our recent work indicates that in addition to promoting MYC degradation, MYC – PIN1 interaction promotes dynamic binding of MYC to chromatin and

Introduction

recruitment of co-activators to increase MYC's oncogenic activity (Farrell et al., 2013). This dual role of PIN1 on MYC is interesting in that MYC's transcriptional activity could be uncoupled from its expression level, bringing another dimension to MYC interaction with DNA and/or the cofactors – temporal. Indeed, many of the biological processes that PIN1 regulates involve rapid response to environmental changes; a disruption of PIN1 controlled molecular timing may support tumorigenesis as will be discussed in the next part of the introduction.

The molecular timer PIN1

Background of PIN1

Phosphorylation-directed proline isomerization is an instrumental posttranslational modification shared by many biological processes. The proline isomerase PIN1 (Protein interacting with never in mitosis A1), by isomerizing specific phosphor Serine / Threonine – Proline (pS/T-P) bonds in certain substrates, controls cell cycle progression, signal transduction, cell fate determination. Deregulation of PIN1 can disrupt the timing of the proline isomerization, rewire the signaling, and in many cases contribute to tumor development, highlighting the importance of understanding the biology of PIN1.

Phosphorylation-directed proline isomerization in signaling cascade

Cells utilize protein phosphorylation as a fast and accurate way to conduct signaling cascades in response to cellular intrinsic and extrinsic stimuli (Blume-Jensen and Hunter, 2001; Pawson and Scott, 2005). These phosphorylation events are often associated with protein conformational changes to have a greater influence on protein functions. One common mechanism that mediates protein phosphorylation and conformation change is the Serine/Threonine

Introduction

phosphorylation-coupled proline isomerization (pS/T-P) (Pawson and Scott, 2005). Close to one third of identified phosphorylation sites in cell are pS/T-P sites, which often provide recognition sites for kinases and phosphatases (Ubersax and Ferrell, 2007). For instance, all MAPKs that are critical for growth responses— including ERKs, p38 MAPKs, and stress-activated protein kinases (SAPKs), as well as all cyclin-dependent kinases (CDKs), which drive cell cycle progression—are Proline-directed kinases (Morgan, 1997; Pearson et al., 2001). Likewise, protein phosphatase 2A (PP2A), which dephosphorylates about one third of all phosphor substrates, is Pro-directed (Zhou et al., 2000). Interestingly, many of the kinases and phosphatases often exist in the same signaling pathway, and depending on the conformation of the substrates, their presence can lead to distinct and sometimes opposite cellular outcomes (reviewed in (Lu and Hunter, 2014; Zhou and Lu, 2016)). Thus, the regulation of pS/T-P is pivotal in cellular functions.

Proline has a its distinct role in protein conformation due to the formation of a 5 carbon-ring in the peptide backbone, resulting in an increase in energy required to convert between cis- or trans-isomers (Fischer and Aumuller, 2003). Peptidyl-prolyl isomerases (PPIases) reduce the energy barrier to accelerate this proline interconversion. pS/T-P not only further increases the energy barrier, but also masks the peptide bonds to conventional PPIases, such as FK506-binding proteins and cyclophilins, leaving the proline accessible only to PIN1 (Göthel and

Introduction

Marahiel, 1999; Ranganathan et al., 1997). As the only identified phosphorylation-dependent proline isomerase, PIN1 plays a crucial role in cell proliferation, motility, apoptosis, and transformation and development of tumor cells.

PIN1 is expressed as a 161aa peptide consisting of an N-terminal WW domain and a C-terminal PPIase, connected by a flexible linker (Figure 1.4). The WW domain is responsible for PIN1 to recognize its targets (Göthel and Marahiel, 1999), whereas the PPIase domain carries the catalytic activity to isomerize proline; both domains are required for PIN1 function *in vivo* (Lu et al., 1999; Ranganathan et al., 1997; Yaffe, 1997; Zhou et al., 2000). The recognition of the WW domain to PIN1's substrates was originally thought to be dependent on the phosphorylation of the S/T-P motif (Ranganathan et al., 1997). Through careful biophysical examination of the interaction between synthetic PIN1 and MYC *in vitro*, however, we found that PIN1 can bind to MYC in a phosphorylation-independent manner, providing an alternative mechanism for how PIN1 recognizes its targets (chapter 2, Helander et al., 2015). Moreover, PIN1 can interact with motifs that are already in *cis* or *trans* and convert them to the opposite conformations; the exact direction depends on the substrate sequences and the context they are in. In the case of pT668-P motifs within amyloid precursor protein (APP), PIN1 has almost the same affinity for both *cis* and *trans* conformations, suggesting that PIN1 catalyzes the inter-conversion of APP (Akiyama et al., 2005; Pastorino, 2006).

Introduction

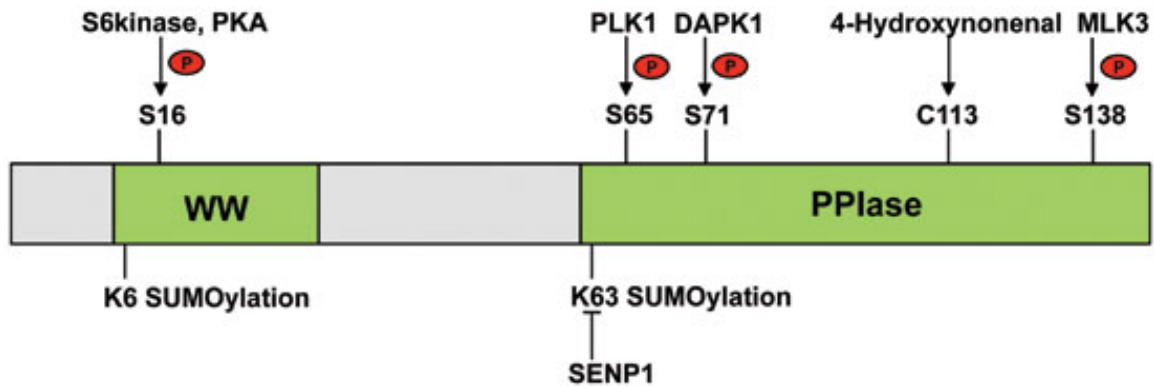


Figure 1.4: Schematic of the structure of Pin1 showing the regulatory posttranslational modification sites (Lu and Hunter, 2014).

PIN1 is composed of N-terminal WW domain and C-terminal PPlase domain. Multiple residues of PIN1 can be post-translationally modified, which will affect the function of PIN1. The phosphorylation sites are annotated as encircled P. Copy permission was obtained from *Cell Research*.

PIN1 expression and regulation

PIN1 is widely overexpressed in human cancer. In a study comparing 60 different human tumor types with corresponding normal tissues, PIN1 is overexpressed in 38 of them, including melanoma, breast, lung, prostate, cervical, and ovarian tumors (Bao et al., 2004). PIN1 overexpression also correlates with poor prognosis and was found to be an independent prognostic factor for esophageal squamous cell carcinoma (Leung et al., 2009). The positive role of PIN1 in tumorigenesis and tumor progression is also supported in mouse models. Depletion of Pin1 decreases the frequency of spontaneously developing tumors

Introduction

and prevents tumor development in tumorigenic mice, such as p53 knockout mice and HER2, HRAS, *eu-myc*, or mutant p53 transgenic mice (Girardini et al., 2011; Takahashi, 2007; Wulf et al., 2004). Recent studies suggest that PIN1 promotes tumorigenesis through its pivotal role in cancer stem cells (CSCs), a population within cancer that processes full tumorigenic potential. In human breast tumors, PIN1 overexpression is more prevalent in CSCs than in non-CSC tumor cells and induces stem-like and epithelial-to-mesenchymal transition (EMT) properties in normal breast cells (Luo et al., 2015; Rustighi et al., 2014a). Consistent with the critical role of PIN1 in CSCs, small interfering RNA-mediated knockdown of PIN1 prevents conversion of normal breast epithelial cells to CSCs by reprogramming factors (Nishi et al., 2014).

PIN1 expression and activity are regulated transcriptionally and post-translationally, although it is not clear if the copy number of PIN1 is amplified in cancer. PIN1 is a direct target of the transcription factor E2F1, which is induced by cell cycle progression or by HER2-RAS signaling (Ryo, 2002). Additionally, a single-nucleotide polymorphism on PIN1 promoter, -842G>C, resulting in a decrease in PIN1 expression, has been associated with less risk of head and neck squamous cell carcinoma (Lu et al., 2009).

In addition to transcriptional control of PIN1, post-translational modification can regulate PIN1's stability, activity, and cellular localization. Multiple

Introduction

phosphorylation sites within the PPlase domain of PIN1, such as pS65, pS71, and pS138, regulate distinct aspects of PIN1 function. Specifically, Death-associated protein kinase 1 (DAPK1)-dependent S71 phosphorylation not only inhibits PIN1's catalytic activity but also prevents its nuclear localization (Lee et al., 2011a). In contrast, the MAPK family member mixed-lineage kinase 3 (MLK3) phosphorylates PIN1 at S138, which—although also within the PPlase domain—increases both PIN1's nuclear translocation and its catalytic activity (Rangasamy et al., 2012). Moreover, PLK1 stabilizes PIN1 through phosphorylating PIN1 at S65, which in turn prevents the ubiquitin-mediated proteasome degradation of PIN1 without affecting its activity (Eckerdt, 2005). Phosphorylation on the WW domain of PIN1 also affects its function. S16 phosphorylation within the WW domain prevents PIN1 from binding to its substrate, thereby inhibiting its activity (Lu et al., 2002b).

PIN1 can also be modified by Small Ubiquitin-like Modification (SUMOylation). SUMOylation of PIN1 on lysine 6 (K6) in the WW domain and on lysine 63 (K63) in the PPlase domain decreases PIN1 activity and oncogenic function. SUMO protease 1 (SENP1) can deSUMOylate PIN1, which increases PIN1 protein stability. In support of this, SENP1 overexpression or disruptions of PIN1 SUMOylation through mutagenesis promotes PIN1 to induce centrosome amplification and cell transformation (Chen et al., 2013).

PIN1 and its diverse targets

The expression of PIN1 has also been found to correlate with other tumor markers in human cancers. For instance, the level of PIN1 correlates closely with cyclin D1 levels in esophageal and oral squamous cell carcinoma and in breast cancer (Miyashita et al., 2003a, 2003b). Indeed, the close relationship between PIN1 and cyclin D1 led to early studies on the molecular mechanisms underlying the oncogenic role of PIN1. PIN1 not only directly stabilizes cyclin D1 protein, but it also increases RNA expression of cyclin D1 by coordinating multiple signaling cascades, including HER2-HRAS-JNK-AP1, WNT- β -catenin, and cytokine-NF- κ B pathways (Liou, 2002; Ryo, 2003; Wulf, 2001). This evidence has led to the concept that PIN1 regulates multiple substrates of multiple pathways to cooperatively promote oncogenesis.

PIN1 and cell cycle regulators

Pin1 knockout mice, although viable, display multiple abnormalities, including smaller body size, neurodegeneration mimicking Alzheimer's disease, retinal degeneration, impaired mammary gland development, and testicular atrophy resulting in infertility (Fujimori et al., 1999; Liou, 2002). These phenotypes indicate a critical role of PIN1 in cell proliferation and cell cycle regulation. In response to growth signaling, PIN1 and many CDKs coordinate with one another to form a positive feedback loop to facilitate cell cycle progression. In quiescent

Introduction

cells, retinoblastoma protein 1 (RB1) binds and inhibits E2F functions. During early G1, RB1 hyperphosphorylation releases E2F, allowing it to activate target gene transcription such as with cyclin D1, which in turn triggers cell cycle progression (Bertoli et al., 2013). As an E2F target gene, the level of PIN1 is elevated at mid-G1 phase, resulting in an increase of PIN1 interaction with RB1. PIN1-catalyzed isomerization renders RB1 in *cis* form, making it resistant to the trans-specific phosphatase PP2A; in this way, PIN1 promotes hyperphosphorylation of RB1, which in turn induces E2F-dependent PIN1 expression (Rizzolio et al., 2012; Tong et al., 2015). This feed-forward loop is further enhanced by PIN1-mediated cyclin D1 upregulation, which in turn activates G1 CDKs to inactivate RB1. PIN1 also downregulates p27 and cyclin E, which are required for proper G1-S transition at different time points (van Drogen, 2006). In support of this, PIN1-deficient fibroblasts have defective G1-S transition (van Drogen, 2006; Fujimori et al., 1999). During S phase, PIN1 interacts with the centrosome to coordinate DNA synthesis and centrosome duplication (Suizu et al., 2006), which is inhibited by PIN1 S71 phosphorylation by DAPK1. During S and G2 phases, PIN1 maintains the stability and activity of the cyclin B1 and CDC2 complex through stabilizing the upstream regulator F-box protein 5 (FBXO5, a F-box containing protein that stabilizes APC ubiquitin substrates), which endures until the G2-M transition (Bernis, 2007; Okamoto and Sagata, 2007; Stukenberg and Kirschner, 2001). As cells progress through mitosis, PIN1 inhibits transcription by switching off the function of RNA polymerase II (RNA

Introduction

PolII), and it induces chromatin condensation by interacting with topoisomerase IIa (Xu and Manley, 2007a, 2007b). Overall, these studies indicate that tight regulation of PIN1 is pivotal to orchestrate many cell cycle regulators spatially and temporally to form abrupt waves of signaling in a coordinated manner (Figure 1.5).

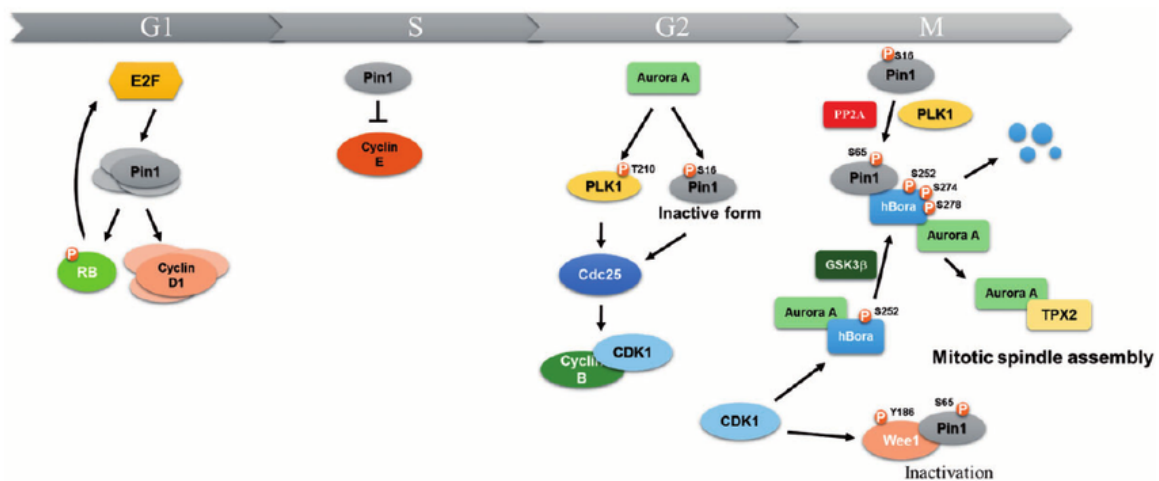


Figure 1.5: PIN1 regulating network in cell cycle (Lin et al., 2015).

During G1, PIN1 promotes cyclin D1 overexpression and RB phosphorylation. The phosphorylated RB releases E2F, which is a transcriptional factor to enhance PIN1 expression. PIN1 stimulates cyclin E degradation in S phase. During G2 phase, Aurora A inactive PIN1 and active PLK result in CDC25 activation triggers G2/M transition. During the G2/M transition, GSK-3 β interacts with and phosphorylates hBora at S274/S278, and in the meantime, Aurora A interacts with and phosphorylates PIN1 at Ser16 to disrupt PIN1 function by suppressing PIN1 binding to phospho-hBora and thus preventing β -TrCP-mediated premature hBora degradation. Therefore, Aurora A forms a complex with phospho-hBora to phosphorylate Plk1 at Thr210 and activates Plk1. Plk1 activates CDC25 result in the activation of the Cyclin-B1/CDK1 complex and promotes mitotic entry. After mitotic entry, PIN1 could recover the binding activity and enhance protein stability through PP2A and PLK1. The active PIN1 promotes the degradation of hBora. Aurora A is then available to bind with TPX2 result in mitotic spindle assembly. Wee1 is phosphorylated at Tyr168 by CDK1 and Pin1 isomerize phosphorylated Wee1 inactivation. Copy permission obtained from *Experimental Biology and Medicine*.

Introduction

PIN1 and protein kinases and phosphatases

Kinases and phosphatases directly control protein phosphorylation, a major mechanism for signal transduction within cells. PIN1 regulates the functions of numerous protein kinases and phosphatases, from plasma membrane to cytosolic and nuclear kinases and phosphatases. For example, in HER2-positive breast cancer, where PIN1 is often overexpressed, PIN1 interacts with ubiquitylated HER2 at the plasma membrane to prevent it from degradation. PIN1 depletion promotes HER2 degradation, which sensitizes the HER2-positive tumor cells to the mTOR inhibitor rapamycin and suppresses tumor cell growth (Lam et al., 2008).

PIN1 also promotes the activation of NOTCH signaling. The binding of NOTCH receptor with ligand induces proteolytic cleavage of the intracellular domain of NOTCH, which is then translocated to the nucleus to activate transcription. There are several isoforms of the NOTCH receptor—e.g., hyper-activated NOTCH1 has been associated with many kinds of tumor development, including breast cancer. PIN1 enhances NOTCH1 activity by increasing NOTCH1 intramembrane cleavage and the release of active intracellular domains to induce transcription of target genes. PIN1 also interacts with NOTCH1 at phosphorylated T2512/P2513, a phosphodegron that facilitates Fbw7a-mediated proteasome degradation. PIN1 controlled prolyl-isomerization of this phosphodegron leads to the

Introduction

dephosphorylation of NOTCH1 by PP2A, preventing the interaction of Fbw7a and subsequent degradation of NOTCH1. Interestingly, NOTCH1 signaling also regulates a distal element on the PIN1 promoter and promotes PIN1 expression. Therefore, NOTCH1 and PIN1 can form a feed-forward loop, which is supported by a strong correlation between PIN1 expression and NOTCH1 activity in human breast cancer (Rustighi et al., 2009, 2014b).

PIN1 also regulates multiple kinases within the MAPK and AKT pathways, which occur mainly in the cytosol. The initiation of the MAPK pathway involves binding of RAS to the RAF-1 kinase, which transmits mitogenic, oncogenic and/or differentiative signals to downstream MEK and ERK kinases. Activated ERK phosphorylates RAF-1 at Serines 29, 289, 296, 301, and 642, blocking the Ras/RAF-1 interaction and RAF-1 activity, creating a negative feedback to shut down the signaling. PIN1 recognizes the hyper-phosphorylated and inactive RAF-1 and catalyzes cis-trans isomerization, which leads to dephosphorylation of RAF-1 by PP2A, restoring RAF-1's signaling competency (Dougherty, 2005). PIN1 regulates other members in the MAPK pathway, as well. For example, in response to EGF stimulation, PIN1 interacts with MEK1 instead of RAF-1, which enhances EGF-induced phosphorylation of MEK1/2 and ERK1/2, leading to downstream target activation such as HER2 and neoplastic cell transformation (Khanal et al., 2010).

Introduction

In addition to MAPK pathways, PIN1 also regulates AKT signaling to regulate many critical cellular functions. PIN1 binds to AKT at the phosphorylated Thr-Pro motif around T92 and T450, which is required for the maintenance of AKT phosphorylation at S473, an indicator of AKT stability and activity. The protective effect on AKT stability is compromised by shRNA-mediated PIN1 depletion. In agreement with this, PIN1 expression level strongly correlates with the level of AKT S473 phosphorylation in many cancer types. In the case of breast cancer, patients with high levels both of PIN1 and AKT-pS473 are associated with poorer prognosis than either factor alone (Liao et al., 2009).

PIN1 and transcription factors.

Many signaling pathways ultimately end up with protein synthesis by turning on or off specific genes; thus, the final acting molecules of signaling cascades are often transcription factors. PIN1 coordinates the activities of various regulators within the same pathway, and therefore PIN1 also regulates a wide range of transcription factors.

PIN1 and β -catenin

PIN1 regulates the stability and subcellular localization of β -catenin, a transcription factor downstream of WNT signaling. The expression of β -catenin is increased in and correlated with overexpressed PIN1 in many human tumors and

Introduction

is decreased in *Pin1* knockout mice (Liou, 2002; Nakashima, 2004; Pang, 2004; Ryo et al., 2001). PIN1 stabilizes β -catenin through isomerization of the phosphorylated Ser246-Pro motif, blocking the interaction of β -catenin with the tumor suppressor APC, which would normally translocate β -catenin to the cytoplasm for degradation. Overexpressed and/or hyperactive PIN1 accumulates β -catenin in the nucleus, resulting in aberrant induction of oncogenic genes, such as *MYC* and *CCND1* (cyclin D1) (Ryo et al., 2001).

PIN1 and AP-1

PIN1 plays an important role in the activity of the transcription factor complex AP-1, which is composed of c-Jun and c-Fos transcription factors. AP-1 is formed through a highly regulated process: following activation of RAS, the c-Jun N-terminal kinases phosphorylate c-Jun at Ser63/73 -Pro motifs, which are recognized and isomerized by PIN1. PIN1-dependent isomerization of these motifs inhibits c-Jun ubiquitylation to increase c-Jun stability and thereby enhance c-Jun's binding to the target promoters (Wulf, 2001). Concordantly, the RAS-ERK signaling phosphorylates multiple residues, including T232, T325, T331, and S374, of the C terminal domain of c-Fos, which then heterodimerizes with c-Jun to form AP-1 (Monje et al., 2005). PIN1 binds to the phosphorylated c-Fos to promote its transcriptional activity. Thus, PIN1 cooperatively regulates c-Jun and c-Fos to facilitate AP-1-dependent gene transcription upon phosphorylation by MAPK family members.

Introduction

PIN1 and ER- α

Estrogen receptor- α (ER- α) is a nuclear hormone receptor that is expressed in breast epithelial cells. Once activated by estrogen, ER- α can translocate to the nucleus and bind DNA to activate gene transcription. ER- α can also be activated via estrogen-independent signaling—for example, PI3K-dependent CDK2 activation can phosphorylate ER- α at S294, inducing an interaction between PIN1 and ER- α . PIN1 recognizes ERK-dependent phosphorylation of ER- α at S118 and S167 in the transcription activation domain, and promotes ER- α dimerization and transcriptional activity (Lannigan, 2003; Lucchetti et al., 2013). PIN1 can also bind and isomerize pS118-P119 motifs directly to stabilize ER- α by blocking ER- α interaction with E6AP, an ubiquitin E3 ligase that facilitates ER- α degradation. Importantly, ER- α expression level positively correlates with PIN1 in human breast carcinoma (Rajbhandari et al., 2012, 2014).

PIN1 and transcription factors associated with stem cells.

The ability to self-renew and the potential to develop and differentiate into various cell types are the unique and prominent characteristics of pluripotent stem cells. The balance of self-renewal and differentiation is fine-tuned by the activities of some key transcription factors. For example, a combination of MYC, Klf-4, Oct4, and Sox2 transcription factors can induce fibroblasts, a fully differentiated skin cell type, to become induced pluripotent stem (iPS) cells (Takahashi and

Introduction

Yamanaka, 2006). Further molecular characterization in murine embryonic stem cells revealed that Sox2, Oct4, and Nanog cooperate with each other to form a feed-forward circuit to maintain stem cell pluripotency (Kashyap et al., 2009; Young, 2011). Intriguingly, both Nanog and Oct4 are substrates of PIN1. PIN1 acts on Nanog phosphorylated at S52, S65, S71, and T287 –Pro motifs to stabilize it by suppressing its ubiquitylation-mediated degradation. Disruption of PIN1-Nanog interaction or inhibition of PIN1 suppresses the capability of embryonic stem cells to form teratomas in immune-deficient mice, an indicator of loss of pluripotency (Moretto-Zita et al., 2010). The importance of PIN1 in maintenance of pluripotency is also demonstrated by its regulation of phosphorylated Oct4. PIN1 interacts with the phosphorylated Ser12-Pro motif of Oct4 to increase its stability and transcriptional activity (Nishi et al., 2011). The reprogramming of iPS increases PIN1 expression, which in turn promotes the efficiency of iPS generation. Consistent with PIN1's role on Nanog and Oct4, inhibition of PIN1 activity significantly reduces the colony formation of human iPS cells and murine embryonic stem cells and induces aberrant differentiation (Nishi et al., 2011).

PIN1 and MYC

For each of the transcription factors discussed so far, PIN1 promotes transcriptional activity through upregulation of protein stability. However, this mechanism does not apply to PIN1 regulation of MYC. As discussed in the

Introduction

section of **Post-translational regulation of MYC**, upon receiving growth signals, MYC is phosphorylated by ERK or CDK or other MAPKs at the Ser62-Pro63 motif, which is likely to display in *trans* as the preferred conformation for MAPK and CDK to act upon (Wulf et al., 2005). PIN1 isomerizes pSer62-Pro63 from *trans* to *cis*, which facilitates the recruitment of MYC and its coactivators, including the histone acetyltransferases GCN5 and p300, to target gene promoters to activate their transcription. Notably, the MYC targets that PIN1 enhances are mainly MYC's transactivated targets, such as E2F2 and Nucleolin, whereas the genes repressed by MYC, such as p15 and p21, are not affected by PIN1 function (Farrell et al., 2013). PIN1 subsequently catalyzes pSer62-Pro63 from *cis* to *trans* following GSK-3 β -mediated phosphorylation at T58. This leads to PP2A-mediated dephosphorylation of pS62 and recognition of the remaining pT58 by Fbw7 for proteasome degradation (Arnold and Sears, 2008; Welcker et al., 2004; Yada et al., 2004). The tumor suppressor Axin1 functions as a scaffold protein to assemble the degradation complex for MYC, containing GSK-3 β , PIN1, and PP2A (Arnold et al., 2009; Zhang et al., 2012). The finding that the degradation complex together with Fbw7 and 19S proteasome can be found at the promoter supports the hypothesis that the proteasome associated with the gene promoter facilitates transcription initiation via removal of activated transcription factors (Durairaj and Kaiser, 2014; Farrell et al., 2013; Geng et al., 2012). Therefore, depending on whether MYC is singly phosphorylated at Ser62 or dually phosphorylated at both Ser62 and Thr58, PIN1 catalyzes MYC

Introduction

from *trans* to *cis* to increase its transcriptional activity or from *cis* to *trans* to promote its protein degradation (Figure 1.6).

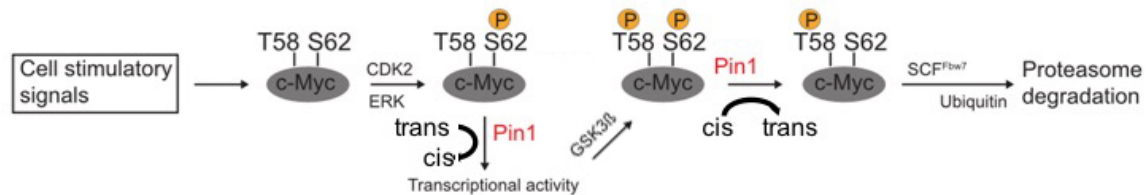


Figure 1.6: PIN1 mediated MYC isomerization depends on the phosphorylation status (modified from Helander et al., 2015).

What, then, accounts for the specificity of PIN1 regulation of MYC? Many biological functions of proteins are tightly associated with the cellular contexts or structures they are within. It has been noted for a long time that pS62 MYC is associated with the nuclear matrix or components of the nuclear periphery. A recent study has indicated an interaction between pS62 MYC and the lamina-associated structure (LAS), which leads to transcriptional activation. This study raises the question of whether PIN1 plays a role in the interaction as well. Moreover, what are the specific components within the LAS that pS62 MYC interacts with? To address these questions, in the next part of the introduction, I will review the current understanding of gene transcription-regulated nuclear compartmentalization, with a focus on the nuclear periphery.

Many facets of transcription at the nuclear periphery

The nucleus is a highly compartmentalized organelle within which gene positioning and chromatin organization in certain compartments both reflects and impacts transcriptional regulation and can change in response to developmental or physiological signals (Francastel et al., 2000; Fraser and Bickmore, 2007). Although transcriptional regulation in various nuclear compartments has drawn the attention of researchers, gene expression under the effect of radial positioning is the most-well understood (Lanctôt et al., 2007; Nguyen and Bosco, 2015), and will thus be the focus of this section. The term radial positioning describes a gene's position in relation to the center or the periphery (nuclear envelope) of the 3D nucleus (Takizawa et al., 2008).

Early observations on chromosome localization during interphase have revealed that organizations relative to one another or to certain nuclear structures such as the nuclear envelope are not random (Cremer and Cremer, 2010). The gene-rich chromosomes are more internally localized, whereas the gene-poor chromosomes are distributed nearer the nuclear periphery (Croft et al., 1999; Scheuermann et al., 2004). For instance, the gene-rich human chromosome 19 is more centrally localized than the gene-poor human chromosome 18 (Tanabe et al., 2002a, 2002b). One of the explanations for this is the association between the radial distribution of a gene and its transcriptional outcome. In general, the nuclear periphery (with the exception of the nuclear pore) is associated with gene

Introduction

repression, whereas the interior or the center of the nucleus is usually transcriptionally permissive (Capelson, 2010; Finlan, 2008; Wu and Yao, 2013). Intriguingly, in a study using inducible transgenes in human cells, transcriptional activation relocalized the transgene from the periphery to the interior of the nucleus. The repositioning of the gene between two nuclear compartments was required for the gene expression and was dependent on the functions of actin and myosin, two nuclear filament proteins that drive chromatin motion (Chuang, 2006). Taken together, these studies indicate that nuclear compartmentalization plays a functional role in gene expression.

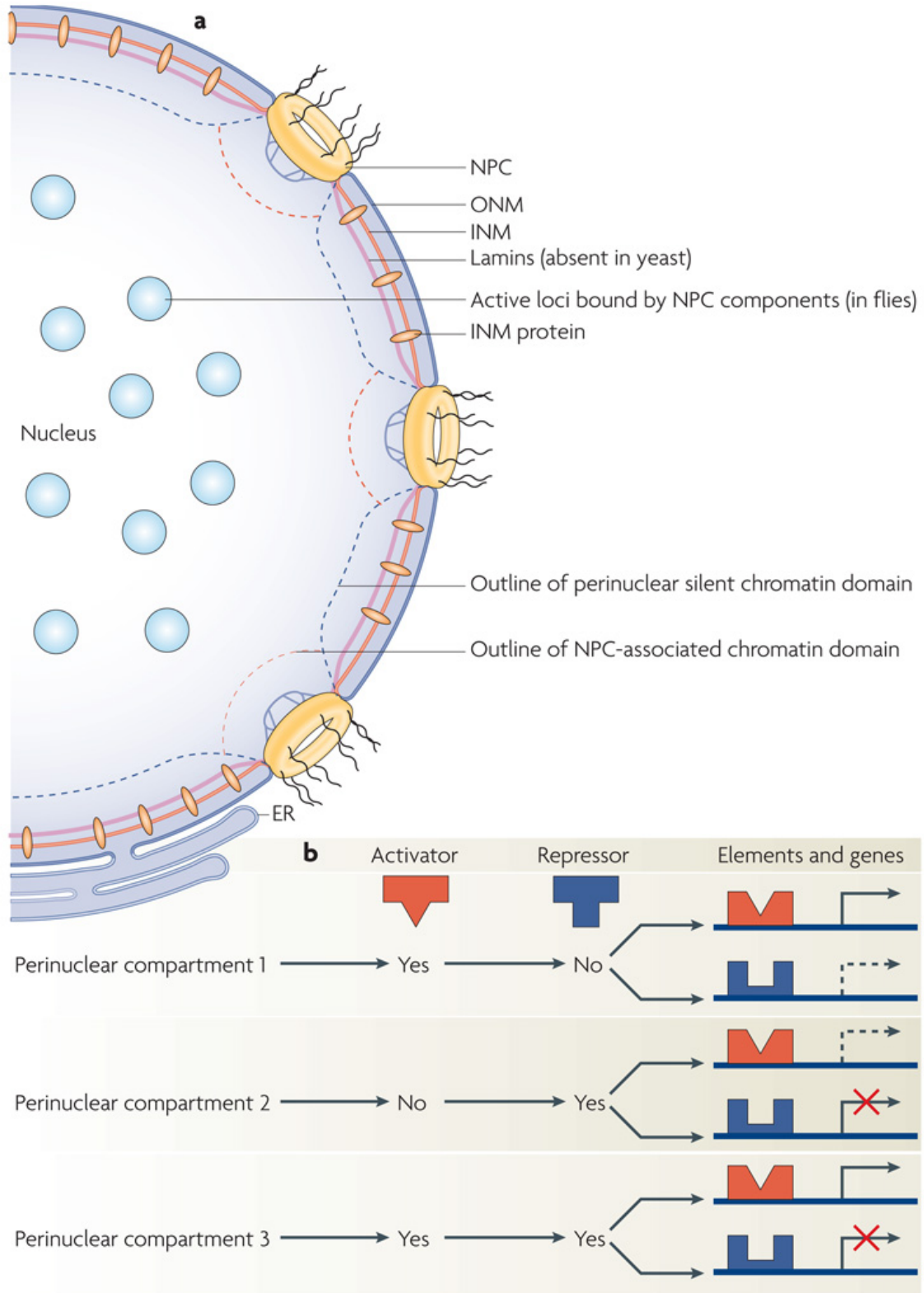
The lamina compartment

The nuclear periphery mainly consists of the inner nuclear membrane, lamina, and the nuclear pore complex that penetrates the nuclear envelope (Akhtar and Gasser, 2007; Hurtley, 2016). The repressive role that the periphery plays in gene transcription is mostly through the lamina compartment (Figure 1.5). The human nuclear lamina is closely attached to the inner membrane of the nuclear envelope, and is composed of three interfilaments: lamin A/C, lamin B1 and B2. Many studies have applied DNA adenine methyltransferases identification (or DamID, a technique to map DNA binding sites of a protein in eukaryotes, reviewed in (Aughey and Southall, 2016)) to examine the role of lamina in regulating the transcription of peripheral chromatin regions and related genes. Genes positioned at the nuclear lamina contain repressive histone markers, including methylated histones such as H3K27me3 and H3K9me2, and are

Introduction

associated with reduced RNA expression. For example, a genome-wide DamID screen in *Drosophila* identified about 500 genes that interact with the lamina, all of which are transcriptionally repressed. These genes are localized relatively close to each other into large chromosome domains termed lamin-associated domains (LADs), which are marked by high levels of repressive histone markers and lack of active histone markers. Many of the lamina-associated genes are developmentally co-regulated and are released upon activation during differentiation (Pickersgill, 2006). Consistently, using DamID in mouse ESCs, researchers found that the lamina-DNA interactions dramatically change during ESC differentiation and lineage commitment (Peric-Hupkes et al., 2010).

Introduction



Introduction

Figure 1.7: Nuclear periphery and gene expression (Mekhail and Moazed, 2010).

(a) An overview of nuclear peripheral compartments. The nuclear envelope consists of an outer nuclear membrane (ONM) and an inner nuclear membrane (INM), which are pierced with nuclear pore complexes (NPCs). In animal cells, filamentous proteins called lamins form a meshwork between the INM and chromatin, connecting nuclear pores to each other and maintaining the spherical geometry of the nucleus. INM proteins and lamins are frequently implicated in transcriptional gene silencing. Nuclear peripheral NPCs can be preferentially associated with active loci. At least in fly cells, nucleoplasmic NPC components are localized to active loci in the nuclear interior. The membrane of the endoplasmic reticulum (ER) is continuous with the ONM. (b) Although active or silent chromatin compartments exist at the nuclear periphery, the effect of gene targeting to a nuclear peripheral compartment depends on the presence or absence (yes or no, respectively) of transcriptional regulators (activators or repressors) at that compartment and the regulatory sequence elements controlling transcription at the targeted locus. Transcriptional effects related to the relocation of two genes to different nuclear peripheral compartments are shown. Scenarios with increased transcription (black arrows), decreased transcription (red X marks) or unaltered transcription (dashed arrows) are shown. Copy permission was obtained from *Nature Reviews Molecular Cell Biology*.

Dissociation of genes from the lamina does not automatically activate their transcription – genes dissociated from the lamina during the ESC transition to the neural progenitor cells remained dissociated but were activated later during differentiation to the astrocytes. This suggests that release of some differentiation-regulated genes render them into an intermediate state, where the genes are transcriptionally poised for rapid response to additional developmental clues (Peric-Hupkes et al., 2010). Additionally, artificially tethering transgenes or endogenous genes to the lamina tend to repress their transcription (Finlan, 2008; Reddy et al., 2008; Zullo et al., 2012). Interestingly, this silencing effect can also be spread to the neighboring genes, supporting the compartmentalization

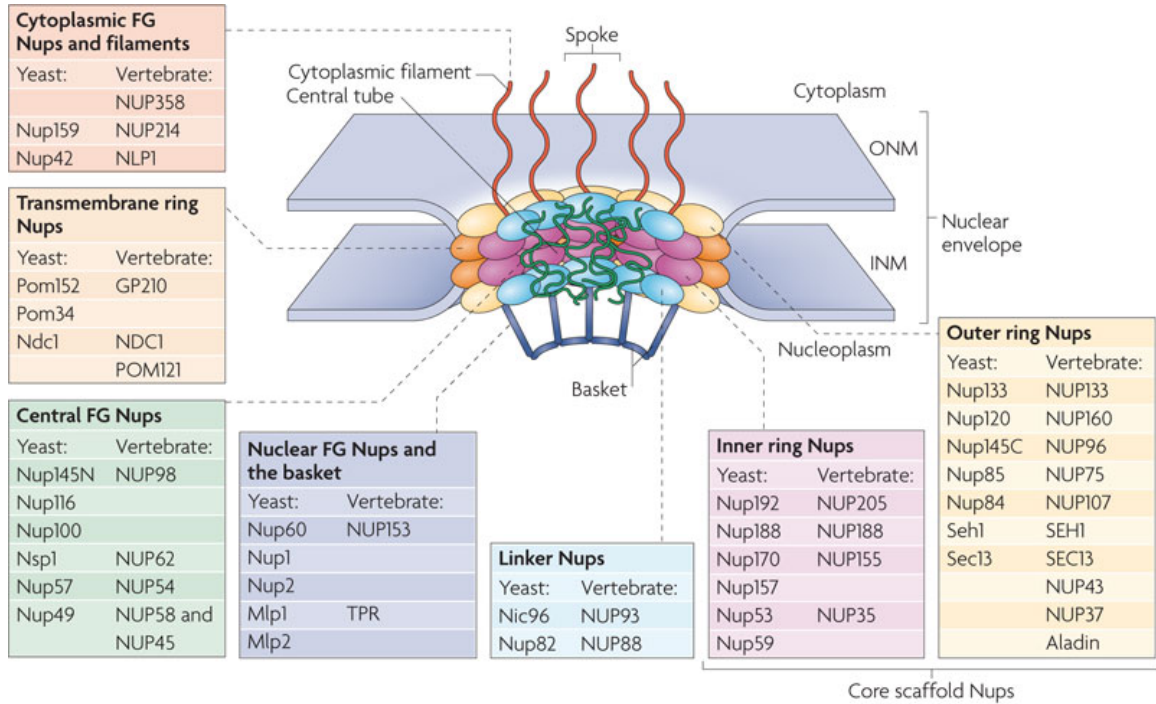
Introduction

function of the lamina (Finlan, 2008). The recruitment of LADs to the lamina involves binding of the transcription factor cKrox and the histone deacetylase HDAC3, as knockdown of either reduces lamina-DNA interactions (Zullo et al., 2012). All together, these experiments demonstrate the repressive functions of the lamina compartment on the genes positioned near it.

The nuclear pore compartment

The nuclear pore complex (NPC) is the assembly of large protein channels that span the nuclear envelope and is composed of multiple copies of 30 different proteins known as nucleoporins (Nups) (Figure 1.6). In addition to its essential role in regulating macromolecule transport between the nucleus and the cytoplasm, the NPC and Nups affect transcription, chromatin structure, and epigenetically inherited transcriptional memory (Ibarra and Hetzer, 2015).

Introduction



Nature Reviews | Molecular Cell Biology

Figure 1.8: Schematic of the nuclear pore complex (NPC) (Strambio-De-Castillia et al., 2010)

Each nuclear pore complex (NPC) is a cylindrical structure composed of eight spokes. The NPC is anchored to the nuclear envelope by a transmembrane ring structure that connects to the core scaffold and encompasses inner ring and outer ring elements. Linker nucleoporins (Nups) anchor the Phe-Gly (FG) Nups such that they line and fill the central tube. NPC-associated peripheral structures consist of cytoplasmic filaments, the basket and a distal ring. The Nups that are known to constitute each NPC substructure are listed, with yeast and vertebrate homologues indicated. GP210, glycoprotein 210; Mlp, myosin-like protein; Ndc1, nuclear division cycle protein 1; Nic96, Nup-interacting component of 76 kDa; NLP1, Nup-like protein 1; Pom, pore membrane protein; Seh1, SEC13 homologue 1; TPR, translocated promoter region. Copy permission was obtained from *Nature Reviews Molecular Cell Biology*.

In contrast to the repressive features of the LAD, genes interacting with the components of the nuclear pore complex tend to be transcriptionally active. A direct evidence comes from the electromicroscopic images of the nuclear

Introduction

periphery, where the NPC and adjacent nuclear areas are exclusive of the dark condensed chromatin that are associated with the nuclear lamina (Belmont et al., 1993; Schermelleh et al., 2008). This feature is mediated by the function of the basket porin TPR, as depletion of TPR—while not inhibiting pore formation—extends the dense chromatin area to the NPC (Krull et al., 2010). Consistent with this, Nup genomic interaction studies in multiple species have revealed that the Nups associate with many highly expressed genes, suggesting an evolutionarily conserved role for Nups in transcription. In yeast, highly expressed genes involved in glycolysis and ribosomal biogenesis constitutively interact with the yeast homologues of TPR, Mlp1 and Mlp2 (Casolari et al., 2004, 2005). Genes also interact with the NPC conditionally upon the induction of environmental stimuli, such as nutrients shifts, heat shock, and mating pheromone treatment (Brickner and Walter, 2004; Cabal, 2006; Casolari et al., 2005; Dieppois et al., 2006; Taddei, 2006).

Although NPC-DNA interactions primarily occur at the nuclear periphery in yeast, some the Nups also interact with genome in the nucleoplasm in higher eukaryotes. For example, in *Drosophila*, the nucleoplasmic Nup50 binds to developmental or heat shock-induced puffs in the larval salivary glands (Kalverda et al., 2010); the nucleoplasmic Nup98 preferentially binds to the genes involved in embryonic development (Kalverda et al., 2010). In contrast, in humans, Nup98 acts on genes involved in the differentiation of embryonic stem cells to the neurons (Liang et al., 2013), suggesting that the functions of Nups are highly

Introduction

dependent on cellular and developmental context. Nonetheless, in both *Drosophila* and human embryonic stem cells, Nup98 binds both strongly and weakly expressed genes that are correlated with different positions within the nucleus: strongly expressed genes are correlated with nucleoplasmic Nup98 binding, whereas weakly expressed genes tend to be bound by NPC-associated Nup98 (NPC-Nup98) at the nuclear periphery (Kalverda et al., 2010; Liang et al., 2013). These weakly expressed chromosomal regions are, however, different from the completely silenced heterochromatic LADs (Kalverda et al., 2010). In fact, many of the developmentally regulated genes associate with the NPC-Nup98 when initially induced in neural progenitor cells, dissociate with the NPC-Nup98 upon stronger induction during differentiation to neurons (Liang et al., 2013). These observations emphasize the dynamic feature of the NPC-genome interactions.

There are several protein factors important for genes interacting with the NPC, including the histone acetyltransferase Spt-Ada-Gcn5-Acetyl (SAGA) complex and the mRNA export factor Sac3, the functions of which are distinct from their traditional roles (Cabal, 2006; Luthra et al., 2007; Rodríguez-Navarro et al., 2004). In yeast, depletion of Ada2, a component of SAGA, or Sac3, or Sus1 (a component shared by the SAGA and Sac3 complexes), dissociates *Gal1* gene with the NPC (Luthra et al., 2007; Rodríguez-Navarro et al., 2004). Similarly in *Drosophila*, knockdown of the homologues of these factors, *E(y)2* and *Xmas-2*,

Introduction

decreases the contacts of the heat shock protein 70 (Hsp70) gene loci from the nuclear envelope (Kurshakova et al., 2007).

The critical role mRNA export factors play in targeting genes to the NPC supports the “Gene Gating” hypothesis, by which actively transcribed genes are brought to the NPC so that the nascent transcripts can interact with the export factors more efficiently (Blobel, 1985). However, some studies suggest that the NPC association does not require gene activation, but rather is determined by cis-regulatory DNA elements. For instance, deleting *Gal2*'s Open Reading Frame (ORF), which transcribes mRNA, does not affect its interaction with the NPC (Dieppois et al., 2006). This is also illustrated by recruitments of the *INO1* gene to the NPC, which is independent of its transcription, but also dependent on two promoter DNA elements upstream of the gene, termed Gene Recruitment Sequences (GRS). Disruption of the two elements dissociates *INO1* from the NPC and localizes it to the nucleoplasm (Ahmed, 2010). Further, *HSP140* possesses a different GRS on its promoter as well (Brickner et al., 2012). Thus, these GRSs function as so-called “DNA Zip codes” to localize genes to the NPC (Ahmed, 2010; Brickner et al., 2012). However, while all the GRSs have been identified in yeast so far, the “zip codes” for DNA-NPC interactions in higher eukaryotes are much less well defined.

Introduction

The interaction of chromatin with Nups tends to promote transcription. In yeast, studies have shown that proper activation of some genes require interaction with the NPC. Specifically, mutating GRS reduces the expression of *INO1* and *TSA2* through disruption of their interactions with the NPC; tethering *INO1* and *HXK1* to the nuclear periphery (yeast does not have the lamina compartment) enhances their expression (Ahmed, 2010; Taddei, 2006). Additionally, tethering the transcription factor Rap1 and its co-factors to the Nup84 subcomplex components stimulates the expression of Rap1 target genes (Morse, 2000).

Nups also promote the expression of certain genes in metazoans, although these effects may not necessarily occur at the nuclear pore. In *Drosophila*, the pore basket subunits Nup153 and MTOR (*Drosophila* homologue of TPR) bind to about 25% of all the genes, the expression of which are reduced upon knockdown of either Nup (Vaquerizas, 2010). Both of these Nups are also required for the hypertranscription of the male X chromosome as a mechanism for *Drosophila* dosage compensation (Mendjan et al., 2006). In the *Drosophila* larva salivary glands, binding of nucleoplasmic Sec13 and Nup98 to the developmentally induced puffs recruit RNA pol II to the puffs to drive associated gene expression (Kalverda et al., 2010).

In humans, as mentioned before, Nup98 binds to developmentally regulated genes during embryonic stem cell differentiation. This binding seems to promote

Introduction

gene expression, since overexpression of wild-type Nup98 increases the expression of the bound genes while expression of a dominant negative Nup98 reduces the expression of a subset of them (Liang et al., 2013). The role of Nup98 in gene transcription is also supported by certain acute myeloid leukemia studies of chromosomal translocation fusing Nup98 to the DNA binding domain of the transcription factor HOXA9 (Kasper et al., 1999). The fusion protein transformed cells through aberrant activation of target genes. The mechanism underlying Nup98-mediated activation involves recruitment of the histone acetyltransferase CBP/p300, which helps to decondense local chromatin (Kasper et al., 1999). All together, these studies indicate a conserved role of certain components of the NPC in transcription activation.

Since the nuclear periphery contains multiple components that can lead to distinct outcomes on transcription regulation – the lamina-associated compartment generally represses transcription while the NPC associated compartment tends to activate transcription – it is necessary to examine in detail which nuclear peripheral component the pS62 MYC is associated with (Myant et al., 2015). There are more questions that need to be addressed mechanistically: what are the regulators of MYC localization to the nuclear periphery? How is MYC's nuclear localization related to its post-translational regulation? Finally, what are the functional consequences? These questions drove our study in Chapter 3.

Chapter Two :

Pre-Anchoring of PIN1 to Unphosphorylated MYC in a Fuzzy Complex Regulates MYC Activity

Pre-Anchoring of Pin1 to Unphosphorylated c-Myc in a Fuzzy Complex Regulates c-Myc Activity^{a,b,c}

Sara Helander,^{1,5,7} Meri Montecchio,^{1,5} Robert Pilstål,^{2,5} Yulong Su,^{3,5} Jacob Kuruvilla,⁴ Malin Elvén,^{1,6} Javed M.E. Ziauddin,¹ Madhanagopal Anandapadamanaban,¹ Susana Cristobal,⁴ Patrik Lundström,¹ Rosalie C. Sears,³ Björn Wallner,² and Maria Sunnerhagen^{1,*}

¹Division of Chemistry, Department of Physics, Chemistry and Biology, Linköping University, 58183 Linköping, Sweden

²Division of Bioinformatics, Department of Physics, Chemistry and Biology, Linköping University, 58183 Linköping, Sweden

³Department of Molecular and Medical Genetics, Oregon Health and Science University, Portland, OR 92739, USA

⁴Department of Clinical and Experimental Medicine, Cell Biology, Faculty of Health Science Linköping University, 58183 Linköping, Sweden

⁵Co-first author

⁶Present address: Department of Clinical Sciences, Dermatology and Venereology, Lund University, 22184 Lund, Sweden

⁷Present address: Division of Drug Research, Department of Medical and Health Sciences, Linköping University, SE-581 85 Linköping, Sweden

*Correspondence: maria.sunnerhagen@liu.se

a. Published in **Structure**. 2015 Dec 1;23(12):2267-79. © 2015 Elsevier Ltd.

b. Due to historical reasons of nomenclature, in this paper c-Myc refers to MYC; Pin1 refers to PIN1.

c. I designed, performed, and analyzed the cell biology experiments for the paper with the help of Drs Sears and Sunnerhagen.

Pre-Anchoring of PIN1 to Unphosphorylated MYC in a Fuzzy Complex Regulates MYC activity

Abstract:

Hierarchical phosphorylation and concomitant Pin1-mediated proline isomerization of the oncoprotein c-Myc controls its cellular stability and activity. However, the molecular basis for Pin1 recognition and catalysis of c-Myc and other multisite, disordered substrates in cell regulation and disease is unclear. By nuclear magnetic resonance, surface plasmon resonance, and molecular modeling, we show that Pin1 subdomains jointly pre-anchor unphosphorylated c-Myc1–88 in the Pin1 interdomain cleft in a disordered, or “fuzzy”, complex at the herein named Myc Box 0 (MB0) conserved region N-terminal to the highly conserved Myc Box I (MBI). Ser62 phosphorylation in MBI intensifies previously transient MBI-Pin1 interactions in c-Myc1–88 binding, and increasingly engages Pin1 PPIase and its catalytic region with maintained MB0 interactions. In cellular assays, MB0 mutated c-Myc shows decreased Pin1 interaction, increased protein half-life, but lowered rates of Myc-driven transcription and cell proliferation. We propose that dynamic Pin1 recognition of MB0 contributes to the regulation of c-Myc activity in cells.

Introduction:

Among the most fundamental processes in cell biology is the regulation of the cell cycle and, thereby, cell growth. A key player in this process is the peptidyl-prolyl isomerase Pin1 that has been shown to function as a molecular timer by acting as a switch of various cell-signaling processes (Liou et al., 2011; Lu and Zhou, 2007). One of the targets of Pin1 is the proto-oncogenic transcription factor c-Myc, which is a universal regulator of cell growth, apoptosis, and proliferation in both normal and tumor cells (Lin et al., 2012b; Meyer and Penn, 2008; Nie et al., 2012). While the pro-proliferative properties of c-Myc are activated by phosphorylation of Ser62, its cellular stability and degradation are controlled by subsequent phosphorylation at Thr58, both sites being located in the conserved Myc Box I (MBI) region of its N-terminal transcriptional activation domain (TAD) (Hann, 2006). The time window of phosphorylation and dephosphorylation at these two sites is affected by Pin1-mediated *cis-trans* isomerization of the Ser62-Pro motif, thereby regulating specific interactions of c-Myc with modifying kinases, predominantly acting on trans substrates (Brown et al., 1999; Lu et al., 2002a) and phosphatases, which control the pathway of c-Myc activation and ubiquitin-mediated degradation (Figure 2.1A) (Farrell and Sears, 2014; Sears, 2004), and which have been shown to act on cis substrates (Werner-Allen et al., 2011). Pin1 also facilitates the dynamic binding of c-Myc to target gene promoters, enhancing association with transcriptional co-activators and transcriptional activation of target genes, thus potentiating c-Myc's oncogenic

Pre-Anchoring of PIN1 to Unphosphorylated MYC in a Fuzzy Complex Regulates MYC activity

activity (Farrell et al., 2013). The importance of regulatory coupling c-Myc activation with its subsequent degradation in maintaining normal cell growth is evidenced by cancer-associated mutations at or near Thr58 and Ser62 that result in maintaining c-Myc in its activated, Ser62-phosphorylated state (Bahram et al., 2000; Wang et al., 2011b), and many regulators of c-Myc that bind to this region are themselves either oncogenes or tumor suppressors (Tu et al., 2015). Although Pin1 promotes c-Myc degradation in normal cells, this activity is uncoupled in cancer cells where both proteins have oncogenic activities and are overexpressed, and Pin1 functions only as a c-Myc co-activator (Farrell et al., 2013). Potential uncoupling mechanisms involve reduced Axin1 function, which scaffolds c-Myc degradation (Arnold et al., 2009; Zhang et al., 2012) and Pin1's downregulation of Fbw7, an E3 ligase controlling degradation of a number of oncoproteins including c-Myc (Min et al., 2012).

Pin1 comprises two independently folded subdomains: Pin1 WW (residues 6–39) and Pin1 PPLase (residues 50–163), connected by a flexible linker (Bayer et al., 2003; Jacobs et al., 2003; Ranganathan et al., 1997). The catalytic proline isomerization activity toward pSer/pThr-Pro motifs entirely resides in Pin1 PPLase (Lu et al., 1999; Ranganathan et al., 1997). The Pin1 PPLase alone binds weakly to native, phosphorylated peptide targets ($K_D > 390 \mu\text{M}$) (De et al., 2012; Verdecia et al., 2000), with significant affinities (K_d range 0.5–90 μM) observed only for peptides selected from library screens (Duncan et al., 2011; Namanja et

Pre-Anchoring of PIN1 to Unphosphorylated MYC in a Fuzzy Complex Regulates MYC activity

al., 2011; Verdecia et al., 2000) or designed inhibitors (Namanja et al., 2011; Zhang et al., 2012). Pin1 WW binds pSer/ pThr-Pro-containing peptides with variable affinities ($K_d > 7 \mu\text{M}$) (Lu et al., 1999; Verdecia et al., 2000), preferably in the extended, trans conformation (De et al., 2012; Namanja et al., 2011; Verdecia et al., 2000; Wintjens et al., 2001). In intact Pin1, the two domains create an interdomain cleft, distant from the Pin1 PPlaseactive site, where phosphorylated target peptides (K_d 5–80 μM) (Verdecia et al., 2000) as well as buffer components such as polyethylene glycol (PEG) bind in well-defined conformations (reviewed in Matena et al., 2013). Pin1 WW binding at phosphorylated pSer/pThr-Pro sites has been proposed to increase the local effective concentration of substrate and activity on neighboring phosphorylated sites (Jacobs et al., 2003; Lu et al., 1999) to facilitate substrate transfer (De et al., 2012; Lu et al., 1999; Wintjens et al., 2001), and/or to sequester trans conformations away from the active site, thereby providing directionality to the cis-trans conversion (De et al., 2012; Lu et al., 1999; Wintjens et al., 2001). Still, the functional reason for binding of targeted peptides to an interdomain cleft distant from the Pin1 active site remains unresolved.

Recent studies suggest that collaborative and possibly allosteric mechanisms jointly involve both Pin1 domains in target binding (reviewed in Peng, 2015). Binding of shorter peptide substrates and small molecules to Pin1 has been shown to affect interdomain mobility and linker dynamics (Jacobs et al., 2003),

Pre-Anchoring of PIN1 to Unphosphorylated MYC in a Fuzzy Complex Regulates MYC activity

and increased affinity and isomerization of phosphorylated peptides binding to Pin1 PPlase has been shown in the presence of PEG-induced transient domain interactions (Matena et al., 2013). Interactions between the two domains have been shown to allosterically affect the isomerization activity by an internal dynamic circuit through the Pin1 PPlase interior (Namanja et al., 2011), as well as through residues in the domain interface (Wilson et al., 2013), both recently supported by molecular simulations (Guo et al., 2015). However, to understand how the dual-domain protein Pin1 acts on its longer, multiply phosphorylated, and often intrinsically disordered substrates (Lu and Zhou, 2007), the interaction with such substrates needs to be studied in structural and dynamic detail, but as yet such studies have not been achieved.

We recently characterized the structural and dynamic properties of the most N-terminal part of the c-Myc TAD domain (c-Myc1–88), by nuclear magnetic resonance (NMR) and surface plasmon resonance (SPR), detailing also its dynamic and multivalent interactions with the tumor suppressor Bin1 (Andresen et al., 2012). We found that c-Myc1–88 contains two transiently ordered regions: the well-characterized MBI region and a less studied, more N-terminal region conserved in c-, N-, and L-Myc (Cowling and Cole, 2006; Legouy et al., 1987) (Figures 2.1B and 2.1C). While MBI is a well-known c-Myc interaction site, and comprises the phosphorylation sites directing c-Myc stability (Meyer and Penn,

Pre-Anchoring of PIN1 to Unphosphorylated MYC in a Fuzzy Complex Regulates MYC activity

2008), so far no clear functional role has been attributed to the transiently ordered region N-terminal to MBI.

Here, we show for the first time how a longer Pin1 substrate, c-Myc1–88, interacts with both domains of Pin1, and how this interaction is affected by phosphorylation. By SPR, NMR, and cellular assays, we show that the transiently ordered, unphosphorylated c-Myc region comprising c-Myc residues 13–32, which we henceforth refer to as “Myc Box 0” (MB0; Figures 2.1B and 2.1C), serves as a dynamic anchoring site for Pin1 on c-Myc1–88, both in the absence and presence of Ser62 phosphorylation. Molecular simulations, restricted by experimental data, show how Pin1 WW and PPlase domains jointly bind the MB0 region in a dynamic complex, thus facilitating MBI interaction with the Pin1 active site. Our results suggest that Pin1 binding to MB0 affects the cellular activity window of the c-Myc oncoprotein.

Results:

Intrinsic Disorder Is Retained in pSer62-c-Myc1–88

To study the Ser62 phosphorylated state of c-Myc, we performed phosphorylation of c-Myc1–88 in vitro with active CDK2 kinase in complex with Cyclin A2, which is known to phosphorylate Ser62-Pro63 in vivo (Hydbring et al., 2010) and in *trans* (Brown et al., 1999). Specific and near-complete pSer62-c-Myc₁₋₈₈ phosphorylation was confirmed by mass spectrometry and NMR, in agreement with the extended properties of the MBI region (Andresen et al., 2012). Chemical-shift perturbations (CSPs) were confined to the well-conserved MBI region (Figures 2.1D and 2.1E). The transverse relaxation rates for c-Myc1–88 are concentration dependent, which agrees with monomer exchange with a small amount of higher molecular weight oligomer not observed by sample inspection or in gel-filtration experiments (Andresen et al., 2012). However, the overall decreased R2 relaxation rates for pSer62-c-Myc1–88 compared with c-Myc1–88 at the same concentration suggest that the additional negative charge introduced by phosphorylation reduces internal interactions. Both ¹⁵N-R1 and {¹H}-¹⁵N-nuclear Overhauser effect (NOE) relaxation of pSer62-c-Myc1–88 correspond well to results obtained for c-Myc1–88 at similar concentrations, suggesting that the intrinsic disorder with transiently structured regions identified for c-Myc1–88 (Andresen et al., 2012) is maintained upon Ser62 phosphorylation.

Pre-Anchoring of PIN1 to Unphosphorylated MYC in a Fuzzy Complex Regulates MYC activity

We used SPR to investigate the binding of Pin1 and its subdomains to c-Myc1–88 and pSer62-c-Myc1–88 (Figures 2.2). Since Pin1 is believed to primarily bind at phosphorylated protein sites (Liou et al., 2011; Lu and Zhou, 2007), we were surprised to find that intact Pin1 binds c-Myc1–88 with an apparent KD of 4 μ M. This Pin1 binding affinity is of similar or higher affinity as previously observed Pin1 binding to phosphorylated peptides, but several orders of magnitude higher than for unphosphorylated Ser/Thr-Pro motifs (Verdecia et al., 2000). Lack of significant Pin1 binding to c-Myc46–69 indicated that the primary binding site for Pin1 to c-Myc1–88 is located distant from the Ser62-Pro motif. Both Pin1 WW and Pin1 PPIase subdomains were consistently found to bind c-Myc1–88 with more than 10-fold weaker affinities compared with intact Pin1 (Figures 2.2B and 2.2C), suggesting both Pin1 subdomains jointly contribute to the higher c-Myc1–88 affinity of the intact protein. SPR measurements of Pin1 affinities to pSer62-c-Myc1–88 showed difficulties in reaching saturation and anomalous binding effects at higher concentrations, which limited the accuracy (Figures 2.2D–2.2F). Notably, however, the phosphorylated substrate may bind the active Pin1 enzyme in several modes with different affinities, due to cis-trans isomerization of pSer62-Pro (De et al., 2012; Jacobs et al., 2003; Namanja et al., 2011). In agreement with this, isothermal titration calorimetry measurements indicate multiple binding events for intact Pin1 binding to pSer62-cMyc1–88, with Kds ranging from 10 to 100 μ M, i.e. in the same range as measured for other phosphorylated peptides (Verdecia et al., 2000). The higher

Pre-Anchoring of PIN1 to Unphosphorylated MYC in a Fuzzy Complex Regulates MYC activity

pSer62-c-Myc1–88 apparent affinities for intact Pin1 compared with its subdomains alone indicate joint subdomain binding contributions also for phosphorylated c-Myc1–88. Finally, while full kinetic analysis was not feasible due to the rapid on- and off-rates in binding, we consistently observed elevated off-rates by visual inspection for Pin1 PPIase binding to pSer62-c-Myc1–88 compared with unphosphorylated c-Myc1–88 (Figures 2.2C and 2.2F), in agreement with increased isomerization turnover of phosphorylated substrates.

Pre-Anchoring of PIN1 to Unphosphorylated MYC in a Fuzzy Complex Regulates MYC activity

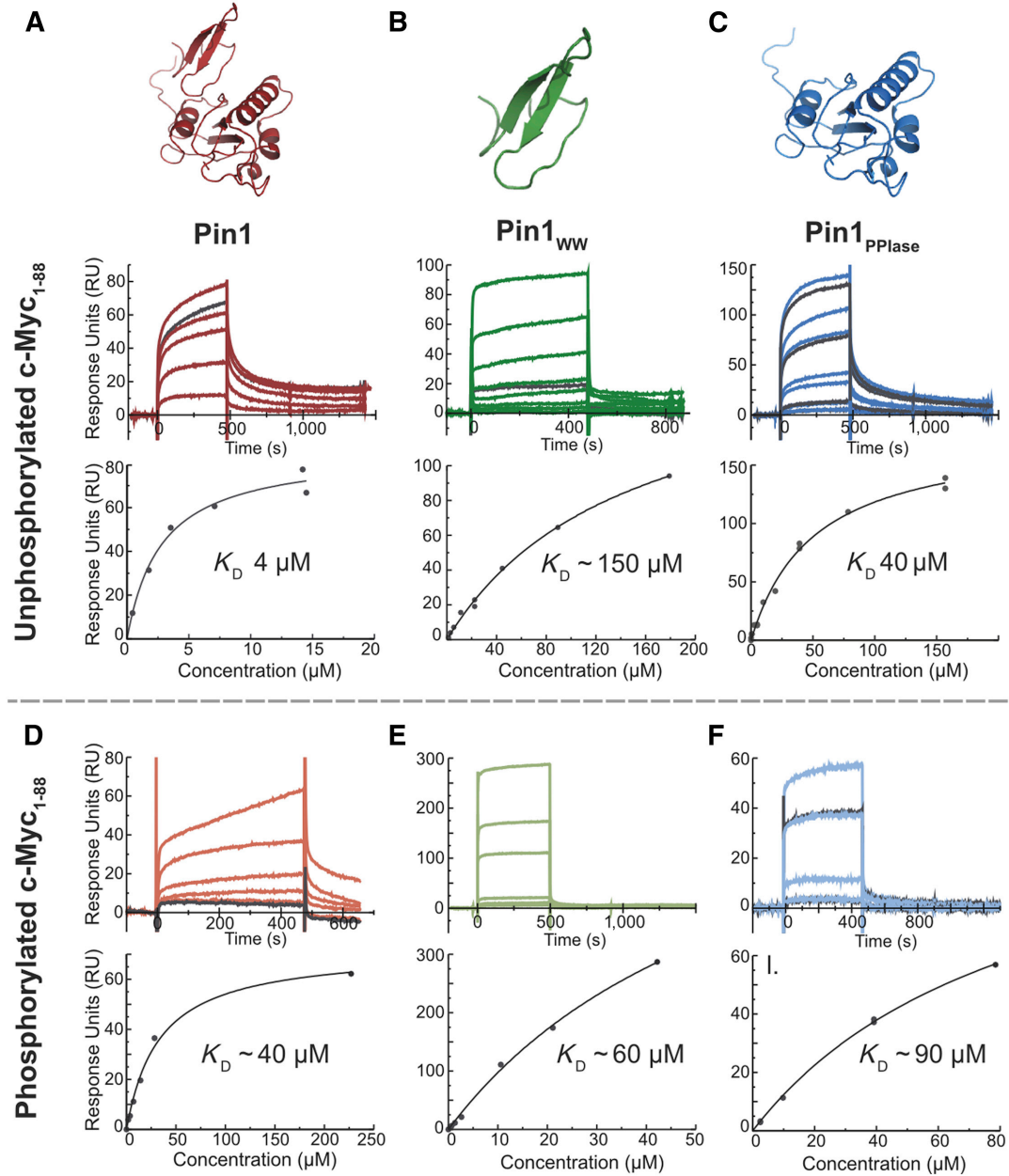


Figure 2.2: Evaluation of c-Myc1–88-Pin1 Affinities by Surface Plasmon Resonance.

Sensorgrams and 1:1 Langmuir fits from steady-state evaluation show binding of Pin1 (red), Pin1 WW (green), and Pin1 PPlase (blue) to both unphosphorylated (A–C) and phosphorylated c-Myc1–88 (D–F). For all measurements c-Myc1–88 were immobilized and Pin1, Pin1 WW, or Pin1 PPlase were injected over the surface.

Pre-Anchoring of PIN1 to Unphosphorylated MYC in a Fuzzy Complex Regulates MYC activity

Pin1 Binds c-Myc1–88 in a Dynamic Complex Anchored at the MB0 Region

By NMR, we further investigated c-Myc-Pin1 interactions on a per-residue level by titrating ^{15}N -labeled c-Myc1–88 and pSer62-c-Myc1–88 with unlabeled Pin1. We found that while for specific c-Myc residues resonance intensities were significantly reduced and not recovered on saturating the binding equilibrium (Figure 2.3), CSPs were very small or nonexistent. While peak intensities in general are lowered upon interaction due to slower molecular tumbling in the complex state, further line broadening leading to reduced intensities can occur as a result of chemical exchange between bound and free states, and/or due to chemical exchange between multiply bound states (Bozoky et al., 2013a, 2013b; Lukhele et al., 2013; Mittag et al., 2008). In the latter case, the signal is not recovered in the bound state due to continued chemical exchange (Bozoky et al., 2013b), which is in agreement with our observations for Pin1/ c-Myc1–88 complexes. Furthermore, we detected no ^{15}N Carr-Purcell-Meiboom-Gill dispersions, showing that line broadening due to chemical exchange occurs on a faster timescale than can be probed by these experiments. These observations are in agreement with the formation of dynamically disordered (Forman-Kay and Mittag, 2013), or “fuzzy” (Fuxreiter and Tompa, 2012), complexes.

Since c-Myc1–88 exhibits low chemical-shift dispersion (Andresen et al., 2012) and very minor CSPs in the bound state, HNC0 intensity ratios (Mittag et al., 2008) were primarily used to characterize the interaction of c-Myc1–88 to intact

Pre-Anchoring of PIN1 to Unphosphorylated MYC in a Fuzzy Complex Regulates MYC activity

Pin1 and its subdomains (Figure 2.3). Binding of intact Pin1 to non-phosphorylated c-Myc1–88 results in major loss of signal intensity primarily in the conserved, transiently ordered MB0 region, but also affects the MBI region (Figures 2.3A and 2.3D). Intact Pin1 binding to pSer62-c-Myc1–88 more clearly affects the phosphorylation site and flanking residues, and perturbations extend into the transiently helical and conserved MBI region around c-Myc1–88-Trp50, while the C-terminal part remains comparatively unperturbed (Figure 2.3D). Binding of either Pin1 WW or Pin1 PPlase resulted in drastically lowered HNCO intensity ratios in the MB0 region of c-Myc1–88, suggesting that both Pin1 subdomains target this region (Figures 2.3B and 2.3C). Pin1 WW primarily affects c-Myc residues 16-YDSVQPYFY-23 (Figure 2.3B), while Pin1 PPlase affects the aromatic residues in the 20-PYFY-23 motif as well as conserved residues 29-ENFY-32 slightly C-terminal to the Pin1 WW binding motif (Figure 2.3C). The proline-aromatic 20-PYFY-23 pattern affected by both Pin1 subdomains is also found in Pin1 binding peptides selected from library screens, both in forward (CTGIPWLYC; Duncan et al., 2011) and reverse sequence orientation (Peptide: WFYpSPFLE; Lu et al., 1999; Verdecia et al., 2000).

On phosphorylation, the binding pattern of Pin1 subdomains to pSer62-c-Myc1–88 alters significantly (Figures 2.3E and 2.3F). While interactions to MB0 are maintained, both Pin1 WW and Pin1 PPlase binding now also leads to severely reduced HNCO peak intensity ratios at c-Myc1–88-pSer62 and adjacent residues

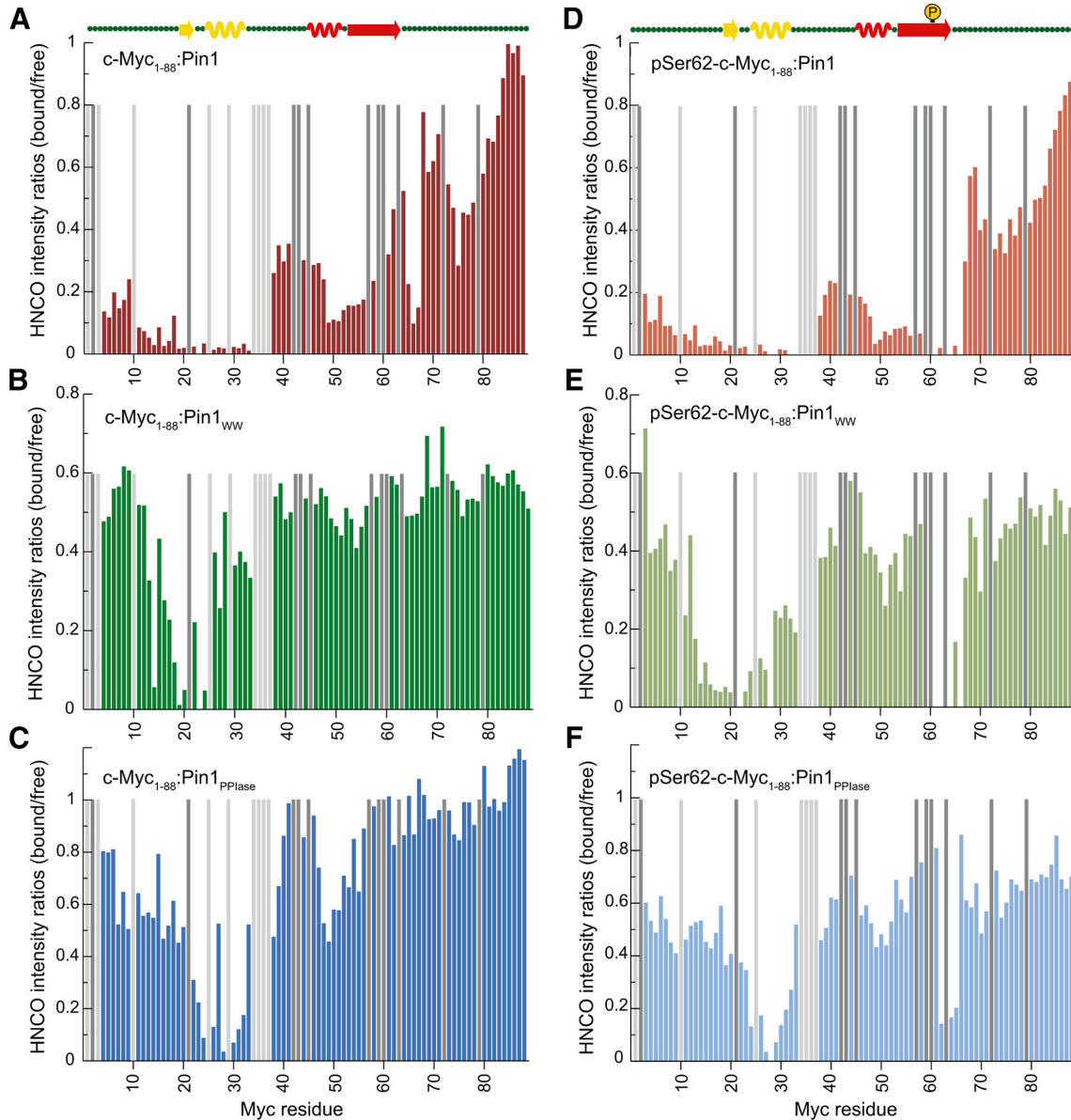
Pre-Anchoring of PIN1 to Unphosphorylated MYC in a Fuzzy Complex Regulates MYC activity

(Figures 2.3E and 2.3F). Furthermore, binding of both c-Myc1–88 and pSer62-c-Myc1–88 to Pin1 results in more extensive effects than would be predicted from Pin1 subdomain binding alone (Figures 2.3A and 2.3D). This suggests that both Pin1 domains jointly bind c-Myc, which agrees with the increased affinity for intact Pin1 compared with its subdomains as observed by SPR (Figure 2.2). Furthermore, the NMR results suggest that the conserved, transiently structured MB0 region in c-Myc1–88 is central for Pin1 interactions with c-Myc1–88 irrespective of the phosphorylation state of Ser62.

To further investigate c-Myc1–88 dynamics upon Pin1 binding, we evaluated ^{15}N -R1, ^{15}N -R1 ρ , and $\{^1\text{H}\}$ - ^{15}N -NOE relaxation experiments for the saturable unphosphorylated c-Myc1–88-Pin1 complex. Although excessive line broadening in the MB0 region limited the evaluation, the residues that showed sufficient signal intensity for analysis had ^{15}N -R1 relaxation rates similar to those of free c-Myc1–88, indicating retained mobility of flanking regions (Figure 2.4A). With retained R1 rates, the c-Myc1-88: Pin1 complex displays higher ^{15}N -R2 relaxation rates compared with free c-Myc1–88, (Figure 2.4B), suggesting transient interactions between Pin1 and regions flanking the MB0 anchor site in agreement with decreased HNCO intensity ratios in the same regions (Figure 2.3). NOE relaxation rates in the c-Myc1–88-Pin1 complex are similar to those in free c-Myc1–88 and correspond well to earlier characterized transient secondary elements (Andresen et al., 2012), suggesting that c-Myc1–88 transient structure

Pre-Anchoring of PIN1 to Unphosphorylated MYC in a Fuzzy Complex Regulates MYC activity

is retained upon Pin1 binding (Figure 2.4C). Taken together, NMR relaxation measurements show retained intrinsic disorder in c-Myc1–88 when binding Pin1, signifying a fuzzy complex (Fuxreiter and Tompa, 2012).



Pre-Anchoring of PIN1 to Unphosphorylated MYC in a Fuzzy Complex Regulates MYC activity

Figure 2.3: NMR Analysis of c-Myc1–88 Per-Residue Interactions with Pin1 and Its Subdomains.

HNCO peak intensity ratios between Pin1-bound and free states were derived for c-Myc1–88 when unphosphorylated (A–C) or Ser62-phosphorylated (D–F) at a c-Myc1–88/Pin1, c-Myc1–88/Pin1WW, or c-Myc1–88/Pin1PPlase ratio of 1:2, with estimated saturation levels ranging from 58% to 96% (see Methods). Prolines (dark gray; give no signal in HNCO) and residues lacking data due to missing assignment or overlap (light gray) are represented by solid histogram bars. Binding to Pin1 (A and D), Pin1 WW (B and E), and Pin1 PPlase (C and F) is color-coded as in Figure 2.2. Gain/loss of interactions in the bound state leads to decreased/increased peak intensity ratios, respectively. Graphical representations (curl and arrow, respectively) indicate the location of previously identified transient secondary structure (Andresen et al., 2012). The phosphorylation site at S62 is indicated with encircled P.

Pre-Anchoring of PIN1 to Unphosphorylated MYC in a Fuzzy Complex Regulates MYC activity

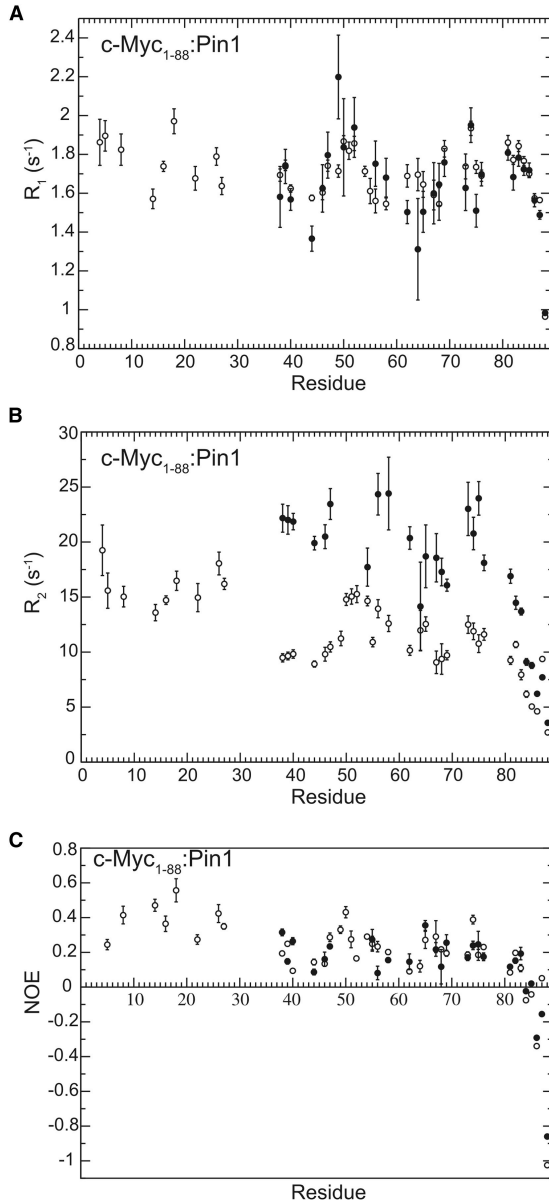


Figure 2.4: NMR Relaxation Analysis of c-Myc1–88 Binding to Pin1.

Relaxation parameters of apo c-Myc1–88 (open circles) and c-Myc1–88 (filled circles) in the presence of 2 mol equivalents of Pin1 (98% saturation). Uncertainties in R1 and R2 were estimated using the jackknife method, and in the heteronuclear NOE as the standard deviation of all permutations of peak ratios in duplicate experiments (Ahlner et al., 2013). (A) R1 relaxation rates. (B) R2 relaxation rates. (C) {¹H}-¹⁵N-NOE.

Pre-Anchoring of PIN1 to Unphosphorylated MYC in a Fuzzy Complex Regulates MYC activity

Pin1 Recognition Pattern Is Altered by Myc1–88 Phosphorylation

To obtain more detailed molecular insight on the extent of Pin1 that interacts with c-Myc, we mapped spectral changes in ^{15}N , ^{13}C -labeled Pin1 on addition of unlabeled c-Myc1–88 and pSer62-c-Myc1–88 by NMR. For both unphosphorylated and phosphorylated c-Myc, small but significant CSPs were observed (Figures 2.5). While CSPs only suggest that the chemical environment around the concerned backbone NH groups has changed, the most likely reasons are a direct binding with an interaction partner or an indirect conformational change due to this interaction.

In the unphosphorylated c-Myc1–88:Pin1 interaction, a near-continuous surface of CSP-displaying residues is formed by Pin1 WW residues centered around Trp34 (Figure 2.5A, blue), and, extending toward the Pin1 PPlase active site, by residues facing the cleft between the two domains (Figure 2.5A, orange). This suggests a Myc binding surface involving the interdomain cleft, which agrees with Pin1 WW and Pin1 PPlase jointly binding the c-Myc MB0 region (Figure 2.3). In the WW domain, affected residues correspond well to those observed in crystal structures to be involved in PEG and phosphopeptide binding (Matena et al., 2013; Namanja et al., 2011; Ranganathan et al., 1997; Verdecia et al., 2000). In addition, a clear pattern of CSPs is observed for Pin1 PPlase residues involved

Pre-Anchoring of PIN1 to Unphosphorylated MYC in a Fuzzy Complex Regulates MYC activity

in substrate recognition and proline ring placement (Figure 2.5A; green) while weak CSPs are observed for residues in the active-site loop (Figure 2.5A; red). Interestingly, the Pin1 interdomain interface and PPlase core region affected by c-Myc1–88 includes many residues in the “Path 1” proposed to mediate allosteric interdomain regulation (Guo et al., 2015).

The pSer62-c-Myc1–88:Pin1 interaction results in a more extensive CSP pattern, which increasingly affects Pin1 residues involved in domain interactions and catalysis (Figure 2.5B). The effects of Pin1 interaction with pSer62-c-Myc1–88 now extends from the Trp34 region to involve WW residues His27 and Ile28 lining the interdomain cleft, as well as Ala140 facing these residues from the PPlase domain. Notably, Pin1-Ile28 was recently shown to be a key residue in regulating substrate binding affinity and isomerase activity by means of its interdomain contact position (Wilson et al., 2013). Furthermore, facing the Pin1 WW domain, the Pin1 PPlase helix 1 (residues 82–98), which was not affected by unphosphorylated c-Myc1-88, now shows significant CSPs (Figure 2.5, orange). Helix1 connects to the active-site loop (Figure 5, red) via highly affected Pin1-His64 (Figure 2.5), which was previously found to be highly perturbed in the binding of both cis- and trans-restricted inhibitors (Namanja et al., 2011). Notably, Pin1 helix1, the interdomain interface, and the WW pocket are also fundamental parts of the second allosteric pathway (“Path 2”) identified by Guo et al. (2015). Pin1 residues proposed to be involved in substrate recognition and proline ring

Pre-Anchoring of PIN1 to Unphosphorylated MYC in a Fuzzy Complex Regulates MYC activity

placement (Namanja et al., 2011) are differently affected: residues 115–117 and 130–131 at the edge of the Pin1 PPIase phosphate binding groove are involved in recognition of phosphorylated c-Myc while unphosphorylated c-Myc affects the surface-exposed β strand and loop structure including residues 120–130 (Figure 2.5; green). Specifically, Pin1 residues I78 and A116, which show enhanced flexibility on ligand binding in previous studies as a possible reflection of substrate recognition (Namanja et al., 2011), are both highly affected by pSer62-c-Myc1–88 binding but not by binding to unphosphorylated c-Myc1–88. Finally, residues 102–105, close to the hydrophobic patch where a second PEG molecule was observed in the Pin1 crystal structure deposited as 1PIN (Ranganathan et al., 1997), now show CSPs, suggesting altered interactions at this site (Figure 2.5, gray). The interaction of Pin1 with c-Myc could be further modulated by phosphorylation, since two of three important phosphorylation sites in Pin1 (Ser16 and Ser71; (Hariharan and Sussman, 2014; Lee et al., 2011b; Lu et al., 2002a) are involved in c-Myc interactions with both phosphorylated and unphosphorylated states (Figure 2.5).

A comparison between HNCO peak intensity ratios for Pin1, in the presence of either c-Myc1–88 or pSer62-c-Myc1–88, reveals a general and uniform reduction of peak intensity ratios for both folded domains of Pin1, in contrast to the residue-specific effects observed for c-Myc1–88. This suggests that the two Pin1 subdomains, which in the free state move independently of each other (Bayer et

Pre-Anchoring of PIN1 to Unphosphorylated MYC in a Fuzzy Complex Regulates MYC activity

al., 2003; Jacobs et al., 2003), experience an increased τ_c as an effect of joint tumbling of the two domains on binding either phosphorylated or unphosphorylated c-Myc1–88, which again supports joint c-Myc binding by Pin1 WW and Pin1 PPlase subdomains.

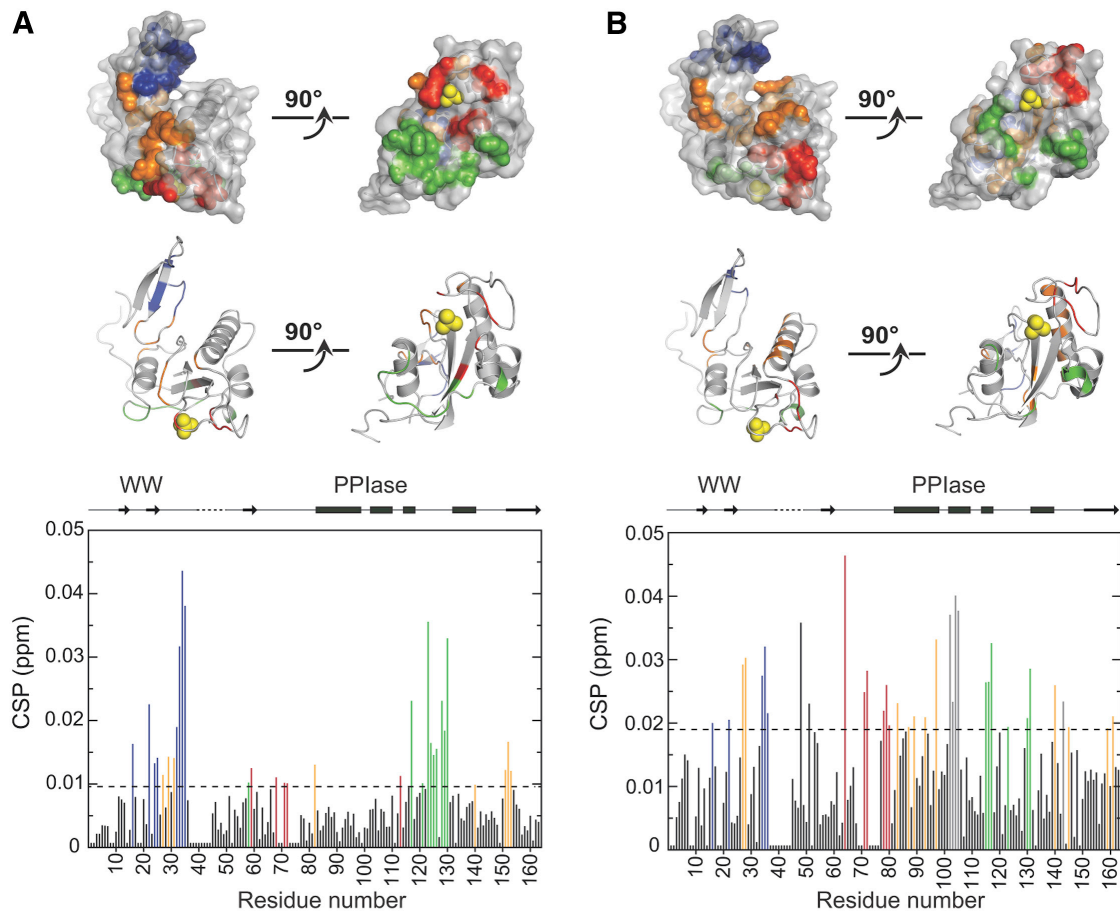


Figure 2.5: NMR Mapping of Pin1 Interactions with c-Myc1–88 and pSer62-c-Myc1–88.

Surface, secondary structure representations, and charts of the CSPs of Pin1, interacting with c-Myc1–88 (A) and pSer62-c-Myc1–88 (B), respectively. Pin1 residues affected by Myc binding are color coded through (A) and (B) as follows: residues in Pin1 WW (blue), subdomain interface (orange), Pin1 PPlase catalytic loop and active site (red), Pin1 PPlase substrate recognition and binding (green). The sulfate group from the crystal structure of PIN1, represented by yellow spheres, indicates the proposed Pin1 active site.

Ensemble Models Describe the Fuzzy Myc-Pin1 Complex

To outline the possibilities for deriving a structural model for the c-Myc-Pin1 interaction, we jointly assessed all our experimental data (Figures 2.2, 2.3, 2.4, and 2.5). SPR measurements showed significant binding of Pin1 to unphosphorylated c-Myc outside of the Pin1-targeted MBI (Figures 2.2), and, in agreement NMR mapping of HNCO intensity ratios, suggests that Pin1 primarily binds to the MB0 region (c-Myc10–35) (Figure 2.3). We focused on investigating how MB0 may interact with Pin1, and how this might affect binding of the unphosphorylated MBI region, since binding to pSer62-c-Myc1-88 seems structurally less resolvable due to the presence of multiple interconverting bound states (Figures 2.2).

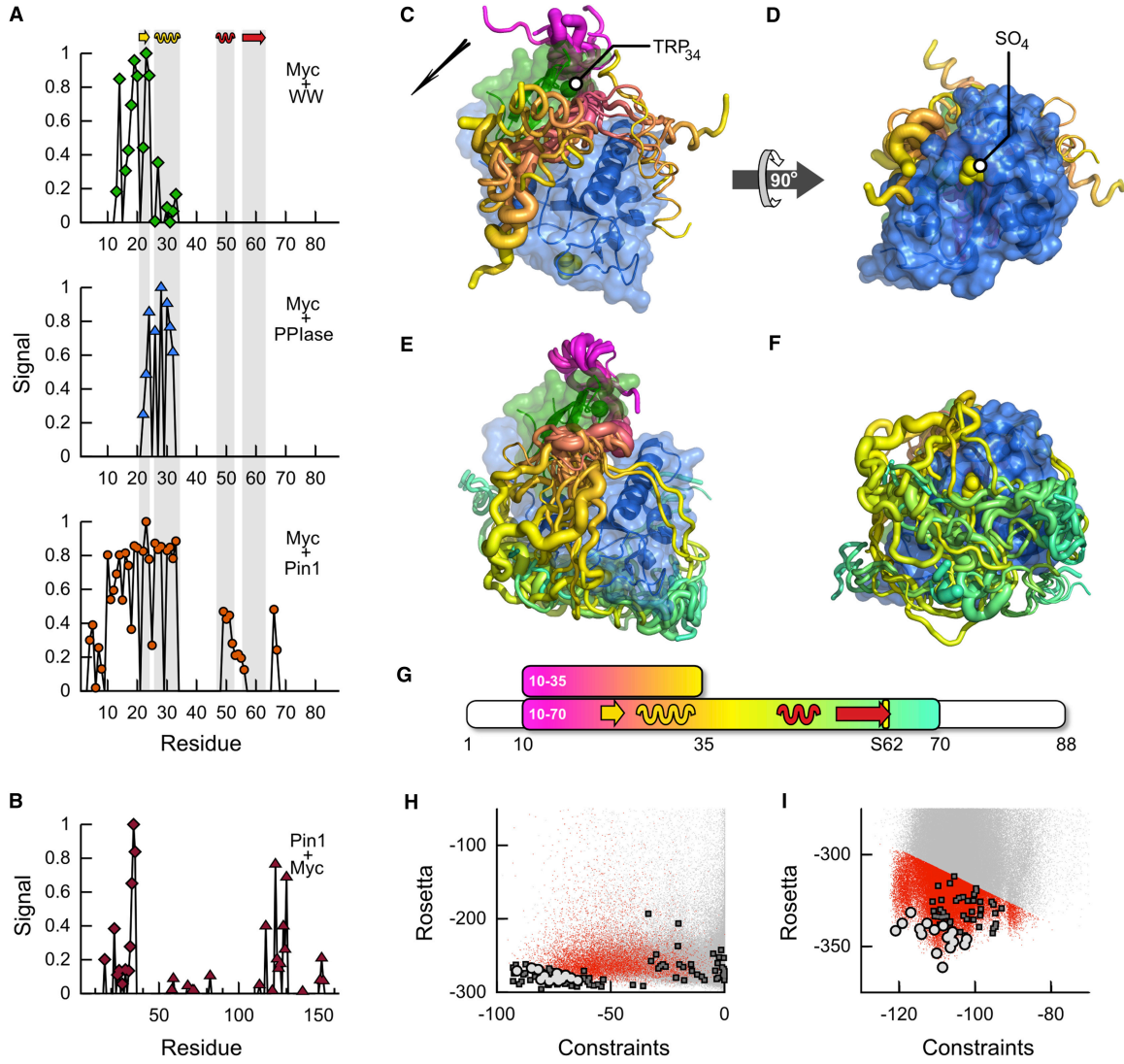
To visualize the structural space accessible to a c-Myc1–88-Pin1 dynamic complex that satisfies our experimental data, we first modeled c-Myc10–35 in complex with Pin1 and then extended this ensemble to include the entire c-Myc10–70 region, using Rosetta docking and loop modeling protocols (see Methods). The docking was guided by experimental constraints derived from HNCO intensity data from c-Myc1–88 binding to Pin1, Pin1 WW and Pin1 PPlase, as well as from Pin1 CSPs on c-Myc1–88 binding (see Methods). The resulting conformations were clustered using a 3-Å root-mean-square deviation

Pre-Anchoring of PIN1 to Unphosphorylated MYC in a Fuzzy Complex Regulates MYC activity

radius cutoff, and the largest clusters, representing a majority of the docked conformations, were sorted based on combined physical and constraint energies. From each of these clusters, the lowest-energy representative that best satisfied the experimental constraints was included in the ensemble describing the bound complexes (Figure 2.6).

The resulting models show a wide ensemble of c-Myc10–35 conformations favorably interacting with both Pin1 WW and Pin1 PPIase by means of the MB0 region (Figures 2.6C, D, G, and H). A preferred direction of binding of MB0 in the interdomain cleft is evident and is introduced by the experimental constraints, since without that contribution to the energy function the bias almost disappears. In the full c-Myc10–70 model, the extent of the linker between MB0 and MBI generously allows for unphosphorylated MBI to interact in a multitude of ways with the Pin1 PPIase active-site region (Figures 2.6E–G, I), in full agreement with experimental data (Figures 2.3, 2.4, and 2.5). Notably, our NMR relaxation data for unphosphorylated c-Myc1–88 show that interactions between Pin1 and regions flanking the MB0 anchor site are dynamically transient, in contrast to the multistate, fuzzy Pin1 binding of MB0 (Figures 2.3 and 2.4). Thus, the entire ensemble of Pin1-bound c-Myc1–70 will also include Myc conformations that are anchored only at MB0, leaving the MBI region disordered and accessible to phosphatases and kinases.

Pre-Anchoring of PIN1 to Unphosphorylated MYC in a Fuzzy Complex Regulates MYC activity



Pre-Anchoring of PIN1 to Unphosphorylated MYC in a Fuzzy Complex Regulates MYC activity

Figure 2.6: Increased PP2A-B56 α activity reduces c-Myc protein levels.

(A) Filtered and rescaled signals used to guide the Rosetta Monte Carlo simulation from HNCO ratios for c-Myc1–88 versus Pin1WW (top), c-Myc1–88 versus Pin1PPlase (middle), and c-Myc1–88 versus full Pin1 (bottom).

(B) Plot of rescaled signals from Pin1 versus c-Myc1–88 Δ CSPs.

(C) A structural representation of the MB0-anchored Myc-Pin1 fuzzy complex, as presented by the ensemble of lowest-energy c-Myc10–35-Pin1 complex conformations from the 15 top-scoring clusters, visualized as ribbon representations of the c-Myc10–35 backbone superimposed on PDB:1PIN. The cross-section area of the ribbon is scaled to the relative size of the cluster. The black arrow indicates the N- to C-terminal c-Myc10–35 binding direction as defined in Figure S5B.

(D) Bottom view of the complex ensemble with SO4 in the superimposed 1PIN structure bound to the active site, represented by yellow spheres.

(E and F) Extended ensemble model showing Myc-Pin1 fuzzy complexes anchored at MB0 with transient MBI-Pin1 interactions. The c-Myc10–70 ensemble comprises the 17 top-scoring clusters, visualized in the same manner as the c-Myc10–35 model.

(G) Relative position of the modeled Myc fragments on c-Myc1–88 with the same coloring gradient of c-Myc10–35 and c-Myc10–70 as in (C) to (F); transient secondary structure elements and the Ser62 phosphorylation site are indicated.

(H) The experimental constraint score versus the Rosetta standard score is plotted as dots for all c-Myc10–35-Pin1 models; red dot if the model belongs to a cluster and gray otherwise. The lowest-energy representative is shown for each cluster irrespective of size (black squares), with the 15 highest-scoring clusters highlighted (gray circle).

(I) Scatterplot of c-Myc10–70 clusters and -Pin1 models; same visualization as in (H) but with the 17 highest-scoring clusters highlighted

Mutations in MB0 Affect Critical Myc Regulatory Functions

The biophysical and computational data suggest that the conserved MB0 region forms a primary interaction site for Pin1 to unphosphorylated c-Myc1–88. To evaluate the importance of this interaction in cells and for c-Myc's cellular functions, we generated point mutations in the MB0 coding region, targeting c-Myc-20-PYFY-23 in human corresponding to c-Myc-20-PYFI-23 in murine, and created murine alanine c-Myc mutants 20-PAAA, 20-PAAI, and 20-AAAI. Consistent with the hypothesis that these residues are important for Pin1 to anchor on c-Myc (Figure 2.3), our co-immunoprecipitation (coIP) experiments reproducibly showed more than 50% reduction in Pin1's ability to bind to MB0 mutated c-Myc compared with wild-type (WT), with AAAI the lowest affinity observed (Figure 2.7A). The cellular data agree well with SPR experiments performed with three corresponding human c-Myc1–88 mutants, c-Myc-20-PYFY/AAAA-23, -PYFY/PAAY, and -PYFY/AAFY. Compared with WT c-Myc1–88, the c-Myc-20-AAAA-23 mutant displays a lower affinity toward human Pin1, 15 μ M, compared with 4 μ M for the WT construct. Measurements were also performed with the other two mutants c-Myc-20-PYFY/PAAY and c-Myc-20-PYFY/AAFY, which were also able to bind Pin1, but showed reduced affinity. In addition, the mutants are phosphorylated at S62 with similar or higher levels compared with WT c-Myc, suggesting that the reduced affinity is not caused by lack of c-Myc S62 phosphorylation, and consistent with a role for Pin1 in facilitating PP2A-mediated S62 dephosphorylation (Yeh et al., 2004a) (Figure

Pre-Anchoring of PIN1 to Unphosphorylated MYC in a Fuzzy Complex Regulates MYC activity

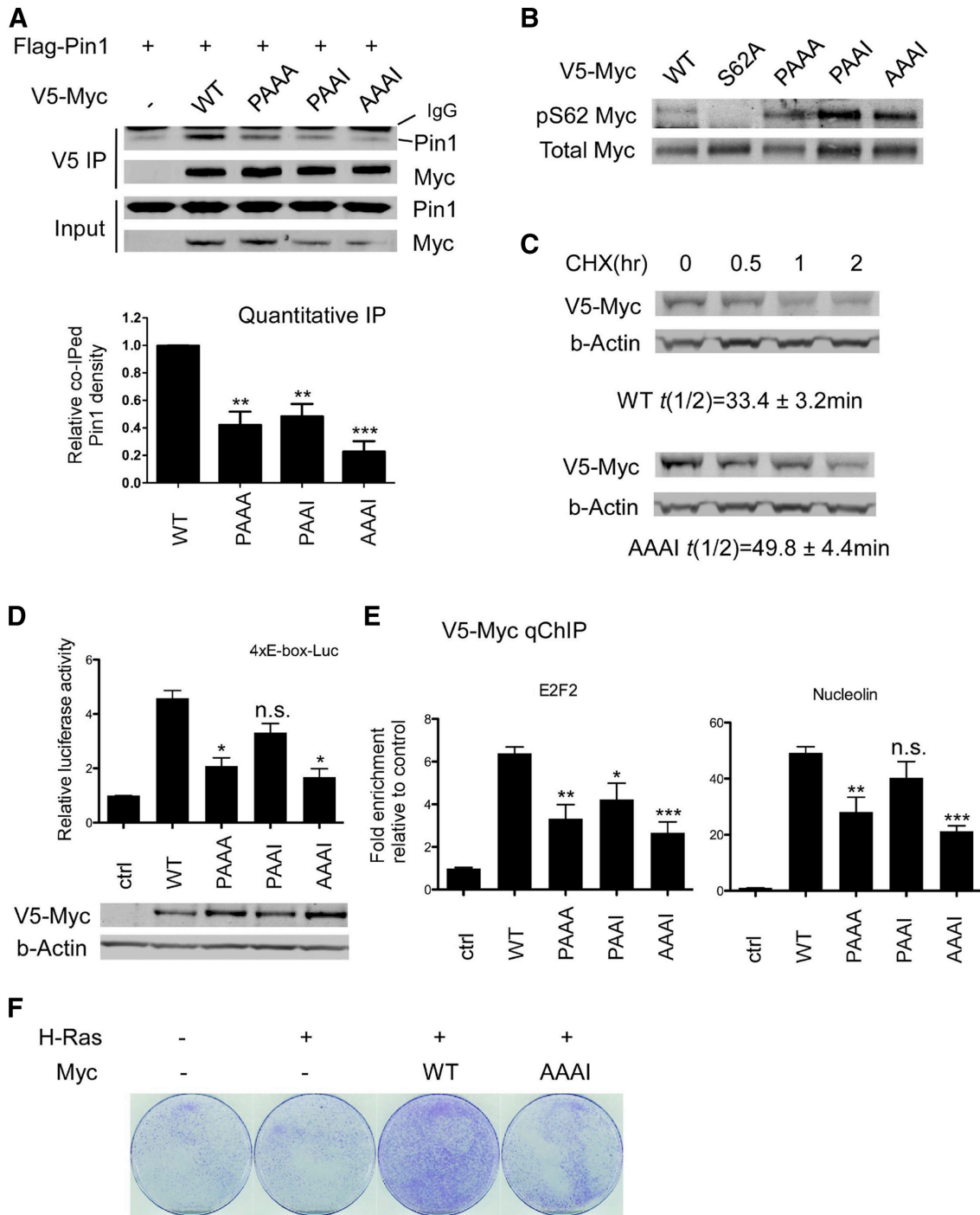
2.7B). We also observed an increase in protein stability in the MB0 mutants reflected by a prolonged protein half-life following inhibition of protein synthesis by cycloheximide treatment (Figure 2.7C) and by a higher steady-state level when transfecting equal amounts of plasmids to the WT (Figure 2.7D, western blot). The increased stability of the MB0 mutants is likely due to downregulation of Pin1's facilitating c-Myc degradation caused by reduced interaction (Yeh et al., 2004).

Since in addition to facilitating c-Myc Ser62 dephosphorylation and degradation, Pin1 initially stimulates c-Myc DNA binding and target gene activation (Farrell et al., 2013), we tested the effects of the c-Myc-20-PYFI mutations on c-Myc transcriptional activity. We measured the luciferase signal driven by the canonical c-Myc binding sequence, 4xE-Box-luc, following expression of c-Myc WT or MB0 mutants. Mutants with disruption of c-Myc-20-PYFI consistently showed decreased ability to drive luciferase signal compared with WT c-Myc (Figure 2.7D). The c-Myc-20-PYFI mutants also have significantly decreased interaction with endogenous target genes, E2F2 and Nucleolin, measured by quantitative ChIP (Figure 2.7E). Interestingly, the degree to which the mutants display impaired activities coordinates well with their abilities to interact with Pin1 (Figure 2.7A), suggesting that Pin1 is the main regulator of the c-Myc-20-PYFI domain and its effects on c-Myc activity. To test the role of c-Myc-20-PYFI in cell proliferation, we conducted colony formation assays in REF52 cells. As shown

Pre-Anchoring of PIN1 to Unphosphorylated MYC in a Fuzzy Complex Regulates MYC activity

in Figure 2.7F, the ability of cells to form colonies with the AAA1 mutant and Ras was dramatically decreased compared with cells with WT Myc and Ras, highlighting the importance of the c-Myc-20-PYFI domain for c-Myc's pro-proliferative function. We find that several pro-proliferative transcription factors that are Pin1 targets (Liou et al., 2011) contain a PYFY-type motif N-terminal to their pSer-Pro sites, suggesting a more general role of this motif in Pin1-regulated pro-proliferative target.

Pre-Anchoring of PIN1 to Unphosphorylated MYC in a Fuzzy Complex Regulates MYC activity



Pre-Anchoring of PIN1 to Unphosphorylated MYC in a Fuzzy Complex Regulates MYC activity

Figure 2.7: Mutations in MB0 Decrease Pin1 Affinity and Regulate c-Myc activity.

Reduced binding affinity with Pin1, less transcriptional activity, and reduced proliferation ability is observed for c-Myc-20-PYFI mutants.

(A) CoIP of cell lysates from HEK293s transfected with indicated plasmids using anti-V5 antibody for immunoprecipitation and anti-Flag antibody for detection of Co-immunoprecipitated Pin1 (bottom band). Co-immunoprecipitated Pin1 band densities were quantified after normalization to input, immunoprecipitated c-Myc level, and controls.

(B) Western analysis of lysates from HEK293 expressing indicated plasmids, V5-immunoprecipitated c-Myc were used for S62 phosphorylation analysis, S62A serves as negative control.

(C) Western analysis of lysates from HEK293 transfected with equal amounts of V5-Myc plasmids (top: WT; bottom: AAAI mutant). Four independent experiments were used to quantify half-life.

(D) 4xE-box driven luciferase signal detected from lysates of HEK293s co-transfected with indicated V5 plasmids or empty vector as control. Luciferase signals were adjusted based on expression levels shown in the immunoblots below.

(E) DNA binding affinity for WT and mutant V5-Myc shown by quantitative ChIP at indicated promoters. ChIP levels were adjusted by respective inputs and protein levels. Lysates of HEK293s transfected empty vector were used as control for normalization.

(F) Colony formation assays were performed in REF52 cells co-transfected with H-Ras and either WT or mutant c-Myc as indicated for up to 3 weeks.

Statistical significance relative to WT was calculated using a two-tailed t test: *p < 0.05; **p < 0.01; ***p < 0.001; n.s., not significant. All quantifications were based on at least three independent experiments.

Discussion:

The Pin1 enzyme is well known for its capability of cis-trans isomerization of phosphorylated (p)Ser/(p)Thr-Pro target sequences, and specifically acts on intrinsically disordered substrates in cell regulation to direct their regulatory activities (Liou et al., 2011; Lu et al., 2007). However, limited light has been shed on how Pin1 interacts with longer substrates, since the present molecular knowledge predominantly has been gained from Pin1 studies of interactions with small molecules or peptides. The present work significantly advances our understanding of Pin1-substrate interactions by showing, using a wide spectrum of biophysical and cellular methods, that Pin1 recognition of its well-known target c-Myc involves pre-anchoring to an unphosphorylated conserved motif distal from the phosphorylated target site for Pin1-mediated proline isomerization, which is biologically critical and structurally significant. Specifically, we find that Pin1 binds unphosphorylated c-Myc in a Pin1 interdomain-anchored dynamic, or fuzzy, complex at a well-conserved region here designated MB0 (Figure 2.1), and we show that such anchoring is structurally compatible with concomitant transient binding to the Pin1PP1ase active site region of the MBI (p)Ser/(p)Thr-Pro Pin1 target site(s) for cis/trans isomerization (Figure 2.6), in full agreement with our NMR data (Figures 2.3, 2.4, and 2.5). Importantly, disturbing Pin1 binding to its unphosphorylated MB0 anchor site results in impaired c-Myc transcriptional activity and reduced c-Myc function in cellular proliferation assays.

Pre-Anchoring of PIN1 to Unphosphorylated MYC in a Fuzzy Complex Regulates MYC activity

A compelling advantage of Pin1 pre-anchoring to unphosphorylated, distal site(s) would be to increase the local concentration of substrate presented to the active site and thereby further increase the catalytic efficiency of Pin1. Our study substantiates this, since we in our NMR experiments directly observe a significant recognition of the unphosphorylated MBI region by intact Pin1 on MB0 binding (Figure 2.3), indicating that this recognition is facilitated by an increase in local concentration due to Pin1-MB0 pre-anchoring. When c-Myc1–88 is phosphorylated at Ser62, we find that Pin1 distinctly recognizes the phosphorylation site in MBI but still affects the N-terminal, non-phosphorylated MB0 (Figure 2.3), suggesting a maintained role of this interaction in the phosphorylated state. Furthermore, the mere localization of MB0 binding to the interdomain cleft (Figures 2.5 and 2.6) may also mediate increased catalytic activity. Recent work has shown enhanced interdomain interactions in Pin1 by small-molecule binding at the Pin1 subdomain interface (Matena et al., 2013), and critical interdomain contact residues such as Ile28 have been shown to affect Pin1 catalytic activity and substrate binding affinity (Wilson et al., 2013). Notably, however, simultaneous tight binding of designed bivalent Pin1 binders to both WW and PPIase creates inhibition of Pin1 activity (Daum et al., 2007), suggesting that intrinsic dynamics in binding both Pin1 sites is required for native substrate activity.

Pre-Anchoring of PIN1 to Unphosphorylated MYC in a Fuzzy Complex Regulates MYC activity

Our results show that mutations in the MB0 Pin1-anchoring region dramatically decrease Ras-dependent transformation and simultaneously show prolonged c-Myc half-life. At first glance this may appear confusing, since several stabilizing c-Myc mutations have been shown to increase cell proliferation (Chang et al., 2000; Salghetti et al., 1999). However, our results are compatible with recent data demonstrating that Pin1 isomerization at pSer62-Pro63 in c-Myc promotes c-Myc DNA binding and target gene activation (Figure 2.1; Farrell et al., 2013) even though it can also facilitate S62-dephosphorylation by protein phosphatase 2A and increase c-Myc turnover (Figure 2.1; (Arnold and Sears, 2006; Yeh et al., 2004a). Thus, a Myc mutant with deficient Pin1 interaction would indeed be more stable and Ser62 phosphorylated, but would not promote transcriptional and/or oncogenic activity. Since our biophysical results indicate that Pin1 binding to the MB0 site N-terminal to the c-Myc pSer62-Pro motif serves to allosterically activate Pin1 and increase the frequency of encounters between the MBI target sequence and the PPlase active site, it is indeed a tenable hypothesis that with disturbed MB0 pre-recognition, both the Pin1 isomerase activity and the affinity between Myc and Pin1 will be too low to be biologically efficient. This would result in a higher prevalence of Myc isomers that are less active in transcriptional activity in the Myc-accessible cellular activity window, with concomitant lowering of cell growth, as shown in our MB0 mutants.

Pre-Anchoring of PIN1 to Unphosphorylated MYC in a Fuzzy Complex Regulates MYC activity

We suggest that the biological requirement for both Pin1 subdomains to reach full Pin1 functionality is based on the biophysical requirements for joint subdomain interaction to longer substrates, which is necessary to allosterically elevate enzymatic activity and specificity to the levels required for efficient biological regulation. Recent studies show that interdomain dynamics is affected by binding of small molecules or substrate peptides/analogs to the active site and/or to the interdomain region (Bayer et al., 2003; Jacobs et al., 2003; Matena et al., 2013; Namanja et al., 2007; Wilson et al., 2013). Our data support and extend these findings by showing how Pin1 integrates recognition to both these sites in binding to a longer substrate. Importantly, we show that not only key residues, such as Pin1^{WW}-Ile28 and its counterpart Ala140 in Pin1^{PPlase}, but a wide range of interdomain residues in both Pin1 subdomains are differentially affected with respect to the phosphorylation state of the binding peptide (Figure 2.5). A recent study performed by molecular dynamics simulations proposes that the two Pin1 domains are allosterically regulated through two pathways: a first quiescent state called Path 1, and a second state (Path 2) which is sequentially activated upon substrate binding to the WW pocket (Guo et al., 2015). Interestingly, in our experimental work with a long substrate, we find that the CSPs in Pin1 created by the binding with c-Myc1–88 resembles the Path 1 pattern, while with pS62-cMyc1–88 a pattern comparable with Path 2 emerges (Figure 2.5). Notably, while the WW pocket is involved in binding both phosphorylated and unphosphorylated c-Myc1–88, it is only in the presence of pS62-c-Myc1–88 that the second

Pre-Anchoring of PIN1 to Unphosphorylated MYC in a Fuzzy Complex Regulates MYC activity

pathway becomes active. Therefore, we propose that the presence of the phosphate in the active site represents the real trigger factor for the activation of Path 2, given joint binding of the substrate protein to the WW pocket. Thus, the allosteric communication between the two Pin1 domains is not a one-way signal initiated by Pin1WW binding, but it is a multistep process whereby Path 1 is activated by substrate binding to the WW domain and Path 2 by the phosphate binding the PPlase active site. Taken together, a comparison between results relating to Pin1 allostery in our experimental data and in the molecular dynamics simulations (Guo et al., 2015) reveals interesting similarities, but also different implications concerning the activation mechanism of allosteric pathways.

The highly dynamic association between non-phosphorylated c-Myc1–88 and Pin1 shows the characteristics of a fuzzy complex (Fuxreiter and Tompa, 2012): alternate conformations are allowed in the bound state, and large parts of the bound c-Myc1–88 peptide have dynamic properties closely resembling the unbound state. The unphosphorylated Myc-Pin1 complex must therefore be considered as an ensemble of conformations where, although one orientation of c-Myc in the interdomain cleft is prevalent, a wide variety of chain-wrapping modes around Pin1 are allowed in the bound ensemble (Figures 2.6). Redistribution among multiple states within the bound ensemble could well occur on Myc phosphorylation, which could also increase the propensities for MBI binding to the Pin1 interdomain cleft, as suggested by Pin1WW binding to both

Pre-Anchoring of PIN1 to Unphosphorylated MYC in a Fuzzy Complex Regulates MYC activity

MB0 and MBI upon Ser62 phosphorylation (Figure 2.3E) as well as by previous crystal structures showing phosphorylated short peptides or peptide analogs bound in the interdomain cleft (Matena et al., 2013; Verdecia et al., 2000). The juggling of substrates on and off the active site, as well as the enzymatic efficiency (De et al., 2012), may thus be controlled by dynamically shifting the ensemble of interdomain Pin1 bound states, as indicated by the requirement of both domains for efficient catalysis and by the multiple modes of Myc-Pin1 recognition identified here. Furthermore, the fuzzy complex with a flexible 30-residue ($>60 \text{ \AA}$) linker between the Myc MB0 and MBI binding sites (Figure 2.6), together with the dynamics of the bound complex (Figure 2.4), will allow for facile kinase/phosphatase access to Ser/Thr-Pro sites in MBI with maintained MB0 association of Pin1 throughout the regulatory cycle (Figure 2.1). Our findings, together with the possible presence of distal motifs in other Pin1-dependent proliferative transcription factors, suggest that dynamic pre-recognition of distal motifs by Pin1 could play a more general role in the timing of cellular events in growth and differentiation.

PIN1 regulates the spatial distribution of transcriptionally active MYC at the nuclear pore

Chapter Three :

**PIN1 regulates the spatial distribution of
transcriptionally active MYC at the nuclear pore**

Abstract:

The transcription factor MYC (also c-Myc) has a broad approach to the genome. High levels of MYC can bind to most active gene promoters and distal open chromatin regions. In addition to MYC's function of controlling Pol II's pause and release, it has also been shown to induce histone modification and chromatin remodeling especially in response to mitogen stimulation. MYC is subject to a series of post-translational modifications that affect its stability and oncogenic activity. Post-translational modifications allow dynamic protein regulation, but how this controls MYC's function on the genome is largely unknown. Recent data suggests a role for MYC in transcriptional control at the nuclear periphery. Here, we report that Serine 62 phosphorylation and PIN1-mediated isomerization of MYC regulate the spatial distribution of MYC, promoting its association with the basket of the nuclear pore, where it recruits the histone acetyltransferase GCN5 to regulate target gene acetylation and expression. We identify a group of MYC binding targets that include pro-migration pathway genes, which as are spatially and dynamically regulated by this mechanism. Taken together, our study indicates that post-translational regulation of MYC controls the temporal and spatial activity of MYC to regulate gene expression.

Introduction:

The proto-oncogenic transcription factor MYC has a broad range of gene targets that control many cellular behaviors including metabolism, proliferation, and morphology, the malfunctions of which contribute to tumorigenesis and cancer progression (Kress et al., 2015). Recent in vivo studies demonstrate that inactivation of MYC can induce tumor collapse and tumor microenvironment normalization. To target MYC for cancer therapeutics, it is crucial to understand the regulation of MYC expression and activity.

MYC protein level and activity are regulated by sequential phosphorylation events on Serine 62 (S62) and Threonine 58 (Hann, 2006; Vervoorts et al., 2006). In response to growth stimulation, multiple RAS induced kinases and cyclin dependent kinases phosphorylate MYC at S62, which is associated with MYC stabilization and activation (Campaner et al., 2010; Hydbring et al., 2010; Sears et al., 2000). The subsequential T58 phosphorylation by GSK3b promotes proteasome degradation of MYC through the pathway of the E3 ligase Fbw7 (Welcker et al., 2004; Yada et al., 2004). These phosphorylation events on the 58-TPPLSP-63 motif lead to MYC's interaction with PIN1 (Yeh et al., 2004b). As the only identified phosphorylation dependent prolyl isomerase, PIN1 catalyzes proline isomerization of pS/pT-P motifs, influencing the protein conformation to alter protein function (Liou et al., 2011). Most known PIN1-mediated isomerization events promote tumor growth and drug resistance (Zhou

PIN1 regulates the spatial distribution of transcriptionally active MYC at the nuclear pore and Lu, 2016). In the case of MYC, in addition to increasing MYC turnover (Yeh et al., 2004b), PIN1 has been shown to promote the oncogenic activity of phosphor Serine 62 (pS62) MYC and its transcriptional control of specific genes (Farrell et al., 2013). However, a global view of PIN1's regulation of MYC's gene regulatory activity, especially under physiological conditions, is still lacking.

Chromatin organization and gene expression are associated with the nuclear structure (Lanctôt et al., 2007; Zhou et al., 2011). In mammalian cells, the nuclear interior is associated with euchromatin and active transcription; The nuclear periphery, especially the Lamina Associated Domain (LAD), is enriched for condensed chromatin and repressive transcription (Guelen et al., 2008; Pombo and Dillon, 2015). However, although also localized to the nuclear periphery, the regions near the nuclear pore is exclusive for heterochromatin and permissive for transcription (Beck and Hurt, 2017; Krull et al., 2010). Interestingly, a recent study has shown that pS62 MYC is enriched at the nuclear periphery and associated with proliferation gene activation (Myant et al., 2015), suggesting that post-translational modification of MYC may regulate its subnuclear localization and activity.

In this study, using Proximity Ligation Assay (PLA) and Stochastic Optical Reconstruction Microscopy (STORM) Imaging, we find that pS62 MYC interacts with the basket of the nuclear pore complex (NPC), which is regulated by Ser62

PIN1 regulates the spatial distribution of transcriptionally active MYC at the nuclear pore phosphorylation and PIN1. PIN1 mediated proline isomerization of MYC promotes its recruitment and co-recruitment of the histone acetyl transferase (HAT) GCN5 to the nuclear pore basket, leading to nearby histone acetylation and gene activation. Using CHIP-seq and FISH, we identified a group of pro-migration genes as MYC binding targets that are affected by this PIN1-mediated sub-nuclear localization of transcriptionally active MYC. Together, we provide mechanistic insights into spatial control of MYC's gene regulatory activity.

Results:

pS62 MYC associates with the inner basket of the nuclear pore.

Previous studies suggest an enrichment of phosphor Serine 62 (pS62) MYC at the nuclear periphery (Myant et al., 2015). Consistent with this report, we visualized pS62 MYC *in vitro* and *in vivo* and found a substantial amount of cells showing rim-like distribution of pS62 signal (Figures 3.1A and S3.1A). Notably, the pattern of pS62 is distinct from phosphor Threonine 58 (pT58) or total MYC signal (Figure 3.1A). The enrichment of pS62 at the nuclear periphery is supported by the presence of pS62 MYC in the nuclear insoluble fraction that includes lamina and the nuclear pore basket component TPR (Figure 3.1C). An early EM study suggested MYC localization to the nuclear pore (Royds et al., 1992). We speculated an involvement of the nuclear pore complex (NPC) in MYC localization at the nuclear periphery. To examine the possibility of MYC association with the nuclear pore, we conducted Proximity Ligation Assay (PLA) between MYC and various nucleoporins (Nups) representing different components of the NPC in HeLa cells (Figure 3.1B). Using antibodies against TPR, Nup98, Nup153, and Nup214, showing specific nuclear peripheral staining (Figure S3.1B), we observed robust PLA signals of MYC association with TPR and Nup153 (pore basket), but not signals of MYC association with Nup98 (inner ring), or Nup214 (cytoplasmic filaments) (Figures 3.1D and 3.1E). These data indicate that MYC and pS62-MYC (Figures 3.1F and S1C) preferentially localizes to the basket of the NPC.

To visualize the detail of MYC protein at the nuclear periphery, we took advantage of the STochastic Optical Reconstruction Microscopy (STORM) imaging technology, which would improve the resolution to ~20nm. We co-stained pS62 or total MYC with TPR, and took images at the nuclear equator and the bottom of the nucleus sequentially. At the focal plane of the equator, both MYC and pS62 MYC signals merged with TPR at the nuclear periphery (Figure 3.1G, a, b, e, and f); at the bottom-plane (Figure 3.1G, c, d, g, and h), both MYC and pS62 MYC signals showed a significant co-localization with TPR, shown by spatial pattern analysis with pair correlation function (Figure 3.1H) (Nickerson et al., 2014). Of note, the occurrence of MYC signal maintains further away (>200nm) from the center of TPR signal (Figure 3.1H left) than the pS62 MYC (Figure 3.1H right), suggesting that the non-TPR-associated MYC are not Ser 62 phosphorylated.

To further examine the relevance of various compartments in MYC's association with the nuclear periphery, we knocked down lamin A/C and Nups to see if the presence of MYC in the nuclear insoluble fraction is affected (Figure 3.1I). Consistent with our PLA results, depletion of the pore basket subunits Nup153 and TPR significantly reduced the level of pS62-MYC and total MYC in the insoluble fraction, whereas knockdown of Nup98 and Nup214 had little effect. Notably, we did not observe an accumulation of MYC in the nuclear soluble

PIN1 regulates the spatial distribution of transcriptionally active MYC at the nuclear pore

fraction, which is consistent with previous observation that MYC in the nuclear soluble fraction is less stable (Figure S3.1D-G; Myant et al., 2015; Tworkowski et al., 2002). In addition, knockdown of Lamin A/C also modestly reduced pS62-MYC and total MYC levels in the insoluble fraction, suggesting a role for the nuclear lamina in storing MYC (Myant et al., 2015) in addition to the NPC, although we can not rule out disruption of NPC structure with the Lamin knockdown. To this point, we could not tease out whether Nup153 or TPR is more important for MYC's association with the basket as depletion of TPR affected Nup153 levels, and depletion of Nup153 interfered the level and distribution of TPR, consistent with the tight structural and functional association of the two proteins (Hase and Cordes, 2003; Krull et al., 2004; Rajanala and Nandicoori, 2012). Given the critical roles of TPR in nuclear pore structure and nuclear peripheral chromatin organization (Krull et al., 2004, 2010), we focused on TPR for the following localization and functional characterization.

PIN1 regulates the spatial distribution of transcriptionally active MYC at the nuclear pore

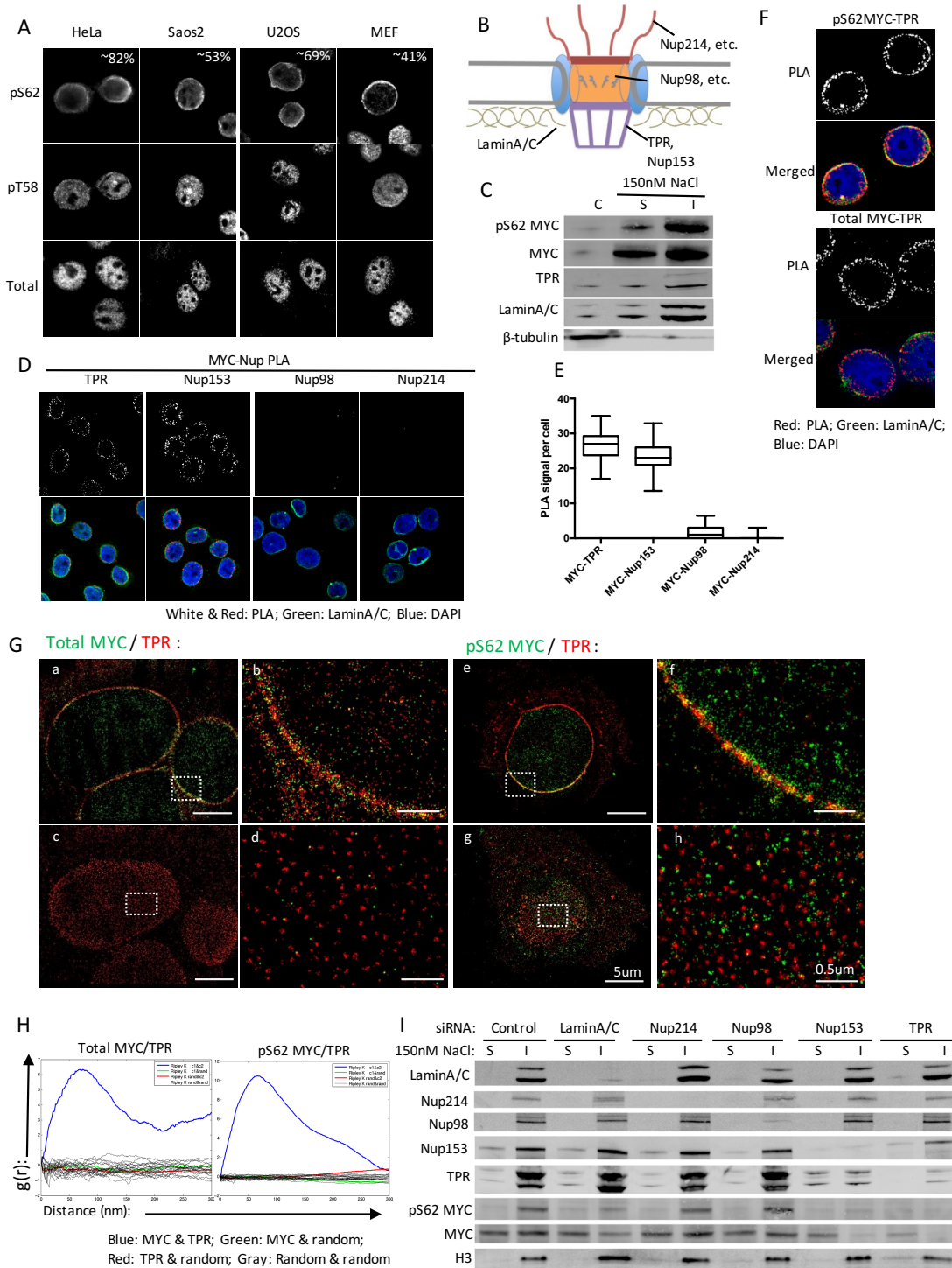


Figure 3.1: pS62 MYC associates with the nuclear pore basket.

(A) Immunofluorescence (IF) staining of pS62 MYC, pT58 MYC, and total MYC in HeLa, Saso2, U2OS, and Mouse Embryonic Fibroblast (MEF) cells.

(B) A schematic of the nuclear pore complex with representative nuclear porins labeled for the following analysis.

(C) Western Blot of subcellular distribution of pS62 MYC and total MYC in cytoplasmic (C), nuclear soluble (S), and nuclear insoluble (I) fractions of HeLa cells by 150nM NaCl nuclear extraction. LaminA/C and TPR represent nuclear markers; β -tubulin represents cellular markers.

(D) PLA of MYC association with nuclear porins (Nups) in HeLa cells. The PLA signals (Red) were overlaid with the immunofluorescence staining of LaminA/C (Green) and DAPI (Blue) in the bottom images.

(E) Quantification of PLA signal in (D), the box represents average and 25-75% intervals of PLA signal per cell from 50 cells.

(F) PLA of pS62 and total MYC association with TPR in HeLa cells.

(G) STORM analysis of co-localization of total and pS62 MYC with TPR. a and c: showing total MYC (Green) and TPR (Red) at a focal plane near the nuclear equator and the bottom of the nucleus respectively. e and g: showing pS62 MYC (Green) and TPR (Red) at a focal plane near the nuclear equator and the bottom of the nucleus respectively. b, d, f, and h: zoom on a part of their left images.

(H) Plot of pair correlation function showing the likelihood ($g(r)$) of finding total and pS62 MYC signals within certain radial distance from TPR signal (blue line). Shown also the plots of (pS62) MYC against random signal (green), TPR against random signal (red), and random signal against random signal (grey).

(I) Western blot of subnuclear distribution of pS62 MYC and total MYC in nuclear soluble (S) and nuclear insoluble (I) fractions of HeLa cells by 150nM NaCl nuclear extraction.

Ser 62 phosphorylation is critical for MYC interaction with the nuclear pore complex.

The enrichment of pS62-MYC at the nuclear periphery and our discovery that pS62-MYC associates with the basket of the NPC led us to test whether Ser62 phosphorylation is important for MYC's association with the NPC. We transfected HeLa cells with constructs expressing V5 tagged Wildtype (WT), S62A, and T58A MYC, and compared their associations with TPR via V5-TPR PLA. The S62A MYC mutant lacks Ser62 phosphorylation whereas T58A MYC, due to the block of downstream signaling, has hyper Ser62 phosphorylation (Arnold and Sears, 2006; Lutterbach and Hann, 1994). The PLA signal from S62A MYC was significantly decreased compared to WT or T58A MYC, suggesting Ser62 phosphorylation facilitates MYC interaction with TPR (Figure 3.2A and 3.2B).

To test the upstream kinases that affect MYC association with the NPC, we focused on ERK and CDK2, which have shown a strong specificity in phosphorylating MYC at Ser62 and increasing MYC stability (Hydbring et al., 2010; Lutterbach and Hann, 1994; Pulverer et al., 1994; Sears et al., 2000). Knockdown of ERK or CDK2 through siRNA reduced Ser62 phosphorylation and total MYC as expected (Figure 3.2C), and this was coupled with a strong reduction in MYC-TPR PLA (Figure 3.2D and 3.2E), suggesting that ERK and CDK2 are upstream kinases involved in Ser62 phosphorylation of MYC and

PIN1 regulates the spatial distribution of transcriptionally active MYC at the nuclear pore

MYC-TPR interaction. As a control, depletion of CDK4, which is a downstream target of MYC (Hermeking et al., 2000; Marval et al., 2004; Mateyak et al., 1999), did not change MYC phosphorylation at Ser62 levels upon knockdown nor the MYC-TPR PLA (Figures 3.2C-E). Consistent with the kinase specificity, we detected robust PLA signals of MYC with ERK and CDK2, but not with CDK4 (Figure 3.2F). Intriguingly, the MYC/ERK PLA signals were displayed ubiquitously in the nucleus; the MYC/CDK2 PLA were enriched in the nuclear periphery, resembling the MYC-TPR interaction pattern (Figure 3.2F). We speculated that while ERK may phosphorylate Ser62 in the nuclear interior, CDK2 might associate with TPR, which is suggested by previous identification of TPR as a CDK2 substrate through Mass Spectrometry (Chi et al., 2008). Indeed, we found robust PLA signal of TPR-CDK2, but only low TPR-ERK, and background levels with TPR-CDK4. Together these results suggest ERK and CDK2 facilitates MYC interaction with NPC by phosphorylating MYC at Ser62. While ERK can phosphorylate MYC in the nucleoplasm, CDK2 may phosphorylate MYC directly at the NPC.

PIN1 regulates the spatial distribution of transcriptionally active MYC at the nuclear pore

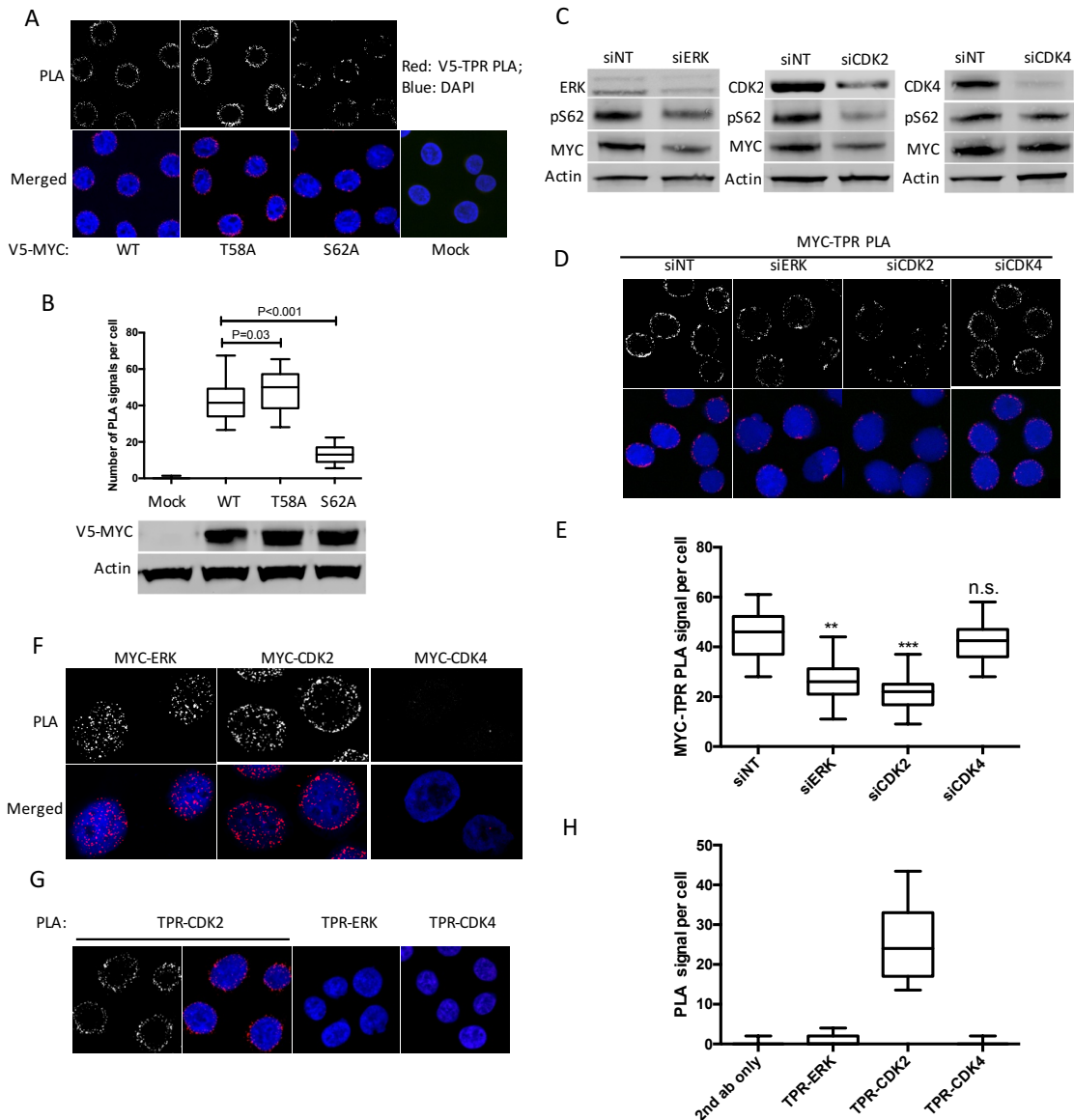


Figure 3.2: Ser62 phosphorylation is important for MYC association with the NPC.

(A) PLA of V5 – TPR association in transfected HeLa cells expressing equal amount of V5 tagged WT, T58A, and S62A MYC. The mock transfection was used as negative control. (B) Quantification of (A) showing average PLA signal per cell from 50 cells and the expressions of the MYC constructs. (C) Western blot of pS62 MYC and total MYC in HeLa cells transfected with siRNAs of indicated kinases. (D) PLA of MYC-TPR association in HeLa cells transfected with siRNAs of indicated kinases. (E) Quantification of (D) showing average PLA signal per cell from 50 cells. (F) PLA of MYC association with indicated kinases in HeLa cells. (G) PLA of TPR association with indicated kinases in HeLa cells. (H) Quantification of (G) showing average PLA signal per cell from 50 cells.

PIN1 regulates the spatial distribution of transcriptionally active MYC at the nuclear pore

PIN1 promotes MYC association with the nuclear pore complex.

PIN1 catalyzes pSer62-Pro63 isomerization where the peptidyl proly bond is in a *trans* conformation following ERK or CDK-mediated phosphorylation to the *cis* conformation, and this increases MYC DNA binding, transcriptional and oncogenic activity (Farrell et al., 2013; Helander et al., 2015). PIN1 subsequently catalyzes pSer62-Pro63 from *cis* to *trans* dependent on secondary phosphorylation at Thr58, and this facilitates PP2A-mediated dephosphorylation of pSer62 and MYC degradation (Yeh et al., 2004b). To test if PIN1 plays a role in pS62 MYC interaction with the NPC, we first looked at the association of PIN1 with total and pS62 MYC by PLA. Interestingly, we found a substantial amount of PLA signal localized to the nuclear periphery in both PIN1-MYC and PIN1- pS62 MYC combinations (Figure 3.3A). Notably, there were also PLA speckles in the nucleoplasm, suggesting PIN1 regulation of MYC may occur in multiple nuclear compartments. We examined the effects of knocking down PIN1 expression via siRNA on the level of MYC in the nuclear soluble and insoluble fractions. While knockdown of PIN1 increased Myc and pS62Myc levels in the soluble fraction, the expression of both total and pS62 MYC in the nuclear insoluble fraction decreased upon PIN1 knockdown (Figure 3.3B). To test the role of PIN1 activity on MYC association with the NPC, we knocked down, PIN1 and found a significant reduction of MYC-TPR PLA signals (Figure 3.3C). Importantly, the defect of MYC interaction with TPR can be rescued by WT PIN1 but not the substrate binding (W33A) or catalytic deficient (C109A) PIN1 (Figure 3.3C),

PIN1 regulates the spatial distribution of transcriptionally active MYC at the nuclear pore

indicating that PIN1's catalytic activity is required to facilitate MYC-TPR interaction.

We have shown previously that PIN1 doesn't recognize S62A MYC, and has a reduced interaction with and effect on T58A MYC, where T58A MYC target gene binding as measured by qChIP is not significantly enhanced by PIN1 as is WT MYC (Farrell et al., 2013; Yeh et al., 2004b). To examine the role of Ser62 and Thr58 phosphorylation in PIN1's regulation of the association of MYC with the NPC, we first transfected HeLa cells with constructs expressing V5 tagged WT, T58A, and S62A MYC, and examined the interaction of PIN1 with these constructs through V5-PIN1 PLA. While S62A MYC lack's phosphorylation on Thr58 and Ser62 due to the hierarchical nature of GSK3-mediated Thr 58 phosphorylation, T58A MYC has increased Ser62 phosphorylation due to the inability of PP2A to dephosphorylate T58A MYC(Hann, 2006; Yeh et al., 2004b). Similar to previous reports, both T58A and S62A MYC showed a significant reduction in interaction with PIN1 compared to WT MYC by PLA (Figure 3.3D) (Yeh et al., 2004, NCB). We then knocked down PIN1 to test if the V5-MYC-TPR interaction is affected. Consistent with the positive role of PIN1 in the endogenous MYC-TPR interaction (Figure 3.3C), the PLA signal between V5-MYC WT and TPR significantly decreased (Figure 3.3E). In contrast, T58A MYC-TPR PLA was resistant to PIN1 depletion, and S62A MYC-TPR PLA remained at baseline level. To further test the promoting role of PIN1 on different forms of

PIN1 regulates the spatial distribution of transcriptionally active MYC at the nuclear pore

MYC, we took advantage of primary mouse embryonic fibroblasts generated from ROSA-LSL-Myc knockin mice, which, once induced by Cre, express WT, T58A, or S62A Myc at physiological levels (Wang, Cancer Res, 2011). When we co-expressed knockin Myc through adenovirus transduction (Ad-Cre) and PIN1 with Ad-PIN1, WT Myc - TPR association was upregulated by 1.5 folds. In contrast, T58A Myc interaction with TPR was already strong and not further affected by PIN1, while S62A Myc again showed minimal interaction that was not affected by PIN1 (Figure 3.3F). Taken together, these data demonstrate that PIN1 promotes MYC association with the NPC in a phosphor-Ser62 dependent manner, while T58A-MYC with hyper-phosphorylated Ser62 interacts with NPC irrespective of PIN1.

PIN1 regulates the spatial distribution of transcriptionally active MYC at the nuclear pore

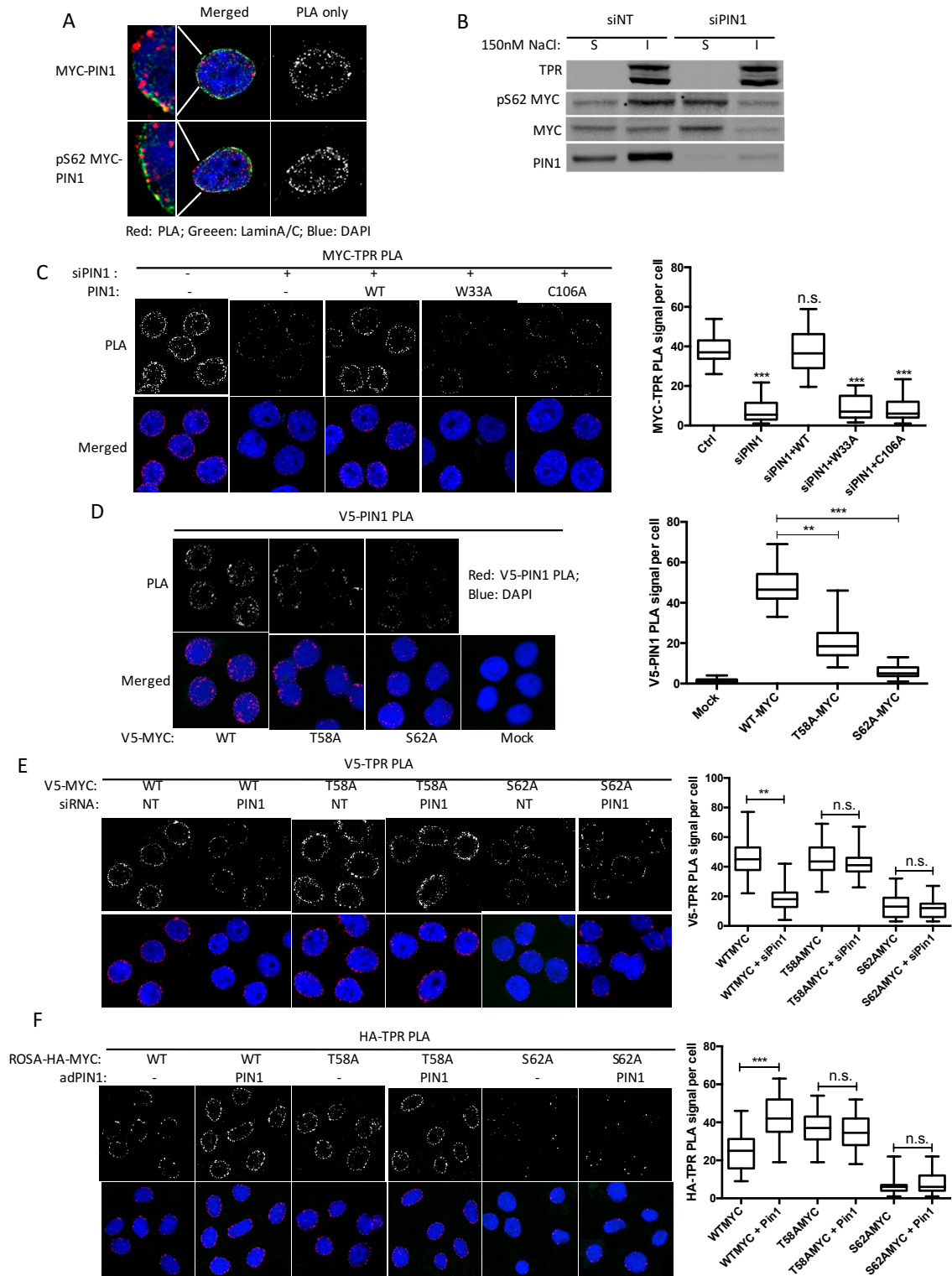


Figure 3.3: PIN1 promotes MYC association with the NPC.

(A) PLA of PIN1 association with total or pS62 MYC. The left two show the detailed colocalization of PIN1-MYC PLA with the nuclear envelope marker LaminA/C.

(B) Western Blot of subcellular distribution of pS62 MYC and total MYC nuclear soluble (S) and nuclear insoluble (I) fractions of HeLa cells transfected with siRNA of PIN1 and extracted by 150nM NaCl.

(C) PLA of MYC-TPR association in HeLa cells transfected with siRNA of PIN1 and indicated PIN1 constructs. Quantification showing average PLA signal per cell from 50 cells.

(D) PLA of V5-PIN1 association in HeLa cells transfected with V5 tagged WT, T58A, and S62A MYC. Quantification showing average PLA signal per cell from 50 cells.

(E) PLA of V5-TPR association in HeLa cells transfected with siRNA of PIN1 and V5 tagged WT, T58A, and S62A MYC construct. Quantification showing average PLA signal per cell from 50 cells.

(F) PLA of HA-TPR association in MEF cells with Cre-dependent expression of HA tagged WT, T58A, and S62A MYC, and infected with adenovirus PIN1 (adPIN1) and adenovirus Cre. Quantification showing average PLA signal per cell from 50 cells.

PIN1 regulates the spatial distribution of transcriptionally active MYC at the nuclear pore

PIN1 mediated MYC interaction with NPC facilitates recruitment of GCN5.

In yeast and higher eukaryotes, the nuclear pore basket helps to maintain a transcriptionally permissive microenvironment (Krull et al., 2010; Mendjan et al., 2006; Taddei et al., 2006), which is potentially mediated by the histone acetyltransferase SAGA (Spt-Ada-GCN5 Acetyltransferase) complex (Cabal et al., 2006; Luthra et al., 2007). The catalytic subunit of SAGA, GCN5, forms a complex with MYC and cooperates with MYC for gene activation (Flinn et al., 2002; Kenneth et al., 2007; Martínez-Cerdeño et al., 2012). In addition, the interaction between MYC and GCN5 is enhanced by PIN1 function (Farrell et al., 2013). Therefore, we tested if GCN5 was involved in the MYC-TPR interaction.

We first visualized the TPR-GCN5 interaction through PLA in HeLa cells, and found robust PLA signal at the nuclear periphery, consistent with the association of GCN5 with Mlp1/2 (the yeast homologue of TPR) in yeast (Luthra et al., 2007). In accordance with PLA of pS62MYC-TPR (Figure 3.1F) and GCN5-TPR, a substantial proportion of pS62 MYC-GCN5 PLA signal also resided at or closely to the nuclear periphery (Figure 4.4A), suggesting that pS62 MYC and GCN5 may exist in the same complex with TPR,

Given the important role of PIN1 in the association of pS62 MYC with the NPC (Figure 3.3C), we hypothesized that both MYC and PIN1 are required for efficient GCN5-TPR association. To test the hypothesis, we quantified the PLA of TPR-

PIN1 regulates the spatial distribution of transcriptionally active MYC at the nuclear pore

GCN5 in response to MYC or PIN1 or both knockdown. Individual depletion of MYC or PIN1 reduced ~40% of the TPR-GCN5 interaction; simultaneous depletion of both MYC and PIN1, however, did not further decrease the PLA signal (Figure 3.4B and 3.4C), suggesting MYC and PIN1 are in the same axis in promoting GCN5 association with TPR.

Since we have now detected potential TPR interactions with CDK2, MYC, and GCN5 via PLA, we asked whether we could also detect these interactions via co-IP experiments and what the effects of PIN1 are on the associations. In agreement with the PLA results, we co-immunoprecipitated (coIPed) CDK2, MYC, GCN5, and PIN1 using a TPR specific antibody. Interestingly, depletion of PIN1 via siRNA substantially reduced the coIPed MYC and GCN5, but had little effect on CDK2 (Figure 3.4D). The TPR coIP data suggests a hierarchy of the assembly of these proteins: CDK2 and other kinases phosphorylate MYC at S62, providing recognition site for PIN1, followed by GCN5 association.

PIN1 regulates the spatial distribution of transcriptionally active MYC at the nuclear pore

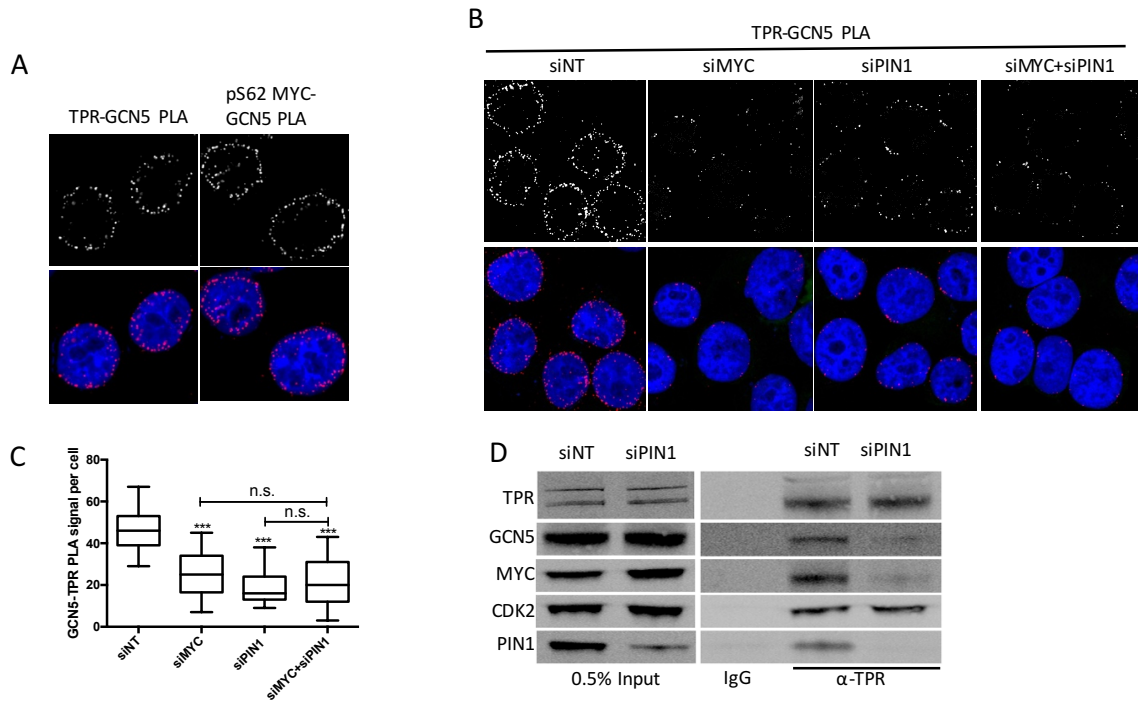


Figure 3.4: PIN1 promotes the formation of TPR-MYC-GCN5 axis.

(A) PLA of GCN5 association with TPR and pS62 MYC in HeLa cells. (B) PLA of TPR-GCN5 association in HeLa cells transfected with siRNAs of MYC and PIN1. (C) Quantification of (B) showing average PLA signal per cell from 50 cells. (D) Western Blot of indicated proteins co-immunoprecipitated (coIPed) with TPR, using TPR specific antibody in HeLa cells.

PIN1 facilitates mitogen induced MYC interaction with the nuclear pore.

PIN1 is viewed as a “molecular timer”, because the signaling pathways and biological processes that PIN1 controls often involve rapid response and adaption to environmental changes(Lu et al., 2007). A role for PIN1 in facilitating the response to growth signals was demonstrated by the phenotype of the mouse embryonic fibroblasts (MEFs) derived from PIN1 knockout mice, which grow normally under asynchronous conditions, but show defects in recovering from serum deprivation and re-stimulation(Fujimori et al., 1999) (Figure S3.5A).

PIN1 regulates the spatial distribution of transcriptionally active MYC at the nuclear pore

Serum stimulation also induces MYC expression through up-regulation of its mRNA and pS62 mediated protein stability as the cells transit through the cell cycle (Frank et al., 2001; Kelly et al., 1983b; Lutterbach and Hann, 1994). Accordingly, MYC knockout cells also exhibit growth arrest (de Alboran et al., 2001). Therefore, we asked whether MYC association with the NPC was serum regulated and if PIN1 is important for this response.

We serum starved primary PIN1 wildtype (WT) and knockout (KO) MEFs generated from isogenic sibling embryos for 48 hrs to render the cells quiescent, then stimulated the cells by changing to serum-complete media, and characterized protein expression and interaction at the indicated time points (Figure 3.5A). The expression of TPR and GCN5 were similar in PIN1 WT and KO MEFs, both gradually increased over the time course (Figure S3.5C). During the process, the pS62 and total MYC levels in WT MEFs were rapidly increased during the first 8 hours and then quickly withdrew to almost baseline level, similar to previous reports (citation). In contrast, the expressions of pS62-MYC and total MYC had a slower induction (0-4hr, Figure S3.5B), and sustained high level expression even at 24 hr in the PIN1 KO MEFs, reflecting a defect in the MYC degradation pathway due to loss of PIN1 (Yeh et al., 2004b). The CDK2 expression was slightly higher in WT MEFs than PIN1 KO MEFs, which could explain the faster induction of MYC Ser62 phosphorylation (Figure S3.5B).

PIN1 regulates the spatial distribution of transcriptionally active MYC at the nuclear pore

In accordance with the MYC expression, in PIN1 wild-type cells, the association between MYC and TPR climbed to peak at 4hrs post stimulation (Figure 3.5A). MYC-GCN5 interaction similarly peaked at 4 hrs in the PIN1 WT cells, and notably, this interaction was at the nuclear periphery (Figure 3.5A and 3.5C). The interaction between MYC and PIN1 also peaked at the 4 hr time point, and it was also localized to the periphery (Figures 3.5A and 3.5C). The rapid inductions of MYC-TPR and MYC-GCN5 at the nuclear periphery were significantly blunted in PIN1 null cells, supporting the critical role of PIN1 in promoting MYC-TPR-GCN5 complex (Figures 3.5A and B). Furthermore, starting around 8 hours, as the MYC-TPR PLA signal begins to decrease in PIN1 wild type cells (Figure 3.5A), there is an intriguing redistribution of MYC-GCN5 and MYC-PIN1 interaction to the nuclear interior (Figures 3.5A and 3.5C); and the MYC-GCN5 spatial redistribution is impaired in the PIN1 deficient cells.

MYC binds DNA with its partner protein MAX (Littlewood et al., 1992; Nair and Burley, 2003). We therefore analyzed the spatial distribution of MYC associated with MAX during the same serum stimulation time course. Notably, the induction of MYC-Max PLA signal occurred both at the nuclear periphery and the interior during early time points in the PIN1 WT cells, with a small shift in distribution toward the interior at 12 hrs (Figure 3.5C). In PIN1 null cells, there was an overall decrease in MYC-MAX association in the first 8 hrs (Figures 3.5A and 3.5B), with the peripheral MYC-MAX PLA signal at early time points showing the most

PIN1 regulates the spatial distribution of transcriptionally active MYC at the nuclear pore

decrease relative to WT cells (Figure 3.5C). By comparing the interaction patterns of MYC-MAX to MYC-TPR, MYC-PIN1 and MYC-GCN5, it appears that a portion of MYC-MAX interaction is involved in the early response MYC-GCN5-PIN1 nuclear pore complex, but that MYC-MAX is also present in the nuclear interior following serum induction.

Overall, these data indicate that during mitogen stimulation, MYC interacts dynamically with different partners at various nuclear compartments: MYC-MAX association is rapidly induced both at the interior and periphery, gradually peaking around 4 to 8 hours, with a modest shift toward the interior at later time points (Figures 3.5A and 3.5C), while MYC-GCN5-PIN1 is initially recruited almost exclusively to the periphery, associating with the nuclear pore basket protein, TPR (Figures 3.5A and 3.5C). PIN1 deletion impairs formation of this complex. At later time points (12hrs), there appears to be a release of MYC-GCN5 from the NPC and re-localization to the nuclear interior, in which PIN1 may also play an active role, as the MYC-PIN1 PLA exhibits similar spatial dynamics (Figures 3.5A and 3.5C) and loss of PIN1 dampens the MYC-GCN5 interior shift in distribution (Figure 3.5C and S3.3D).

PIN1 regulates the spatial distribution of transcriptionally active MYC at the nuclear pore

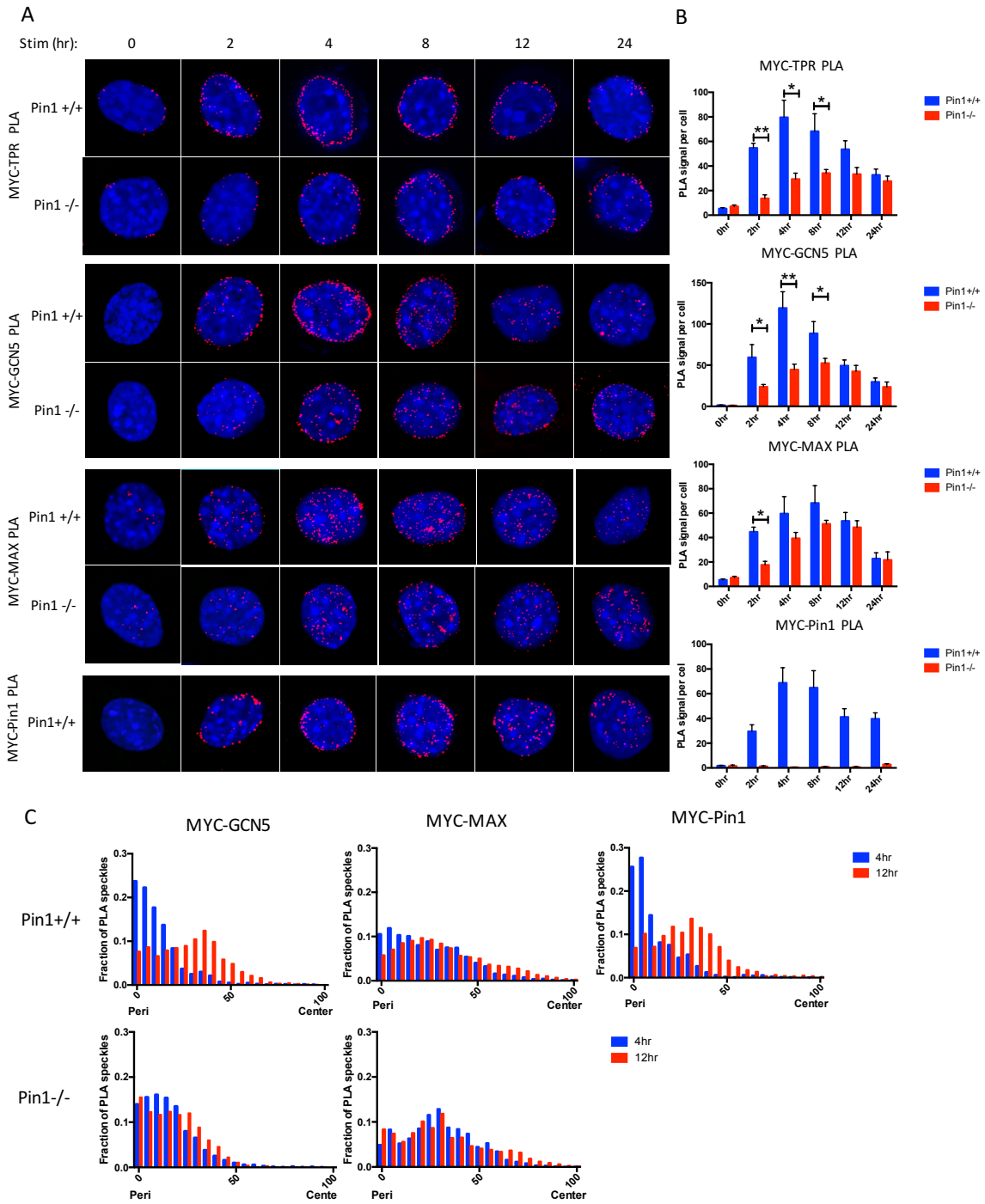


Figure 3.5: PIN1 is critical for mitogen induced MYC association with the NPC.

(A) PLA of MYC association with TPR, GCN5, MAX, and PIN1 (from top to bottom) in Pin1^{+/+} and ^{-/-} MEFs at indicated time points post serum stimulation. (B) Quantification of (A) showing average of PLA signal per cell Pin1 ^{+/+} MEFs (Blue) and Pin1 ^{-/-} MEFs (Red) from three biological replicates. (C) Detection of radial distribution shift between early time points (4hr, blue) and late time points (12hr, red) of indicated PLA signals. Histograms of the normalized distance distribution were generated from at least 500 PLA speckles.

PIN1 promotes MYC-driven transcription at the nuclear periphery

To assess the global DNA binding of MYC regulated by PIN1 and its association with MYC's localization near the nuclear pore, we performed MYC ChIP-seq in PIN1 WT and KO MEFs at 4hr post serum stimulation, when expression levels of MYC were similar, but differences in the MYC-TPR PLA was the largest (Figures 3.5A, B and S3.3C). We focused on the MYC binding within 1kb upstream and downstream of the transcription start sites of genes. Using Gene Set Enrichment Analysis (GSEA) of the MYC bound genes, we found several pathways enriched in PIN1 WT versus null MEFs including cell motion, protein acetylation, and polysome pathways (Figure S3.4A), aligning with the increased cell growth and increased histone acetylation following serum stimulation in PIN1^{+/+} versus PIN1^{-/-} cells (Figure S3.4A-C). Consistent with a role for PIN1 in promoting MYC DNA binding (Farrell et al., 2013), 673 genes had increased MYC binding peaks more than 1.5 fold in Pin1 WT versus PIN1 KO (Figure 3.6A), among them we chose to study genes encoding several transcription factor involved in cell motility

PIN1 regulates the spatial distribution of transcriptionally active MYC at the nuclear pore including TWIST, SNAIL, and cell proliferation regulators, CDC45 and RPL36 to investigate spatial relationships by DNA Fluorescence in situ Hybridization (FISH). We hypothesized that these genes where MYC binding was affected due to loss of PIN1 would localize to the nuclear periphery during early induction. We observed that the FISH signals for Cdc45, Rpl36, Twist1, and Snai1, at 0 and 4hr time points, were localized to the nuclear periphery (Figure 3.6B and 3.6C). Interestingly, at 12hr post stimulation, when the MYC-PIN1 and MYC-GCN5 PLA shifted to the nuclear interior, we observed a shift toward more interior FISH signals for these genes in the PIN1 WT cells, but this was not the case for the control lamin associated IgH gene (Figure 3.6B and 3.6C). In contrast, the position changes of these genes was reduced in the PIN1 null cells (Figure 3.6C), which is consistent with earlier results showing that the MYC-GCN5 and MYC-MAX PLA interior shift at 12 hrs was blunted by loss of PIN1 (Figure 3.5C). The nuclear peripheral localization of these genes during early time points and departure from the nuclear pore at later time points are also supported by their interaction with TPR captured by TPR qChIP, which are at a higher level at 0 and 4 hr time points and decreased at 12hr time point in the PIN1 WT cells, but this is reduced in the PIN1 null cells and the control IgH gene is not captured by TPR qChIP (Figure S3.4B).

To test the hypothesis that loss of PIN1 impairs the functions of MYC and GCN5 at these genes, we performed qChIP using primers for the promoters of Cdc45,

PIN1 regulates the spatial distribution of transcriptionally active MYC at the nuclear pore

Rpl36, Twist1, Snai1, and IgH to examine the occupancy of MYC and GCN5 on these representative genes following serum stimulation. In PIN1 WT cells, MYC and GCN5 occupancy at these genes were rapidly induced at 4 and 12 hrs (Figures 3.6D and S3.4C). These inductions were blunted in PIN1 null cells, which may explain the reduced histone acetylation on these regions detected by qChIP with a pan H3ac antibody in PIN1 null cells (Figure S3.4D). Consistent with the induction of H3ac level, which marks chromatin opening, the mRNA of the gene targets was also induced to a greater degree in the PIN1^{+/+} versus PIN1^{-/-} cells (Figure 3.6E). As negative control, the lamin associated IgH (ref) exhibited virtually no MYC or GCN5 binding, no mRNA induction, and was depleted of H3ac during the stimulation process (Figures 3.6C-E, and S3.4B-D).

The above data suggests that in response to extracellular stimuli, PIN1 is critical for the efficient recruitment of MYC to the NPC, which by interacting with GCN5, affects local chromatin histone acetylation and transcription outcome.

PIN1 regulates the spatial distribution of transcriptionally active MYC at the nuclear pore

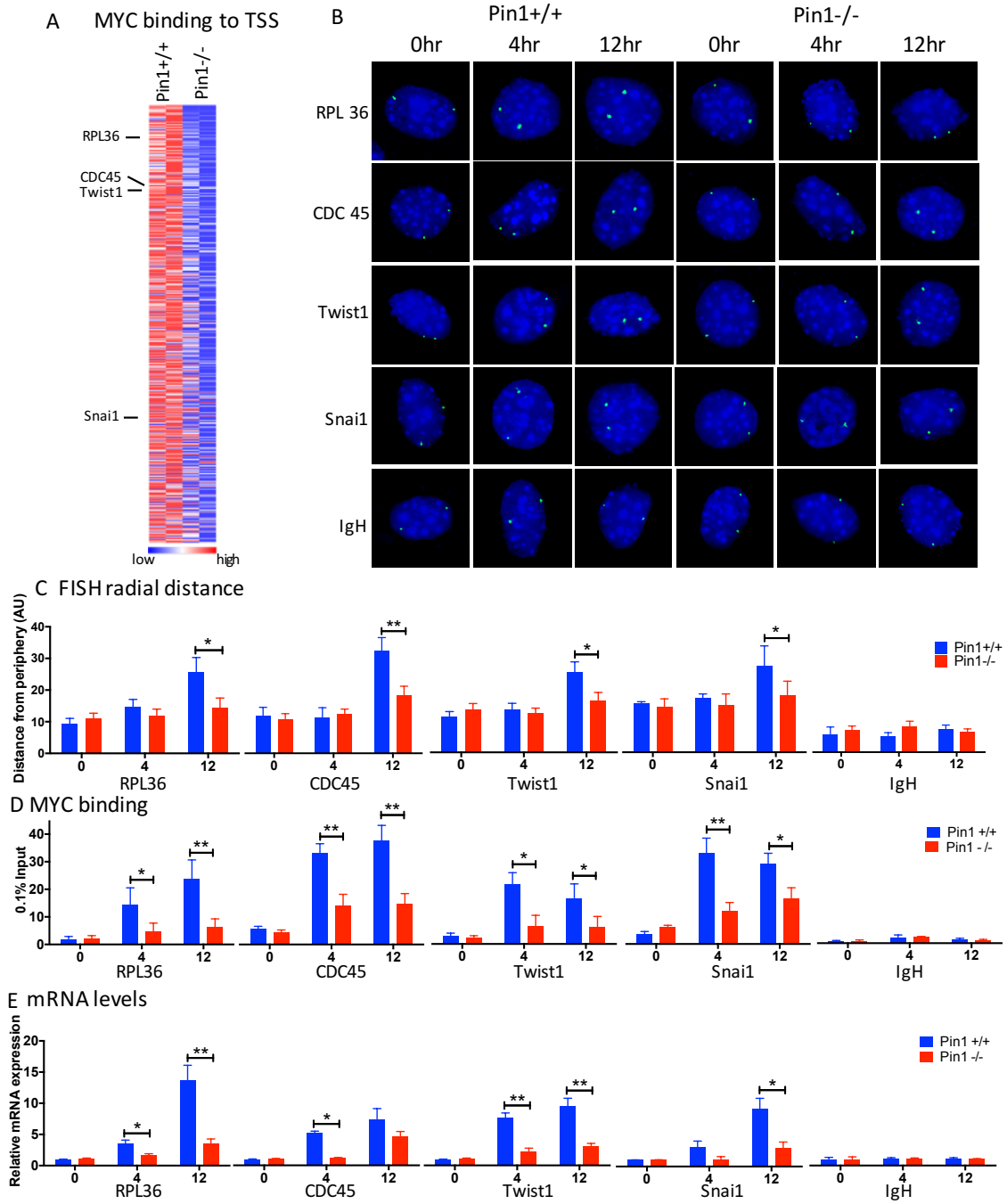


Figure 3.6: PIN1 promotes MYC binding to the nuclear peripheral targets.

(A) Heatmap of gene targets showing more MYC binding at the transcription start sites (TSS) in Pin1^{+/+} MEFs than Pin1^{-/-} MEFs (>1.5 fold). Genes were ranked by fold change of wildtype / knockout combining two biological replicates.

(B) Representative FISH images of indicated loci (green) in Pin1^{+/+} and Pin1^{-/-} MEFs at 0, 4, and 12 hr timepoints in response to serum stimulation.

(C) Detection of radial distribution shift of FISH signal of indicated loci during serum stimulation in Pin1^{+/+} (Blue) and Pin1^{-/-} (Red) MEFs. Y-axis is the normalized distance from periphery (0) to center (100). Shown are the average of distance from over 50 cells.

(D) Quantitative Chromatin IP (qChIP) of MYC binding to the indicated target genes in Pin1^{+/+} (Blue) and Pin1^{-/-} (Red) MEFs during serum stimulation.

(E) RT-PCR of the mRNA of indicated genes in Pin1^{+/+} (Blue) and Pin1^{-/-} (Red) MEFs during serum stimulation.

PIN1 deficient mice have defects in wound healing.

To investigate whether the above observed defects in gene regulation in PIN1 null cells is associated with functional changes, we performed *in vitro* scratch assays on the PIN1 WT and null MEFs. PIN1^{-/-} cells showed a delay in migration into the scratch area (Figure 3.7A). This defect was rescued by infection of cells with adenovirus expressing T58A MYC (Figure 3.7A), a form of MYC that can interact with the nuclear pore independent of PIN1 (Figures 3.3E and 3.3F), suggesting MYC mediates PIN1 function in migration *in vitro*. In addition, we conducted skin punch wound healing assays in PIN1 WT and Null mice. It took around 10 days for WT mice to heal from the punch biopsy on the back, whereas PIN1 KO mice took more than 15 days (Figures 3.7B and 3.7C). At day 8, the WT mice exhibited thickened epidermis at the wound area, whereas the epidermis at

PIN1 regulates the spatial distribution of transcriptionally active MYC at the nuclear pore

the wound area of the PIN1 null mice mostly only had a single basal (K14 positive) layer (Figure 3.7D). Immunofluorescent analysis of the day 8 skin showed a strong decrease in expression of E-cadherin and Integrin B1 at both wound and adjacent skin in PIN1 knockout mice. Studies have shown that E-cadherin promotes collective cell migration *in vivo* (Cai et al., 2014), and that Integrin b1 mediates keratinocytes migration and epidermal stem cell maintenance (Georges-Labouesse et al., 1996; Jones and Watt, 1993; Kim et al., 1992). Additionally, the PIN1 KO showed less Ki67 positive cells at the wound area (Figure S3.5A) and at the adjacent epidermis regions (Figure S3.5A arrows), suggesting that the defects of both proliferation and migration in PIN1 KO mice contribute to the impaired wound healing. To test if MYC is involved in this process, we performed PLA of MYC with TPR and PIN1. In WT mice, Both MYC-TPR and MYC-PIN1 associations were induced towards the wound area; in contrast, MYC association with TPR was significantly reduced in the wound area of PIN1 KO mice (Figure S3.5B). Together, these data suggest PIN1 mediated MYC-TPR association facilitates proper wound healing. Lastly, the defects of wound healing of PIN1 KO mice mimicked the phenotype of mice with overexpression of MYC in the skin (Waikel et al., 2001), consistent with PIN1 positively regulating MYC transcriptional activity.

PIN1 regulates the spatial distribution of transcriptionally active MYC at the nuclear pore

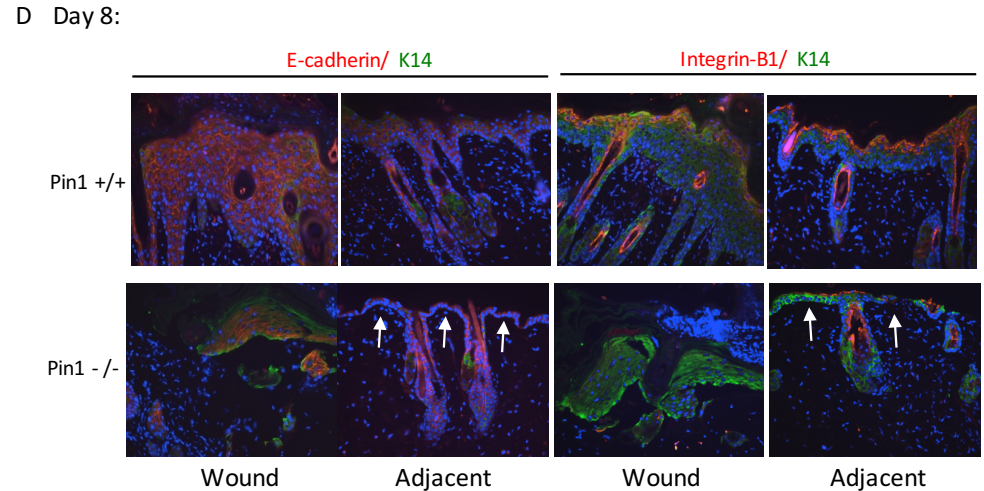
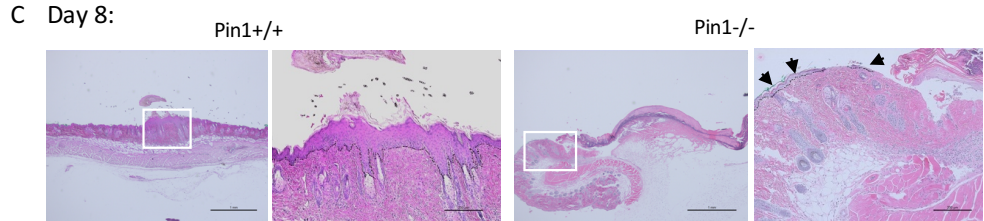
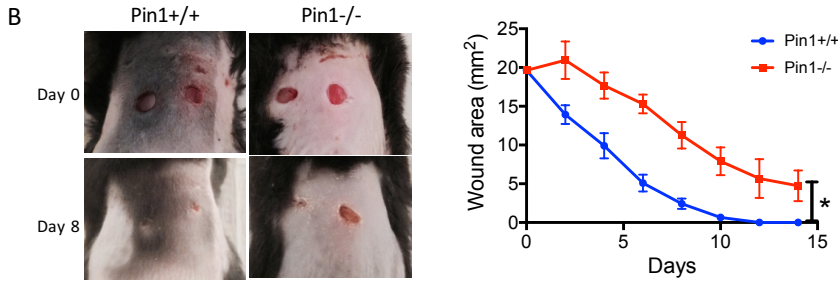
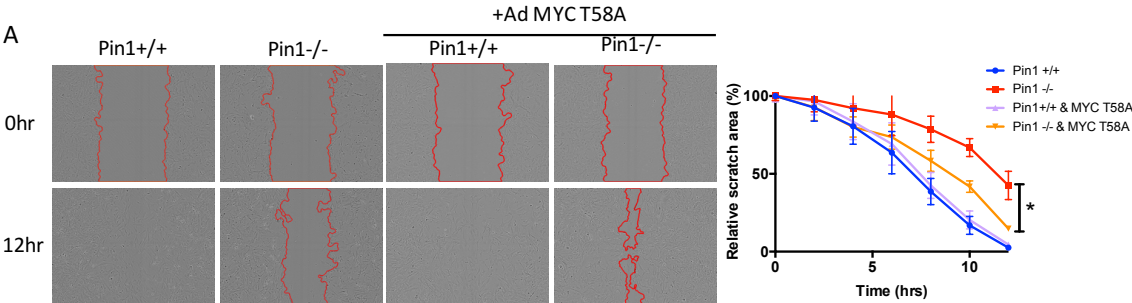


Figure 3.7: Pin1 knockout mice exhibit defects in wound healing.

(A) Representative phase contrast images of scratch assay of Pin1^{+/+}, Pin1^{-/-} MEFs and their infections of adenovirus expressed T58A MYC. Shown is the boundaries of the scratches (red) at indicated time points. Shown at the right is the quantification of the scratch area relative to the beginning (%) at indicated conditions.

(B) Wound pictures of Pin1 ^{+/+} and Pin1 ^{-/-} mice after skin punch biopsy at indicated time points. Bottom is the quantification of the average wound area from three pairs of matched siblings.

(C) H & E staining of the wound areas of Pin1^{+/+} and ^{-/-} mice 8 days post skin punch biopsy.

(D) IF staining of E-cadherin (red), Integrin-B1 (red), and Keratin 14 (K14, green) of the wound and adjacent skin samples.

Statistical significance relative to WT was calculated using a two-tailed t test: *p < 0.05; **p < 0.01; ***p < 0.001. All quantifications were based on at least three independent experiments.

Discussion:

Although the nuclear peripheral localization of MYC has been observed for a long time, both the significance and mechanistic regulation remained an enigma (Eisenman et al., 1985; Vríz et al., 1992). Early reports suggested that both the nuclear pore and the lamina were involved in MYC association with the nuclear periphery (Royds et al., 1992; Winqvist et al., 1984). Particularly, a recent study indicated that CIP2a regulates pS62 MYC association with the LaminA/C-associated structures (LAS) (Myant et al., 2015). The LAS compartment is likely to include the pore components since the nuclear pore is embedded in the lamina meshwork (Figures 1C and 1I), and Myant et al., suggested this possibility in their discussion. The nuclear pore complex (NPC), one of the largest protein complexes, is composed of three scaffold rings and peripheral elements including the cytoplasmic filaments and the pore basket (Beck and Hurt, 2017). Through PLA and STORM imaging, we demonstrate that pS62 MYC associates with the pore basket represented by TPR and NUP153. The association between MYC and TPR is controlled by Ser 62 phosphorylation downstream of ERK and CDK2 (and potentially other kinases). CDK2 may directly phosphorylate MYC (Chi et al., 2008) at the pore as suggested by the PLA signal from TPR-CDK2. Despite the potential role of ERK at the pore (Vomastek et al., 2008), we did not detect the interaction in our PLA. Ser 62 phosphorylation of MYC promotes its interaction with the prolyl-isomerase PIN1 (Farrell et al., 2013; Yeh et al., 2004b). We demonstrate that PIN1's catalytic activity facilitates the association between MYC

PIN1 regulates the spatial distribution of transcriptionally active MYC at the nuclear pore and TPR both in HeLa and MEFs, which is distinct from PIN1's promoting MYC degradation. In HeLa cells, enhanced MYC-TPR interaction by PIN1 were often presented with lower MYC expression; In MEFs after 4 hours exposure to serum stimulation, when MYC levels were similar, MYC-TPR and MYC-GCN5 PLA signals were greatly reduced by the loss of PIN1. Because the Proline 63 *trans*-form of MYC is a substrate for Serine 62 dephosphorylation and proteasome degradation, we suggest that the favorable conformation of NPC associated MYC is in *cis*. The regulation of MYC at the pore may involve many other players and post-translation modifications. The nuclear pore associated SUMO protease SENP1 (Chow et al., 2014; David-Watine, 2011; Schweizer et al., 2013) deSUMOlates and increases PIN1 activity (Chen et al., 2013), indicating that SENP1 may also regulate, directly or indirectly, MYC at the nuclear pore. Future investigation into the interplay between MYC, PIN1, SENP1, and potential other post-translational regulators at the nuclear pore will likely provide additional insights into the nuclear spatial control of MYC.

Aside from affecting site-specific chromatin states and gene expression, MYC has been shown to influence global chromatin architecture. For instance, depletion of N-MYC in neuronal progenitors causes global nuclear condensation marked by a decrease in H3 and H4 acetylation (H3ac and H4ac) and an increase in H3K9me3 (Knoepfler et al., 2006). MYC's broad influence on chromatin occurred through upregulation of the histone acetyl transferase GCN5,

PIN1 regulates the spatial distribution of transcriptionally active MYC at the nuclear pore which increases genome-wide H3ac and H4ac. MYC may also interact with GCN5 and cooperate in this genome-wide effect (Flinn et al., 2002; Martínez-Cerdeño et al., 2012). It is unknown, however, the connection between the nuclear localization of MYC and its influence on the genome architecture. Consistent with the yeast studies indicating GCN5 association with the nuclear pore basket (Cabal et al., 2006; Luthra et al., 2007), we observed GCN5-TPR and GCN5-MYC interactions in the nuclear periphery. Combining with the positive role of PIN1 in promoting MYC-TPR and MYC-GCN5 association at the periphery (Figure 4 and Farrell et al., 2013), a picture of a PIN1-regulated TPR-MYC-GCN5 axis has emerged.

Using MYC ChIP-seq, we identified a group of genes co-regulated by MYC and PIN1 with roles in cell cycle and cell movement (Figure 6A and S6A). In accordance with a PIN1-regulated TPR-MYC-GCN5 complex, genes with MYC binding affected by PIN1 tended to localize to the nuclear periphery at early time points following serum stimulation and subsequently showed a shift to the nuclear interior, indicating a genome re-organization as cells progress through the cell cycle (Strickfaden et al., 2010; Vazquez et al., 2001). These dynamic movements were impaired by loss of PIN1, as was MYC DNA binding, histone acetylation, and gene transcription (Figure 6). Genome organization and histone modification status are tightly associated with each other (Huang et al., 2015; Zhou et al., 2011). It was shown that global histone acetylation following

PIN1 regulates the spatial distribution of transcriptionally active MYC at the nuclear pore

treatment with a HDAC inhibitor induced genomic reorganization including promoter region, euchromatin domains and differentially expressed gene recruitment to the nuclear pore (Brown et al., 2008). Interestingly, in mouse oligodendrocyte progenitor cells, silencing of MYC was associated with a decrease in the histone acetylation level on target genes and the induction of premature nuclear peripheral chromatin compaction (Magri et al., 2014). In our system, H3 acetylation levels were significantly reduced in PIN1 KO cells at early time points following serum stimulation (Figure S5b), and this was seen at individually interrogated genes associated with reduced GCN5 and MYC DNA binding and gene expression in the PIN1 KO cells. This further correlated with reduced MYC and GCN5 association with TPR in the PIN1 null versus WT cells. In addition, the initiating level of H3ac at *Cdc45*, *Rpl36*, *Snai1*, and *Twist1* were significantly higher than *IgH*, suggesting the increase of H3ac on these genes was an expansion of already existing eu-chromatin rather than a switch from completely heterochromatin (Figure S6D). Finally, the “detachment” of these loci from TPR binding (Figure S6B) and their movement toward the nuclear interior at later time points in the WT cells may reflect a transition from individual gene induction at the periphery to a coordinated expression with other genes in the interior, consistent with the steady increase in mRNA expression observed during the time course (Figure 6E), all of which were dampened in the PIN1 null cells. For future studies, a detailed map of chromatin loop formation can be revealed by

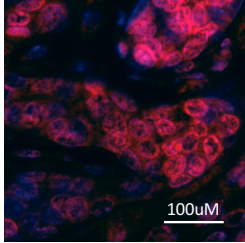
PIN1 regulates the spatial distribution of transcriptionally active MYC at the nuclear pore

the Chromatin Conformation Capture technologies (Davies et al., 2017; Schmitt et al., 2016).

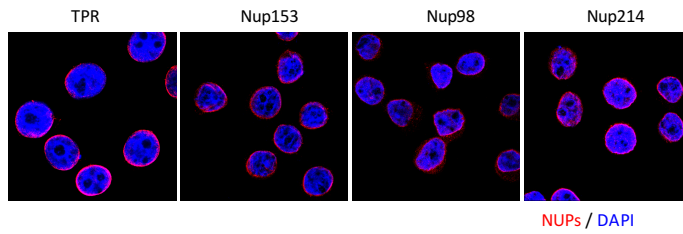
In summary, our study addresses post-translational regulation of MYC localization within the nucleus. We characterized the association between MYC and the nuclear pore basket, which is tightly regulated by Ser62 phosphorylation and PIN1 catalysis. Our study suggests that MYC proteins in the PIN1 depleted cells, although they may have elevated expression level (Yeh et al., 2004b), lack the conformation controlled by PIN1 to efficiently localize to certain nuclear compartments to facilitate the timely regulation of target genes (Farrell et al., 2013). We find that the association of MYC at the pore basket activates sets of genes including pro-growth and pro-migration genes by facilitating histone acetylation through GCN5, these gene subsequently migrate toward the interior of the nucleus, which is comprised of larger euchromatin domains. Both the movement of MYC and these gene loci are impaired in PIN1 KO cells. At this point it is not clear how PIN1 affects chromatin reorganization. This study provides important mechanistic insight into MYC subnuclear localization and its effects on gene regulation. Future understanding of dynamic spatial and temporal control of transcription factors and genome architecture to accurately control gene expression is essential to understand phenotype plasticity in cellular response to environmental changes that underlie normal and diseased states.

Supplemental Figures

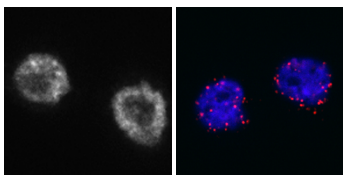
A ROSA-LSL-Myc; NeuNT; Blg-cre.



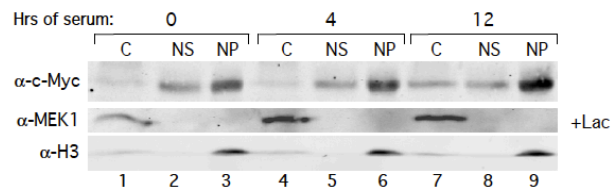
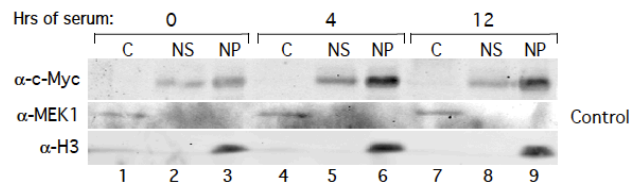
B



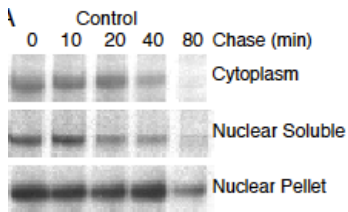
C pS62 MYC pS62 MYC-TPR



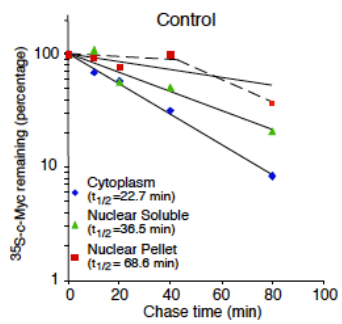
D



E



F



G

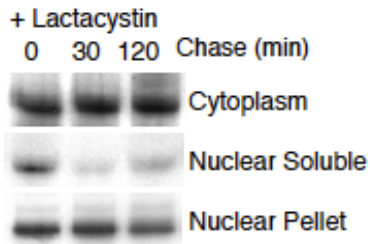


Figure S3.1, related to Figure 3.1

(A) IF staining of pS62 MYC in mouse breast tumor driven by Blg-cre induced MYC and oncogenic Her2 (NeuNT) showing nuclear peripheral signal.

(B) IF staining of nucleoporins (Nups) as controls for Figure 3.1 D.

(C) PLA between pS62 MYC and TPR using a different pS62 MYC antibody (Farrell et al., 2014; Zhang et al., 2012), in support of Figure 1F.

(D) Quiescent REF52 fibroblasts were maintained in low-serum media for 18hr, and stimulated by 20% FBS for 4hr and 12hr as indicated. At 3.5hr prior to harvesting, 10uM lactacystin (proteasome) was added as indicated. Harvested cells were lysed in low-salt and low-detergent lysis buffer to obtain the cytoplasmic fraction (C). After a cytoplasmic was, the nuclear soluble fraction (NS) was collected in the same lysis buffer with 0.5M NaCl and the nuclear pellet (NP) was solublized by boiling in 2X SDS sample buffer.

(E-F) Quiescent REF52 cells were infected with Ad-MYC (rel.MOI=0.12). Infected cells were maintained in low-serum (0.25%) for an additional 18hr. Cells were serum stimulated with 20% FBS for 13 hrs and then pulse labeled with ³⁵S-methionine/cysteine and chased with medium containing excess unlabeled methionine and cysteine. Cells were harvested after various chase times and fractionated in (C). All fractions were adjusted to immunoprecipitation conditions and ³⁵S labelled MYC was immunoprecipitated and sperated by SDS-PAGE. Percent of MYC remaining was graphed on semi-log plots and best-fit exponential lines were calculated by Excel. The equation for the line was used to calculate the half-life.

(G) Cells were treated as in (E) except 4hr prior to harvesting, 10uM lactacystin was added and pulse/chase analysis was in the continued presence of lactacystin.

D - G were done by former lab member, Kristi Piehl.

PIN1 regulates the spatial distribution of transcriptionally active MYC at the nuclear pore

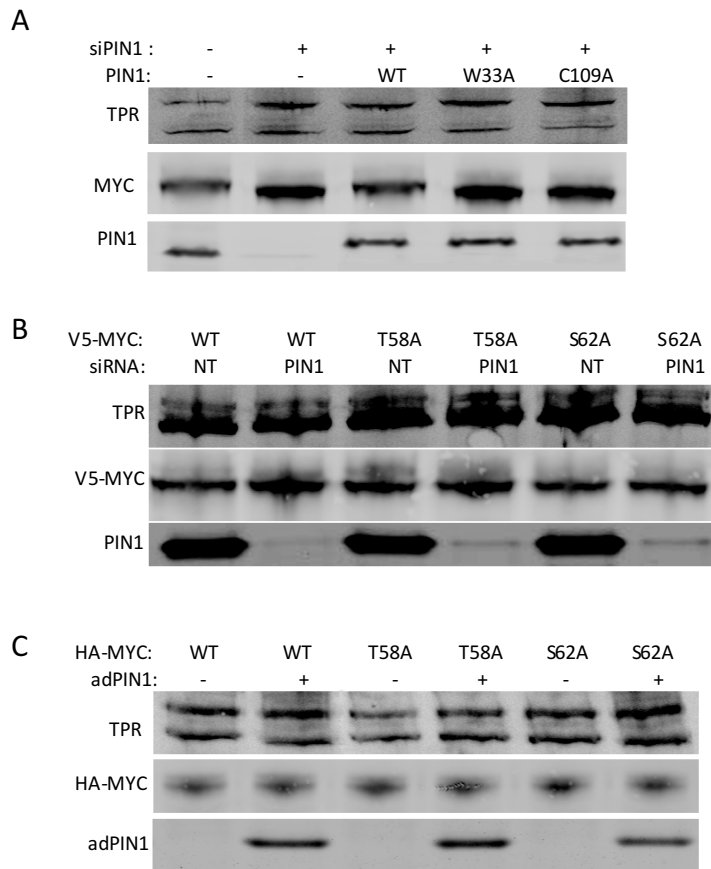


Figure S3.2, related to Figure 3.3

(A) Western Blot of the expression of TPR, MYC, and PIN1 for Figure 3.3 C.

(B) Western Blot of the expression of TPR, V5, and PIN1 for Figure 3.3 E.

(C) Western Blot of the expression of TPR, HA, and PIN1 for Figure 3.3 F.

PIN1 regulates the spatial distribution of transcriptionally active MYC at the nuclear pore

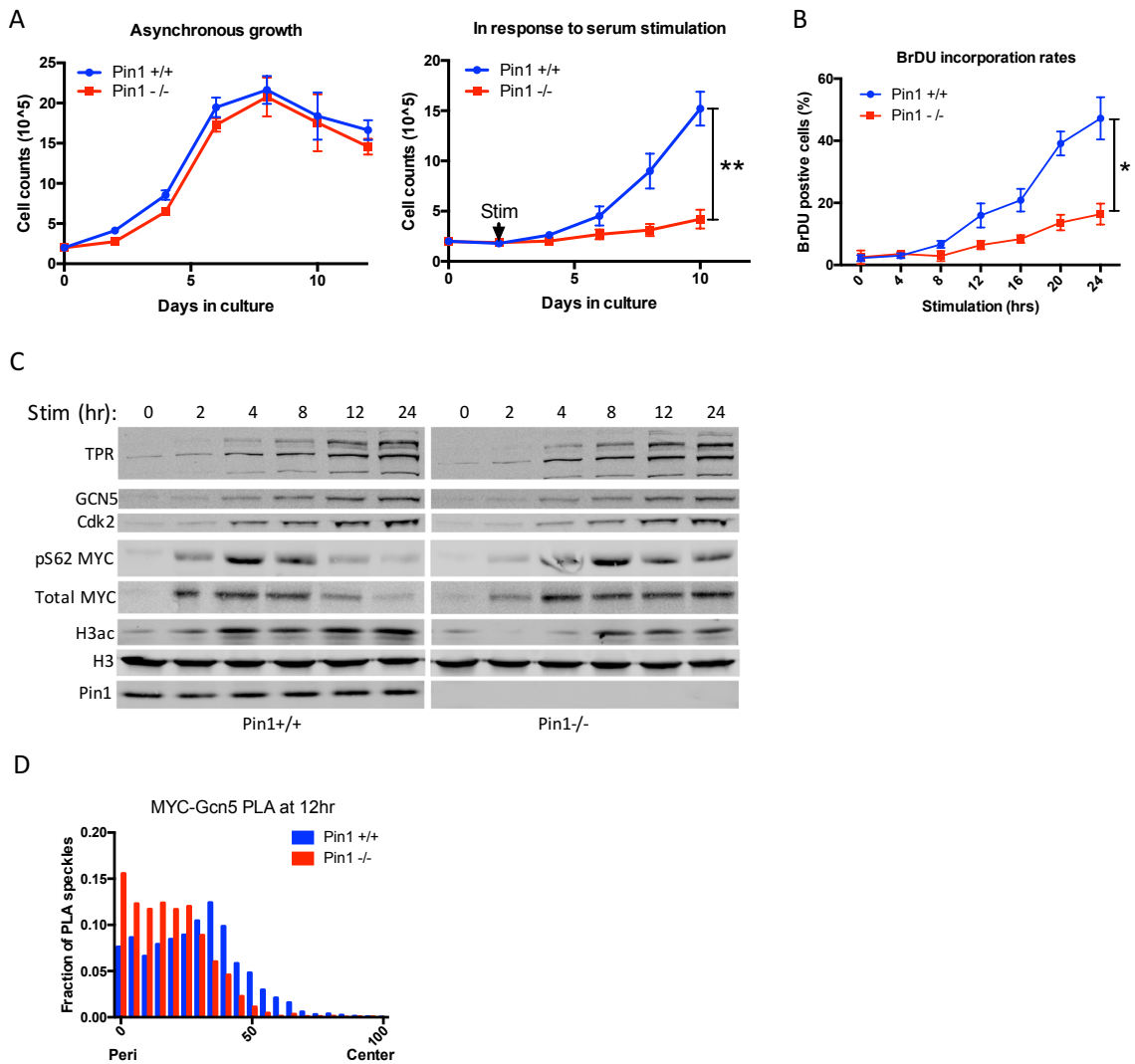
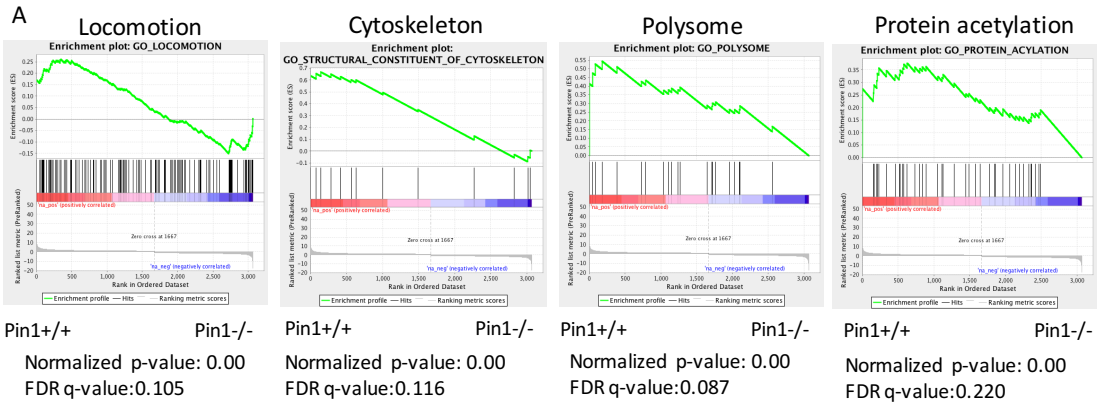


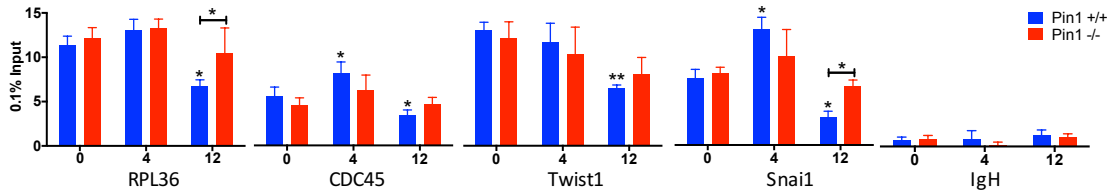
Figure S3.3, related to Figure 3.5

(A) Quantification of MEF cell growth under asynchronous and serum stimulation conditions. (B) BrDU incorporation of MEF cells during serum stimulation. (C) Western Blot of the expression of TPR, GCN5, CDK2, pS62 MYC, total MYC, Histone 3 acetylation (H3ac), H3, and Pin1 for Figure 3.5. (D) Difference of MYC-GCN5 PLA radial distribution between Pin1+/+ (blue) and Pin1-/- (red) MEFs at 12 hr post serum stimulation.

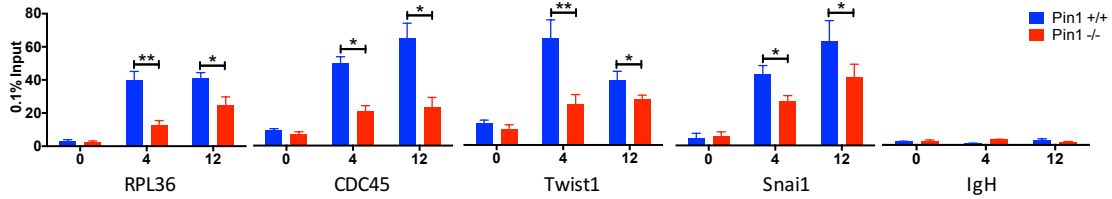
PIN1 regulates the spatial distribution of transcriptionally active MYC at the nuclear pore



B TPR binding



C GCN5 binding



D H3ac level

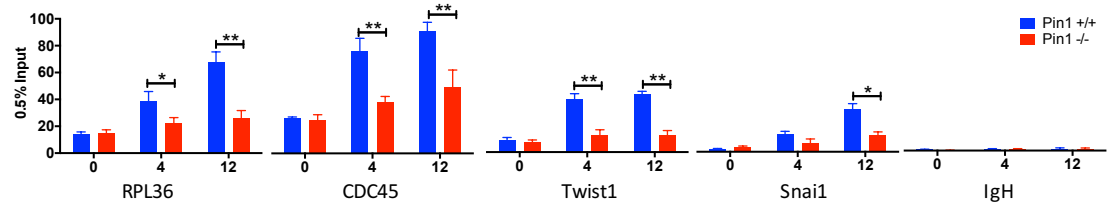


Figure S3.4, related to Figure 3.6

(A) Genes preferentially bound by MYC in Pin1 ^{+/+} MEFs (left) and Pin1 ^{-/-} MEFs (right) were used as ranked list and tested for enrichment of pathways via Gene Set Enrichment Analysis (GSEA). Shown were some of the most significantly enriched pathways of all C5 gene sets.

(B) qChIP of TPR binding to the indicated target genes in Pin1^{+/+} (Blue) and Pin1 ^{-/-} (Red) MEFs during serum stimulation. Statistical significance relative to 0hr was calculated using a two-tailed t test: *p < 0.05; **p < 0.01; ***p < 0.001. and labeled at the top of individual column.

(C) qChIP of GCN5 binding to the indicated target genes in Pin1^{+/+} (Blue) and Pin1 ^{-/-} (Red) MEFs during serum stimulation.

(D) qChIP of Histone 3 acetylation (H3ac) level of indicated target genes in Pin1^{+/+} (Blue) and Pin1 ^{-/-} (Red) MEFs during serum stimulation.

Statistical significance relative to WT was calculated using a two-tailed t test: *p < 0.05; **p < 0.01; ***p < 0.001. All quantifications were based on at least three independent experiments.

PIN1 regulates the spatial distribution of transcriptionally active MYC at the nuclear pore

A Ki67 staining at Day 8

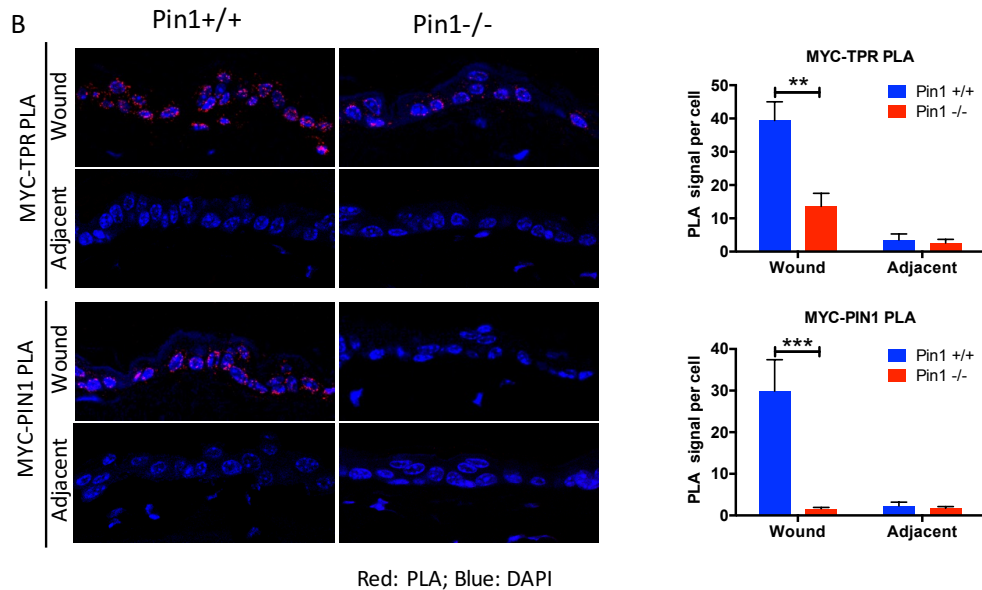
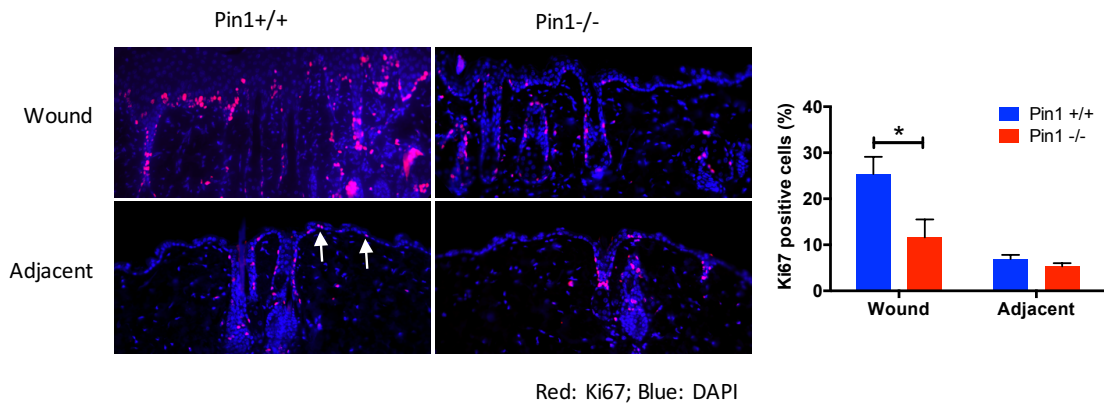


Figure S3.5, related to Figure 3.7

(A) IF of Ki67 (Proliferation marker) of the wound and adjacent skin samples at day 8 post skin punch biopsy. Shown at the right is the quantification of Ki67 positive cells.

(B) PLA of MYC association with TPR and PIN1 (from top to bottom) in Pin1^{+/+} and ^{-/-} mouse skin samples at at day 8 post skin punch biopsy. Shown at the right at the quantification of PLA.

Statistical significance relative to WT was calculated using a two-tailed t test: *p < 0.05; **p < 0.01; ***p < 0.001. All quantifications were based on at least three independent experiments

Acknowledgements

We thank Dr. Matt Thayer and Dr. Susan Olson's laboratories for their help on FISH. Dr. Gail Mandel's laboratories for discussion, and Dr. Stefanie Petrie for help on confocal imaging.

Summary and Discussion

Chapter Four :

Summary and Discussion

Summary and Discussion

The proto-oncoprotein MYC functions as a transcription factor that, by orchestrating a pro-cancer transcription program, drives tumorigenesis and tumor progression. Overexpression of MYC is associated with more than half of solid tumors and multiple blood-borne cancers (reviewed in Dang, 2012). Withdrawal of MYC in mouse tumor models leads to tumor regression (D’Cruz, 2001; Felsher and Bishop, 1999; Pelengaris et al., 1999), highlighting the importance of targeting MYC as a strategy for cancer treatment. However, despite decades of studies on MYC, it is still challenging to target MYC. In this thesis, I presented two studies focused on post-translational modifications of MYC, and specifically on PIN1-mediated proline isomerisation: one addressing the biophysical features of PIN1-MYC interaction, and the other providing insights into how PIN1 controls the nuclear distribution of MYC and associated transcriptional activities.

A novel motif of MYC that primes PIN1 binding

The prolyl isomerase PIN1 is unique in its ability to catalyze the *cis/trans* switch of pSer/pThr-Pro motifs, as demonstrated by studies of PIN1 interactions with small molecules or short peptides. However, most cellular substrates of PIN1 are long peptides with multiple potential target sites for PIN1, many of which reside at or near intrinsically disordered regions (IDRs) that lack a fixed three-dimensional structure, making it hard to understand the real interactions between PIN1 and its targets (van der Lee et al., 2014; Lu et al., 2007). To better model PIN1 interaction with long-peptide substrates as well as to investigate how PIN1

Summary and Discussion

regulates the function of MYC, we took advantage of the most N-terminal part of the MYC TAD domain (MYC₁₋₈₈), a previously characterized IDR of MYC. By a wide range of biophysical and cellular assays, we showed that PIN1 recognizes MYC by pre-anchoring to an unphosphorylated conserved motif N-terminal to MYC Box I (MB1) and thus designated as MB0. Such anchoring potentiates PIN1 to interact with the (p)Ser62-Pro63 motif of MYC and catalyze *cis/trans* isomerization. Importantly, disrupting PIN1 binding to MB0 via mutagenesis impairs MYC transcriptional activity and its capacity to promote cell proliferation.

Why does PIN1 bind to an unphosphorylated region distal to the acting site of its substrate? There are two putative explanations, which are complimentary and could both be applicable. The first is that increases in the local concentration of substrate presented to PIN1 thereby increases its catalytic efficiency. In support of this, PIN1 binds to MB0 prior to Ser62 phosphorylation and expands to the Pro63 region when Ser62 is phosphorylated; disruption of MB0 decreases overall interaction of PIN1 and MYC, suggesting the pre-anchoring of PIN1 to MB0 facilitates its interaction with the pSer62-Pro63 site. The second is that PIN1's binding to MB0 changes the structure of PIN1's interdomain cleft, affecting multiple residues within, including Ile28. Contacts between Ile28 and a small molecule can elevate PIN1's substrate binding and catalytic activity. The changes of PIN1's interdomain cleft may allow PIN1 to sample multiple conformations of its target representing different regulated states of its substrate (Schelhorn et al.,

Summary and Discussion

2015). Interestingly, a wider range of interdomain residues are affected when MYC is phosphorylated at Ser62, suggesting a multi-step activation of PIN1 during its recognition of its targets and that PIN1 binding to MB0 serves to “warm up” PIN1.

Consistent with a potentiating role of MB0 in PIN1’s interaction with MYC, we found that disrupting MB0 through targeted mutagenesis interrupts PIN1-MYC binding in cells, leading to decreased MYC binding to target gene promoters and reduced ability to promote cell proliferation in cooperation with RAS, although it also prolonged MYC half-life. The seemingly contradictory role of PIN1 on MYC is illustrated by a previous study demonstrating that PIN1 isomerization at pSer62-Pro63 in MYC promotes its DNA binding and recruitment of co-factors; the subsequent Thr58-mediated isomerization by PIN1 releases MYC from the promoter associated with its ubiquitin-mediated degradation, rendering MYC to a rapid “on and off” pattern to activate gene transcription (Farrell and Sears, 2014; Farrell et al., 2013). Thus, a MYC mutant with deficient PIN1 interaction might be more stable but would not promote transcriptional or oncogenic activity.

Lastly, this study may help to target PIN1 or MYC for potential cancer therapeutics. Coincidentally, a previously published cyclic peptide (CTGI**PWLYC**) that can inhibit the activity of PIN1 shares a similar sequence with the MYC MB0 motif (PYFY) (Duncan et al., 2011). The possible mechanism is that the

Summary and Discussion

sequence similarities with MB0 allows it to be recognized by PIN1, but the cyclic structure locks the peptide into a certain proline conformation that prevents its release from PIN1, thus blocking PIN1 binding to other substrates. Now, with the knowledge of PIN1's binding to MB0, we can either modify the cyclic peptide with better efficacy or design novel MB0 mimics that may compete off the cooperation between MYC and PIN1 that drives cancer.

PIN1 regulates the subnuclear localization of MYC

Our second study addressed the fundamental question of how the nuclear localization of MYC affects its activity.

It is more and more evident that nuclear architecture and gene positioning have a substantial influence on gene transcription (Fraser and Bickmore, 2007; Nguyen and Bosco, 2015). Particularly, genes in the nuclear interior are usually associated with open chromatin and transcriptionally permissive, whereas genes localized at the nuclear periphery tend to be transcriptionally repressive and associated with condensed chromatin. A notable exception are genes associated with the nuclear pore, which although localized to the periphery, are usually transcriptionally active (Ishii et al., 2002; Krull et al., 2004; Luthra et al., 2007; Rajanala and Nandicoori, 2012; Strambio-De-Castillia et al., 2010). A recent study indicated that pS62 MYC is enriched at the nuclear peripheral lamin A/C-

Summary and Discussion

associated structure (LAS), but also that the LAS is a relatively crude component that may include the lamina-embedded nuclear pore complex (NPC). In fact, in some early electron microscopy images, MYC signals localized in the vicinity of the nuclear pores. Moreover, in response to DNA damage, sustenance of pS62 MYC in the nuclear periphery resulted in transactivation of Myc target genes (Myant et al., 2015). Together with the transcriptionally permissive feature of genes associated with the nuclear pore, we speculated that the NPC might be a key location for MYC at the periphery.

In support of our hypothesis, both imaging and subcellular fractionation data indicate that pS62 MYC can interact with TPR, a subunit of the nuclear pore basket. This interaction is dependent on Ser62 phosphorylation, downstream of the functions of ERK and CDK2 kinases. The importance of Ser62 phosphorylation on MYC's association with the NPC is mediated by PIN1-dependent isomerization: overexpression of PIN1 enhances pSer62 MYC localization to TPR, whereas knockdown of PIN1 dissociates pSer62 MYC from TPR. Consistent with the previous observation that PIN1 promotes MYC interaction with the histone acetyl transferase GCN5 and that GCN5 interacts with the nuclear pore basket, we found that PIN1-mediated MYC interaction with TPR further recruits GCN5, thus forming the TPR-MYC-GCN5 complex.

Summary and Discussion

What is the function of this complex? How is it regulated by PIN1? To address these questions, note that the physiological function of PIN1 may be most evident upon the cellular response to environmental changes. For instance, *Pin1* knockout fibroblasts grow similarly to wild-type in asynchronous cultures but exhibit defects when recovered from serum starvation. Taking advantage of this process, we found that the formation of the TPR-MYC-GCN5 complex at the nuclear periphery following serum stimulation was suppressed by loss of PIN1. Concomitantly, associated MYC target genes were less induced by serum stimulation, marked by lack of histone acetylation and reduced transcripts in PIN1-deficient cells. This impaired MYC target gene transcription persists in the *Pin1* knockout cells during the late stage of serum response when MYC-GCN5-PIN1 complex is translocated to the interior of the nucleus in wildtype cells.

How does the complex localization correlate with the movement of MYC target genes, and what is the biological meaning of this regulation? Using FISH, we observed a nuclear peripheral localization of MYC target genes (*Rpl36*, *Cdc45*, *Twist1*, and *Snai1*) at 0 and 4hr time points, when the complex involving MYC, GCN5, and PIN1 exhibit a similar pattern. This supports the hypothesis that formation of MYC-GCN5-PIN1 complex at the nuclear pore interacts with neighbouring chromatin and genes. At the 12 hr time point, when the MYC-GCN5-PIN1 complex, indicated by PLA signal, migrates to the nuclear interior, I observed a shift of the FISH signal to the interior in the wildtype cells but not the

Summary and Discussion

Pin1 knockout cells, suggesting that PIN1 promotes cell-cycle associated chromatin reorganization (Bridger et al., 2000; Kind et al., 2013). The co-shift of MYC protein complex with targets genes to the nuclear interior was associated with stronger induction of gene expression at 12hr in the PIN1 WT cells, consistent with a more permissive transcriptional environment at the nuclear interior indicated by previous studies (Geyer et al., 2011; Pombo and Dillon, 2015). However, we do not know whether MYC or PIN1 or both play an active role in driving the movement of chromatin, as retaining the FISH signal at the periphery in PIN1^{-/-} cells could be the result of the defect in cell cycle progression due to loss of PIN1. This question could be addressed in the future by inhibiting cell cycle progression in wild-type cells and measuring the target gene movements. One way to achieve cell cycle inhibition without interfering upstream of MYC would be p21 overexpression (Sears et al., 2000). Moreover, loss of PIN1 seems to not affect the chromatin organization prior to mitogen stimulation, as the localizations of the representative genes are similar between *Pin1* wildtype and knockout cells at 0hr timepoint: the MYC target genes are localized at the nuclear pore (suggested by TPR binding in qChIP experiments) regardless of the PIN1 presence. Interestingly, the H3ac levels of MYC target genes, although low at 0hr, are higher than the *IgH* locus, which has been demonstrated to be associated with lamina and repressed in fibroblast cells (Malhas et al., 2007). Thus, the chromatin of MYC target genes might be at a poised state that in response to mitogen stimulation can be rapidly activated. The association of

Summary and Discussion

responsive genes with the nuclear pore can be explained by a mechanism that the nuclear pore preserves the epigenetic transcriptional memory to allow rapid induction of many genes during the cell cycle (Light and Brickner, 2013; Tan-Wong et al., 2009). Based on these evidence, I propose a model in which upon extracellular stimuli (e.g. mitogen stimulaiton), PIN1 recruits MYC to the nuclear pore to activate neighbouring poised genes by induction of histone acetyaltion, which leads to chromatin remodeling and relocalize of these genes to the nuclear interior for sustained expression. This model can be tested by high throughput chromatin conformation capture technologies (Hi-C) in the near future (Schmitt et al., 2016).

A role for PIN1 in controlling the dynamic movement of MYC through the nucleus may extend to relocalization for MYC turnover as we have observed in some preliminary studies. This work was based on an interesting study on the regulation of Cyclin E by PIN1, which indicated that PIN1 facilitates the translocation of Cyclin E following priming ubiquitinylation by FBW7 α in the nucleoplasm to the nucleolus, where it is further polyubiquitinylated by FBW7 γ for proteasomal degradation (Bhaskaran et al., 2013). Since MYC is similarly ubiquitinylated by both FBW7 α in the nucleoplasm and FBW7 γ in the nucleolus, and the latter appears to be the predominant location for MYC turnover (Arabi et al., 2003; Grim et al., 2008), it is possible that PIN1 plays a similar role in regulating MYC sub-nuclear localization. To test this hypothesis, we first utilized

Summary and Discussion

an experimental system where treatment with proteasome inhibitors (e.g. MG132 and Lactacystin) will accumulate MYC in the nucleolus. Depletion of PIN1 by siRNA severely inhibited the accumulation of MYC in three commonly used cell lines, and this was recapitulated in *Pin1* knockout cells (Figure 4.1). Secondly, based on a previous study in which the MYC deubiquitination enzyme USP36 inhibits MYC proteasomal degradation in the nucleolus (Sun et al., 2015), we designed epistasis experiments between USP36 and PIN1 (Figure 4.2). We found that overexpressing USP36 prevented PIN1-mediated MYC degradation and that knockdown of PIN1 reduced USP36-driven stabilization of MYC in the nucleolus, suggesting that PIN1 is upstream of USP36 function potentially through shuttling MYC to the nucleolus. To further confirm the role of PIN1 in shuttling MYC to the nucleolus, we measured MYC driven pre-rRNA synthesis, which occurs exclusively in the nucleolus, in response to changes in PIN1 levels. Consistently, knockdown of PIN1 reduced and PIN1 overexpression promoted the pre-rRNA synthesis induced by MYC (Figure 4.3).

Summary and Discussion

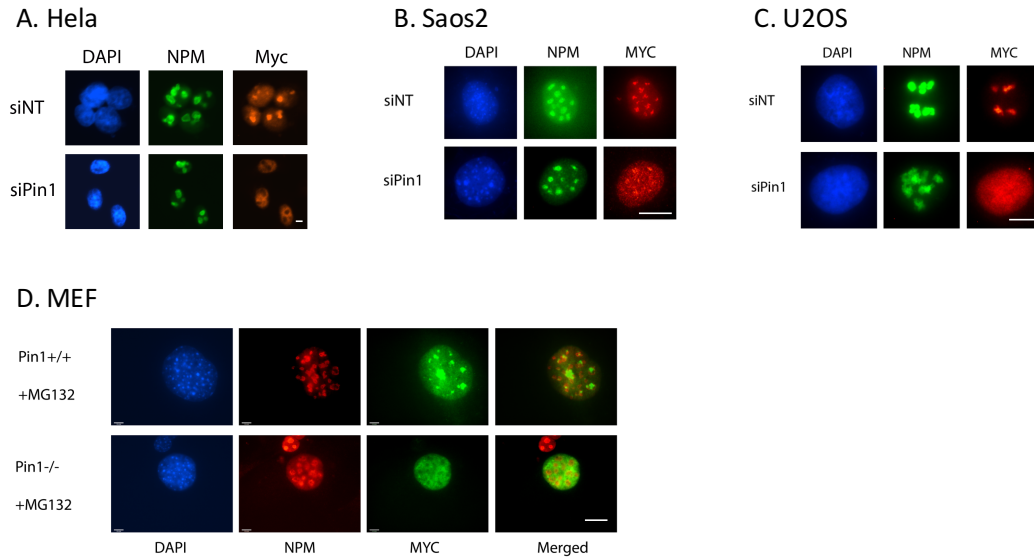


Figure 4.1: PIN1 regulates MYC translocation to the nucleolus.

(A-D) Immunofluorescence (IF) staining of MYC together with nucleolar marker Nucleophosmin (NPM) in human cell lines HeLa, Saos2, U2OS, and in Pin1 wild-type (+/+) or knockout (-/-) mouse embryonic fibroblast (MEF). (A-C) Cells were transfected with 20nM siRNA of PIN1 or non-target (NT) for 48hrs before proteasome inhibition treatment. (A-D) Cells were grown to ~80% confluence, and treated with 10uM proteasome inhibitor MG132 for 4hrs before analysis. Scale bars represent 5µm in length.

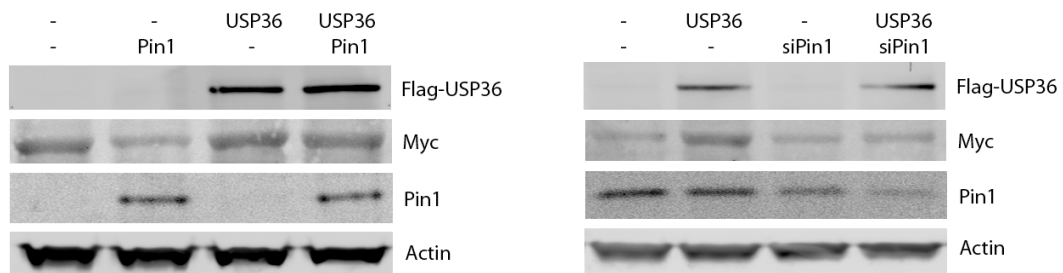


Figure 4.2: PIN1 is the upstream of USP36 in the MYC degradation pathway.

Western Blot of MYC expression (detected by ab32073, Abcam) in 293 cells transfected with USP36 (Sun et al., 2015), PIN1 (Farrell et al., 2013), and siRNA of PIN1 (Dharmacon) for 48hrs.

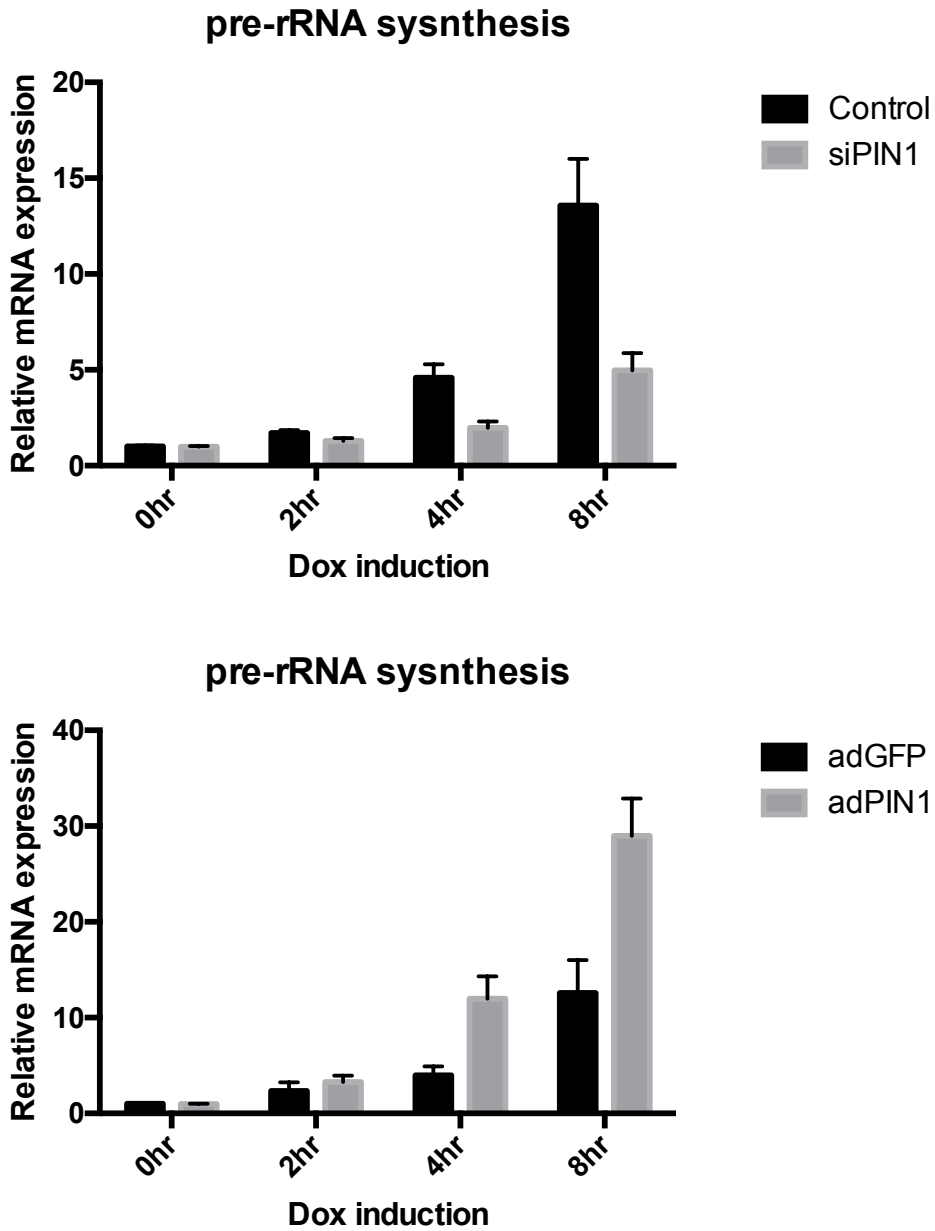


Figure 4.3: PIN1 promotes MYC driven pre-rRNA synthesis.

qPCR of pre-rRNA (primers from Dr. Mushui Dai's lab) in dox inducible MCF10A cells (Farrell et al., 2013). Cells were treated with 1.5uM Dox for indicated time for harvesting RNA using Qiagen Rneasy kit.

Summary and Discussion

Thus, based on published results with Cyclin E, and published and unpublished data on MYC, PIN1 and MYC proline isomerization may play an important role in the sub-nuclear movement of MYC as it transitions through its mitogen-stimulated life-cycle—from S62 phosphorylation and association with the nuclear periphery (including the NPC) to Pol II target gene binding and regulation in the nucleoplasm to nucleolar translocation and Pol I rDNA transcription, and proteasomal degradation (Figure 4.4).

Together, a dynamic picture of PIN1-mediated MYC regulation is emerging (Figure 4.4). Whether this regulation allows for selective MYC target gene control that could help explain the observed effects of PIN1 on selective MYC functions, such as proliferation versus apoptosis or stemness versus differentiation, is a critical question requiring further elucidation.

Summary and Discussion

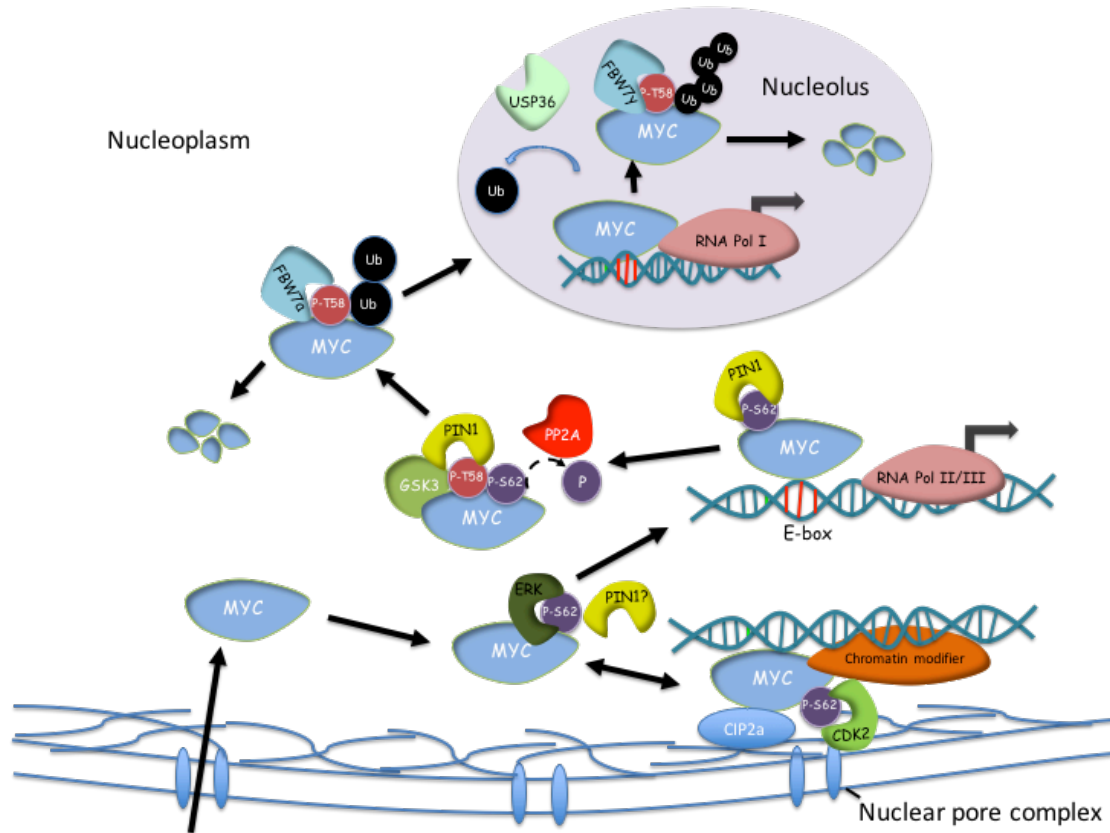


Figure 4.4: PIN1 mediated dynamic MYC localization in the nucleus.

A schematic of our proposed model of dynamic localization of MYC in the nucleus: After import to the nucleus, MYC is phosphorylated at Ser62 by ERK in the nucleoplasm or CDK2 at the nuclear pore complex in response to growth stimulatory signals. The pS62 MYC is catalyzed by PIN1 to be in the *cis* conformation, facilitating its interaction with the nuclear pore basket. This may be stabilized by the PP2A inhibitor CIP2A. The nuclear pore associated MYC recruits chromatin modifiers such as GCN5 to decondense adjacent chromatin for active gene transcription. The pS62 MYC in *cis* also binds to open chromatin or gene targets that are localized at the nucleoplasm to facilitate Pol II/III mediated transcription. The subsequent isomerization by PIN1 renders MYC into *trans*, releasing MYC from chromatin, promoting GSK3b-mediated phosphorylation on T58 and PP2A-mediated dephosphorylation on S62. The pT58 MYC is either degraded in the nucleoplasm by Fbw7 α -mediated ubiquitylation or translocated to the nucleolus to activate rRNA synthesis by Pol I. Finally, the nucleolus-specific Fbw7 γ ubiquitinates MYC and promotes its proteasomal degradation in the nucleolus.

Chapter Five :

Materials and Methods

Plasmids and siRNA

Construction of expression plasmids CMV-empty, CMV-βgal, CMV-Myc, pCEP-small-T-antigen, pD40-His/V5-c-Myc, pD40-His/V5-c-Myc^{T58A}, and pD40-His/V5-c-Myc^{S62A}, as well as reporter constructs, E2F2-Luc, and E2F2(-E-box)-Luc have previously been described (Sears et al. 1997; Yeh et al. 2004).

siRNA were purchased from the following resources and performed according to manufacturers:

<http://dharmacon.gelifesciences.com/sirna/sigenome-lamin-a/c-control-sirna/>

https://www.thermofisher.com/order/genome-database/SIRNA/gene/NUP153_137886

https://www.thermofisher.com/order/genome-database/SIRNA/gene/NUP205_261156

https://www.scbt.com/scbt/product/nup214-sirna-h-shrna-and-lentiviral-particle-gene-silencers?requestFrom=search_sc-106320

https://www.scbt.com/scbt/product/cdk4-sirna-h-shrna-and-lentiviral-particle-gene-silencers_sc-29261

https://www.thermofisher.com/order/genome-database/browse/sirna/gene/NUP98_Cat.#_AM16708

Table 5.1: Primer sequences.

RT-PCR Primers

Target	Foward	Reverse
Cdc45	tatagcgtggtccggttc	ctctcctggttcgctccac
Rpl36	caccaaacacaccaagttcg	ctttattgggggagggttc
Twist1	ggacaagctgagcaagattca	cggagaaggcgtagctgag

Materials and Methods

Snai1	gcgtgtgtggagttcaccttc	ggttgaggacctcgggc
IgH	ttctgagcattgcagactaatcttg	cctagacagttatttcccaacttctc

ChIP Primer

Target	Foward	Reverse
Cdc45	AATCGGTCACGAACATAGCC	CTGTCCCCAGTAGGAACCAA
Rpl36	ATCAGGTAAGTGGGCCTCGT	TGTGTCTCGGCTTACTGACG
Twist1	gcaccaaggctgctctatct	tctcaagacgtggccacatc
Snai1	cggagttgactaccgacctt	gacctaggtagtcgggggtcac
IgH	CCCAGACCCATGTCTCAACT	GTCACAATGTGCCTGGTTTG

Cell-lines and Transfection

HEK293 and REF52 cells were cultured as previously described (Farrell et al., 2013; Yeh et al., 2004). Specifically, cells were maintained in Dulbecco's modified Eagle's medium (DMEM) supplemented with 10% standard fetal bovine serum (FBS), 2.5 mM L- glutamine, and 1 x penicillin-streptomycin. HEK293s were passaged every 2 days, REF52 were passaged every 3-4 days. Plating of cells was done to achieve 60– 80% confluency 24 h post-split for transfection. All transfections were performed using Lipofectamine 2000 (Life technology, U.S.). Total transfected DNA was held constant (unless otherwise indicated) by the addition of empty control plasmid and included 50 ng of CMV-b-gal to normalize for transfection efficiencies between experimental conditions.

Antibodies

List of antibodies used:

S62 MYC (abcam 78318 mouse) tissue IF (homemade)

Total MYC (N262 rabbit; santa cruz C33 mouse)

pT58 MYC (Abm, Y011034)

Tpr (mous SC121094; rabbit SC67116)

Gcn5 (rabbit sc20698)

Cdk2 (rabbit sc-163)

Cdk4 (rabbit sc-160)

H3ac (Millipore 06-599)

H3 (upstate 31560)

Erk (rabbit CSG 4695S)

Nup153 mouse ab24700

Nup214 rabbit ab70497

Nup98 mouse sc-74578

LaminA/C mouse sc-7292; rabbit sc-20681; goat sc-6215

V5 invitrogen mouse 1718556

HA Abm G036 mouse

Pin1 Novas Biologicals 2f2 mouse; rabbit sc-15340

Western Blotting

Cell lysates were run on SDS-PAGE gels and transferred to Immobilon-FL membranes (Millipore). The membranes were blocked with Odyssey blocking buffer (LI-COR Biosciences, Lincoln, NE). Primary antibodies were diluted in 1:1 Odyssey blocking buffer-PBS with 0.05% Tween 20. Primary antibodies were detected with secondary antibodies labeled with the near-infrared fluorescent dyes IRDye800 (Rockland, Philadelphia, PA) and Alexa Fluor 680 (Molecular Probes, Eugene, OR). Secondary antibodies were diluted 1:10,000 in 1:1 Odyssey blocking buffer-PBS with 0.05% Tween 20. Blots were scanned with an Odyssey infrared imager (LI-COR Biosciences) to visualize proteins.

RT-PCR analysis

Transfected HEK-293 cells were collected in 1XPBS with 1mM EDTA, 5% of the cells were reserved for β gal assay and western analysis. RNA was isolated from cells exhibiting transfection efficiencies within 5% of each other using TRIzol reagent from Invitrogen (Carlsbad, CA). cDNA was made using the M-MLV Reverse Transcriptase according to manufacturer's protocol (Invitrogen). 2X Immunomix Red from BIOLINE (Randolph, MA) was used for PCR analysis of cDNA (see supplemental information for primer sequence and thermocycler setup).

qRT-PCR analysis

RNA was isolated from 293tr-V5-Axin1 cells collected in 1mL TRIzol reagent (Invitrogen) according to manufacturer's protocol. Isolated RNA was DNase treated in 100mM MgCl₂, 10mM DTT, RNasin (Promega), RNase free DNase (Roche) for 15 minutes at 37°C and purified using RNeasy (Qiagen). cDNA was made from DNase treated RNA using M-MLV Reverse Transcriptase (Invitrogen) according to manufacturer's protocol with oligo dT primers. qRT-PCR analysis was done using primers for *c-myc* and *18S* as designed by Applied Biosystems on a 7300 qRT-PCR machine (Applied Biosystems) according to manufacturer's preset qRT-PCR cycle conditions.

Cyclohexamide half-life

100mM dishes of HEK-293 cells were cotransfected with 50ng CMV-βgal, 0.5ug pD40-His/V5-c-Myc and 4ug pSUPER-empty or B56α for c-Myc/PP2A-B56α experiments or pENTR-H1/TO-scramble, Axin1, or B56α for c-Myc/Axin1 experiments under 10% FBS serum conditions for 24hrs. Each transfection was split into six 60mM dishes and maintained for 24hrs in DMEM supplemented with 10% FBS and L-glutamine and then starved in DMEM supplemented with 0.2% FBS and L-glutamine for 48hrs. Cells were treated with 100ug/mL cyclohexamide for 5-15 minutes and then the indicated time points were collected.

Coimmunoprecipitation

HEK293 cells were transfected with V5 tagged Myc and other indicated plasmids for 2 days. A total of $\sim 5 \times 10^6$ HEK293 cells were washed with phosphate-buffered saline (PBS) once, and then resuspended in 1 ml of co-IP buffer (20 mM Tris, pH 7.5, 12.5% glycerol, 0.5% NP-40, 150 mM NaCl, 2 mM EDTA, 2 mM EGTA, and 1 mM DTT) plus protease and phosphatase inhibitors. Cellular lysates were sonicated for 10 pulses (output 1; 15% duty cycle; Branson Sonifier 450), incubated on ice for 20 min, and cleared by centrifugation at 14,000 rpm for 10 min at 4°C. The supernatants were adjusted for transfection efficiency as measured by β -Gal activity and incubated with 2 μ g of V5 antibody for 1 hour at room temperature and then added protein A Sepharose beads (Repligen, Waltham, MA) for 1 hour at 4°C. The immunoprecipitates were washed 3 times with 1 ml of co-IP buffer and analyzed by Western blotting for Myc phosphorylation status or other co-IPed proteins.

Colony Formation Assay

REF52 cells were grown about 80% confluence in p100 plates for transfection. Expression vectors containing c-Myc WT or mutant (pEntr-Dest40, 1 μ g/plate) and H- rasG12V (pBabe, 1 μ g/plate) were used for transfections. Where indicated, transfections were supplemented with respective empty vectors as

Materials and Methods

controls. 72-hour posttransfections, cells were re-plated into p100s at low density (5k – 25k cells/plate). Following re-plating, cells were maintained in DMEM containing 4% fetal bovine serum, and the colonies were visualized by staining with crystal violet blue 2 weeks later.

FISH Assay

The protocol is based on Vysis LSI (Locus Specific Identifier) DNA Probe FISH Procedure and (Shachar et al., 2015). Cells were fixed in 4% PFA in PBS for 15 min, permeabilized in 0.5% Saponin (Sigma Aldrich) / 0.5% Triton X-100 / PBS for 20 min at RT and incubated in 0.1 N HCl for 15 min at RT. Cells were precipitated by 5 min incubation each in a gradient of EtOH at 70%, 85%, and 100%. Cells were kept in 50% formamide/23% SSC for at least 30 min at RT. A probe mix containing 7ul LSI/WCP Hybridization Buffer, 1ul fluorescently labeled probes and 2 ul purified H₂O was then added, denatured together with cells at 74 °C for 7 min and left to hybridize at 37 °C overnight. Excess probe was washed three times with each: 2X SSC/0.1% NP-40 at 42 °C for 5 min. Cells were finally stained with DAPI in PBS (5 ng/ml) before imaging.

Luciferase Assay

Approximately 5x10⁵ HEK293 cells were washed with PBS once, and then resuspended in 200ul of cell lysis buffer (Promega, Madison, WI) with protease and phosphatase inhibitors. Cellular lysates were sonicated for 10 pulses at

Materials and Methods

output 1, 10% duty cycle (Branson Sonifier 450), then incubated on ice for 20 min. The supernatant lysates were collected after centrifugation at 14,000 rpm for 10 min at 4°C. Luciferase activity was measured using the standard Promega luciferase assay kit and a Berthold (Bundoora, Australia) luminometer. Luciferase activity was adjusted by β -Gal activity. Fold changes in luciferase activities were measured relative to empty vector or control transfections.

ChIP-seq analysis

ChIP-seq and the analysis were done based on the previously published (Xie et al., 2011). Basically, ChIP data was filtered to remove sequences duplicated more than 5 times (first 5 sequences are used). A sliding window of 2300 bp was then used to call peaks with a peak FDR (False Discovery Rate) threshold of 0.05. Only peaks that were at least 4 fold over background were accepted (using YS_Pin1_null_b1_INPUT as background input). Peaks within 5kb of satellite repeats were also rejected. Next, "consistency analysis of peak calling on replicates" by Qunhua Li and Anshul Kundaje (Oct,2010)

(see: <https://github.com/spundhir/idr>) was applied to each pair of replicate ChIP peaks to select consistently detected peaks with an IDR (Irreproducibility Discovery Rate) FDR threshold of 0.10. These IDR peaks from both WT replicates and Pin1 null replicates were merged to give a set of enriched and reproducible peaks to further analyze. The original ChIP sequencing data was then filtered to allow only sequence alignments in these regions. Counts were

Materials and Methods

then normalized to total sequence counts in these regions. Finally, sums of these filtered and normalized sequence counts were generated for 5kb windows centered on the TSS (Transcription Start Sites) for RefSeq genes.

Proximity Ligation Assay and Immunofluorescence

The PLA assay was performed following the manufacturer's protocol (Duolink Sigma). Briefly, cells plated on chamber slides were grown to 70% confluence, fixed with 4% PFA for 15min, blocked with blocking solution for 30 mins, followed by incubating the primary antibodies at 4°C shaker overnight. The next day, samples were incubated with PLA probes for 1hr at RT and 1hr at 37°C, followed by ligation at 37°C for 1hr. After brief wash, amplifications were carried out at 37°C for 2hr, before staining for DAPI for 5-10 mins and processed to confocal imaging (Zeiss LSM880). Subsequently, cells were washed with buffer A, and the PLA probe was incubated in a pre-heated humidity chamber for 1 hr at 37°C, followed by ligase reaction in a pre-heated humidity chamber for 1 hr at 37°C. Next, amplification polymerase solution for PLA and the secondary antibodies (if counter staining needed) were added, followed by incubating the cells in a pre-heated humidity chamber for 100 min at 37°C.

For tissue samples, formalin-fixed slides were dewaxed in xylene and rehydrated in decreasing concentrations of alcohol, followed by washing two times in tap water. The slides were then incubated in antigen retrieval buffer (Lab Vision

Materials and Methods

citrate buffer, Thermo Scientific) for 30 min at 99°C, followed by cooling down to room temperature and rinsing the slides in distilled water (dH₂O). Next, the slides were blocked for 15 min in 1.5% H₂O₂ solution in PBS, followed by rising in dH₂O and rinsing once in Tris-buffered saline with Tween 20 (TBST) buffer. Finally, the PLA assay was performed following the PLA protocol for cell staining from blocking slides by blocking solution.

Appendix

Contribution to Figures:

Figure 2.1 – 2.6: Dr. Sunnerhagen's group performed the experiments and generated the figures.

Figure 3.1: Dr. Tao Huang from Dr. Xiaolin Nan's group performed the STORM analysis.

Figure 3.4: Colin Danial performed the colP experiment.

Figure 3.7: Dr. Xiaoyan Wang helped with tissue section and the histology analysis.

Figure S3.1 (D-G): Dr. Kristi Piehl performed the experiments and generated the data.

References

- Ahmed, S. (2010). DNA zip codes control an ancient mechanism for gene targeting to the nuclear periphery. *Nat. Cell Biol* 12, 111–118.
- Akhtar, A., and Gasser, S.M. (2007). The nuclear envelope and transcriptional control. *Nat. Rev Genet* 8, 507–517.
- Akiyama, H., Shin, R.W., Uchida, C., Kitamoto, T., and Uchida, T. (2005). Pin1 promotes production of Alzheimer's amyloid [beta] from [beta]-cleaved amyloid precursor protein. *Biochem Biophys Res Commun* 336, 521–529.
- de Alboran, I.M., O'Hagan, R.C., Gärtner, F., Malynn, B., Davidson, L., Rickert, R., Rajewsky, K., DePinho, R.A., and Alt, F.W. (2001). Analysis of C-MYC Function in Normal Cells via Conditional Gene-Targeted Mutation. *Immunity* 14, 45–55.
- Alt, J.R., Greiner, T.C., Cleveland, J.L., and Eischen, C.M. (2003). Mdm2 haplo-insufficiency profoundly inhibits Myc-induced lymphomagenesis. *EMBO J* 22, 1442–1450.
- Alvarez, E., Northwood, I.C., Gonzalez, F.A., Latour, D.A., Seth, A., Abate, C., Curran, T., and Davis, R.J. (1991). Pro-Leu-Ser/Thr-Pro is a consensus primary sequence for substrate protein phosphorylation. Characterization of the phosphorylation of c-myc and c-jun proteins by an epidermal growth factor receptor threonine 669 protein kinase. *J. Biol. Chem.* 266, 15277–15285.
- Andresen, C., Helander, S., Lemak, A., Farès, C., Csizmok, V., Carlsson, J., Penn, L.Z., Forman-Kay, J.D., Arrowsmith, C.H., Lundström, P., et al. (2012). Transient structure and dynamics in the disordered c-Myc transactivation domain affect Bin1 binding. *Nucleic Acids Res.* 40, 6353–6366.
- Arabi, A., Rustum, C., Hallberg, E., and Wright, A.P.H. (2003). Accumulation of c-Myc and proteasomes at the nucleoli of cells containing elevated c-Myc protein levels. *J. Cell Sci.* 116, 1707–1717.
- Arnold, H.K., and Sears, R.C. (2006). Protein Phosphatase 2A Regulatory Subunit B56 α Associates with c-Myc and Negatively Regulates c-Myc Accumulation. *Mol. Cell. Biol.* 26, 2832–2844.
- Arnold, H.K., and Sears, R.C. (2008). A tumor suppressor role for PP2A-B56[alpha] through negative regulation of c-Myc and other key oncoproteins. *Cancer Metastasis Rev* 27, 147–158.
- Arnold, H.K., Zhang, X., Daniel, C.J., Tibbitts, D., Escamilla-Powers, J., Farrell, A., Tokarz, S., Morgan, C., and Sears, R.C. (2009). The Axin1 scaffold protein promotes formation of a degradation complex for c-Myc. *EMBO J.* 28, 500–512.

References

- Askew DS, Ashmun RA, Simmons B, and Cleveland JL (1991). Constitutive c-Myc expression in an IL-3 dependent myeloid cell line suppresses cell cycle arrest and accelerates apoptosis. *Oncogene* 6, 1915–1922.
- Aughey, G.N., and Southall, T.D. (2016). Dam it's good! DamID profiling of protein-DNA interactions. *Wiley Interdiscip. Rev. Dev. Biol.* 5, 25–37.
- Ayer, D.E., Kretzner, L., and Eisenman, R.N. (1993). Mad: a heterodimeric partner for Max that antagonizes Myc transcriptional activity. *Cell* 72, 211–222.
- Ayer, D.E., Lawrence, Q.A., and Eisenman, R.N. (1995). Mad-Max transcriptional repression is mediated by ternary complex formation with mammalian homologs of yeast repressor Sin3. *Cell* 80, 767–776.
- Bahram, F., von der Lehr, N., Cetinkaya, C., and Larsson, L.G. (2000). c-Myc hot spot mutations in lymphomas result in inefficient ubiquitination and decreased proteasome-mediated turnover. *Blood* 95, 2104–2110.
- Bao, L., Sauter, G., Sowadski, J., Lu, K.P., and Wang, D. (2004). Prevalent overexpression of prolyl isomerase Pin1 in human cancers. *Am J Pathol* 164, 1727–1737.
- Bayer, E., Goettsch, S., Mueller, J.W., Griewel, B., Guiberman, E., Mayr, L.M., and Bayer, P. (2003). Structural analysis of the mitotic regulator hPin1 in solution: insights into domain architecture and substrate binding. *J. Biol. Chem.* 278, 26183–26193.
- Beck, M., and Hurt, E. (2017). The nuclear pore complex: understanding its function through structural insight. *Nat. Rev. Mol. Cell Biol.* 18, 73–89.
- Belmont, A.S., Zhai, Y., and Thilenius, A. (1993). Lamin B distribution and association with peripheral chromatin revealed by optical sectioning and electron microscopy tomography. *J. Cell Biol.* 123, 1671–1685.
- Bernis, C. (2007). Pin1 stabilizes Emi1 during G2 phase by preventing its association with SCF (betatrcp). *EMBO Rep* 8, 91–98.
- Beroukhim, R., Mermel, C.H., Porter, D., Wei, G., Raychaudhuri, S., Donovan, J., Barretina, J., Boehm, J.S., Dobson, J., Urashima, M., et al. (2010). The landscape of somatic copy-number alteration across human cancers. *Nature* 463, 899–905.
- Bertoli, C., Skotheim, J.M., and de Bruin, R.A.M. (2013). Control of cell cycle transcription during G1 and S phases. *Nat. Rev. Mol. Cell Biol.* 14, 518–528.
- Bhaskaran, N., Drogen, F. van, Ng, H.-F., Kumar, R., Ekholm-Reed, S., Peter, M., Sangfelt, O., and Reed, S.I. (2013). Fbw7 α and Fbw7 γ Collaborate To Shuttle Cyclin E1 into the Nucleolus for Multiubiquitylation. *Mol. Cell. Biol.* 33, 85–97.
- Bissonnette, R.P., Echeverri, F., Mahboubi, A., and Green, D.R. (1992). Apoptotic cell death induced by c-myc is inhibited by bcl-2. *Nature* 359, 552–554.

References

- Blackwell, T.K., Kretzner, L., Blackwood, E.M., Eisenman, R.N., and Weintraub, H. (1990). Sequence-specific DNA binding by the c-Myc protein. *Science* *250*, 1149–1151.
- Blobel, G. (1985). Gene gating: a hypothesis. *Proc. Natl. Acad. Sci. U. S. A.* *82*, 8527–8529.
- Blume-Jensen, P., and Hunter, T. (2001). Oncogenic kinase signalling. *Nature* *411*, 355–365.
- Bouchard, C. (2001). Regulation of cyclin D2 gene expression by the Myc/Max/Mad network: Myc-dependent TRRAP recruitment and histone acetylation at the cyclin D2 promoter. *Genes Dev* *15*, 2042–2047.
- Bouchard, C. (2007). FoxO transcription factors suppress Myc-driven lymphomagenesis via direct activation of Arf. *Genes Dev* *21*, 2775–2787.
- Bozoky, Z., Krzeminski, M., Muhandiram, R., Birtley, J.R., Al-Zahrani, A., Thomas, P.J., Frizzell, R.A., Ford, R.C., and Forman-Kay, J.D. (2013a). Regulatory R region of the CFTR chloride channel is a dynamic integrator of phospho-dependent intra- and intermolecular interactions. *Proc. Natl. Acad. Sci. U. S. A.* *110*, E4427-4436.
- Bozoky, Z., Krzeminski, M., Chong, P.A., and Forman-Kay, J.D. (2013b). Structural changes of CFTR R region upon phosphorylation: a plastic platform for intramolecular and intermolecular interactions. *FEBS J.* *280*, 4407–4416.
- Bretones, G., Acosta, J.C., Caraballo, J.M., Ferrándiz, N., Gómez-Casares, M.T., Albajar, M., Blanco, R., Ruiz, P., Hung, W.-C., Albero, M.P., et al. (2011). SKP2 Oncogene Is a Direct MYC Target Gene and MYC Down-regulates p27KIP1 through SKP2 in Human Leukemia Cells. *J. Biol. Chem.* *286*, 9815–9825.
- Brewer, G., and Ross, J. (1988). Poly(A) shortening and degradation of the 3' A+U-rich sequences of human c-myc mRNA in a cell-free system. *Mol. Cell. Biol.* *8*, 1697–1708.
- Brickner, J.H., and Walter, P. (2004). Gene recruitment of the activated INO1 locus to the nuclear membrane. *PLoS Biol* *2*, e342.
- Brickner, D.G., Ahmed, S., Meldi, L., Thompson, A., Light, W., Young, M., Hickman, T.L., Chu, F., Fabre, E., and Brickner, J.H. (2012). Transcription Factor Binding to a DNA Zip Code Controls Interchromosomal Clustering at the Nuclear Periphery. *Dev. Cell* *22*, 1234–1246.
- Bridger, J.M., Boyle, S., Kill, I.R., and Bickmore, W.A. (2000). Re-modelling of nuclear architecture in quiescent and senescent human fibroblasts. *Curr. Biol. CB* *10*, 149–152.
- Brodeur, G.M., Seeger, R.C., Schwab, M., Varmus, H.E., and Bishop, J.M. (1984). Amplification of N-myc in untreated human neuroblastomas correlates with advanced disease stage. *Science* *224*, 1121–1124.

References

- Brown, C.R., Kennedy, C.J., Delmar, V.A., Forbes, D.J., and Silver, P.A. (2008). Global histone acetylation induces functional genomic reorganization at mammalian nuclear pore complexes. *Genes Dev.* *22*, 627–639.
- Brown, N.R., Noble, M.E., Endicott, J.A., and Johnson, L.N. (1999). The structural basis for specificity of substrate and recruitment peptides for cyclin-dependent kinases. *Nat. Cell Biol.* *1*, 438–443.
- Cabal, G.G. (2006). SAGA interacting factors confine sub-diffusion of transcribed genes to the nuclear envelope. *Nature* *441*, 770–773.
- Cabal, G.G., Genovesio, A., Rodriguez-Navarro, S., Zimmer, C., Gadal, O., Lesne, A., Buc, H., Feuerbach-Fournier, F., Olivo-Marin, J.-C., Hurt, E.C., et al. (2006). SAGA interacting factors confine sub-diffusion of transcribed genes to the nuclear envelope. *Nature* *441*, 770–773.
- Cai, D., Chen, S.-C., Prasad, M., He, L., Wang, X., Choessel-Cadamuro, V., Sawyer, J.K., Danuser, G., and Montell, D.J. (2014). Mechanical feedback through E-cadherin promotes direction sensing during collective cell migration. *Cell* *157*, 1146–1159.
- Campaner, S., Doni, M., Hydring, P., Verrecchia, A., Bianchi, L., Sardella, D., Schleker, T., Perna, D., Tronnersjö, S., Murga, M., et al. (2010). Cdk2 suppresses cellular senescence induced by the c-myc oncogene. *Nat. Cell Biol.* *12*, 54–59.
- Cao X, Bennett RL, and May WS (2008). c-Myc and caspase-2 are involved in activating Bax during cytotoxic drug-induced apoptosis. *J Biol Chem* *283*, 14490–14496.
- Capelson, M. (2010). Chromatin-bound nuclear pore components regulate gene expression in higher eukaryotes. *Cell* *140*, 372–383.
- Casolari, J.M., Brown, C.R., Komili, S., West, J., Hieronymus, H., and Silver, P.A. (2004). Genome-wide localization of the nuclear transport machinery couples transcriptional status and nuclear organization. *Cell* *117*, 427–439.
- Casolari, J.M., Brown, C.R., Drubin, D.A., Rando, O.J., and Silver, P.A. (2005). Developmentally induced changes in transcriptional program alter spatial organization across chromosomes. *Genes Dev.* *19*, 1188–1198.
- Chandramohan, V., Jeay, S., Pianetti, S., and Sonenshein, G.E. (2004). Reciprocal Control of Forkhead box O 3a and c-Myc via the Phosphatidylinositol 3-Kinase Pathway Coordinately Regulates p27^{Kip1} Levels. *J. Immunol.* *172*, 5522–5527.
- Chang, D.W., Claassen, G.F., Hann, S.R., and Cole, M.D. (2000). The c-Myc transactivation domain is a direct modulator of apoptotic versus proliferative signals. *Mol. Cell. Biol.* *20*, 4309–4319.
- Chappell, S.A., LeQuesne, J.P., Paulin, F.E., deSchoolmeester, M.L., Stoneley, M., Soutar, R.L., Ralston, S.H., Helfrich, M.H., and Willis, A.E. (2000). A mutation in the c-

References

- myc-IRES leads to enhanced internal ribosome entry in multiple myeloma: a novel mechanism of oncogene de-regulation. *Oncogene* 19, 4437–4440.
- Chen, C.-H., Chang, C.-C., Lee, T.H., Luo, M., Huang, P., Liao, P.-H., Wei, S., Li, F.-A., Chen, R.-H., Zhou, X.Z., et al. (2013). SENP1 deSUMOylates and regulates Pin1 protein activity and cellular function. *Cancer Res.* 73, 3951–3962.
- Chi, Y., Welcker, M., Hizli, A.A., Posakony, J.J., Aebersold, R., and Clurman, B.E. (2008). Identification of CDK2 substrates in human cell lysates. *Genome Biol.* 9, R149.
- Chow, K.-H., Elgort, S., Dasso, M., Powers, M.A., and Ullman, K.S. (2014). The SUMO proteases SENP1 and SENP2 play a critical role in nucleoporin homeostasis and nuclear pore complex function. *Mol. Biol. Cell* 25, 160–168.
- Chuang, C.H. (2006). Long-range directional movement of an interphase chromosome site. *Curr Biol* 16, 825–831.
- Ciurciu, A., Komonyi, O., Pankotai, T., and Boros, I.M. (2006). The *Drosophila* histone acetyltransferase Gcn5 and transcriptional adaptor Ada2a are involved in nucleosomal histone H4 acetylation. *Mol. Cell. Biol.* 26, 9413–9423.
- Cowling, V.H., and Cole, M.D. (2006). Mechanism of transcriptional activation by the Myc oncoproteins. *Semin. Cancer Biol.* 16, 242–252.
- Cremer, T., and Cremer, M. (2010). Chromosome territories. *Cold Spring Harb. Perspect. Biol.* 2, a003889.
- Croft, J.A., Bridger, J.M., Boyle, S., Perry, P., Teague, P., and Bickmore, W.A. (1999). Differences in the Localization and Morphology of Chromosomes in the Human Nucleus. *J. Cell Biol.* 145, 1119–1131.
- Cross, D.A., Alessi, D.R., Cohen, P., Andjelkovich, M., and Hemmings, B.A. (1995). Inhibition of glycogen synthase kinase-3 by insulin mediated by protein kinase B. *Nature* 378, 785–789.
- Dalla-Favera, R., Bregni, M., Erikson, J., Patterson, D., Gallo, R.C., and Croce, C.M. (1982). Human c-myc onc gene is located on the region of chromosome 8 that is translocated in Burkitt lymphoma cells. *Proc. Natl. Acad. Sci. U. S. A.* 79, 7824–7827.
- Dang, C.V. (2012). MYC on the Path to Cancer. *Cell* 149, 22–35.
- Dani, C., Blanchard, J.M., Piechaczyk, M., El Sabouty, S., Marty, L., and Jeanteur, P. (1984). Extreme instability of myc mRNA in normal and transformed human cells. *Proc. Natl. Acad. Sci. U. S. A.* 81, 7046–7050.
- Dansen TB, Whitfield J, Rostker F, Brown-Swigart L, and Evan GI (2006). Specific requirement for Bax, not Bak, in Myc-induced apoptosis and tumor suppression in vivo. *J Biol Chem* 281, 10890–10895.

References

- Das, P.P., Shao, Z., Beyaz, S., Apostolou, E., Pinello, L., De Los Angeles, A., O'Brien, K., Atsma, J.M., Fujiwara, Y., Nguyen, M., et al. (2014). Distinct and combinatorial functions of Jmjd2b/Kdm4b and Jmjd2c/Kdm4c in mouse embryonic stem cell identity. *Mol. Cell* 53, 32–48.
- Daum, S., Lücke, C., Wildemann, D., and Schiene-Fischer, C. (2007). On the benefit of bivalency in peptide ligand/pin1 interactions. *J. Mol. Biol.* 374, 147–161.
- David-Watine, B. (2011). Silencing Nuclear Pore Protein Tpr Elicits a Senescent-Like Phenotype in Cancer Cells. *PLOS ONE* 6, e22423.
- Davies, J.O.J., Oudelaar, A.M., Higgs, D.R., and Hughes, J.R. (2017). How best to identify chromosomal interactions: a comparison of approaches. *Nat. Methods* 14, 125–134.
- D'Cruz, C.M. (2001). c-MYC induces mammary tumorigenesis by means of a preferred pathway involving spontaneous Kras2 mutations. *Nat. Med* 7, 235–239.
- De, S., Greenwood, A.I., Rogals, M.J., Kovrigin, E.L., Lu, K.P., and Nicholson, L.K. (2012). Complete thermodynamic and kinetic characterization of the isomer-specific interaction between Pin1-WW domain and the amyloid precursor protein cytoplasmic tail phosphorylated at Thr668. *Biochemistry (Mosc.)* 51, 8583–8596.
- Dieppo, G., Iglesias, N., and Stutz, F. (2006). Cotranscriptional recruitment to the mRNA export receptor Mex67p contributes to nuclear pore anchoring of activated genes. *Mol Cell Biol* 26, 7858–7870.
- Dougherty, M.K. (2005). Regulation of Raf-1 by direct feedback phosphorylation. *Mol Cell* 17, 215–224.
- van Drogen, F. (2006). Ubiquitylation of cyclin E requires the sequential function of SCF complexes containing distinct hCdc4 isoforms. *Mol Cell* 23, 37–48.
- Duncan, K.E., Dempsey, B.R., Killip, L.E., Adams, J., Bailey, M.L., Lajoie, G.A., Litchfield, D.W., Brandl, C.J., Shaw, G.S., and Shilton, B.H. (2011). Discovery and characterization of a nonphosphorylated cyclic peptide inhibitor of the peptidylprolyl isomerase, Pin1. *J. Med. Chem.* 54, 3854–3865.
- Durairaj, G., and Kaiser, P. (2014). The 26S Proteasome and Initiation of Gene Transcription. *Biomolecules* 4, 827–847.
- Eckerdt, F. (2005). Polo-like kinase 1-mediated phosphorylation stabilizes Pin1 by inhibiting its ubiquitination in human cells. *J Biol Chem* 280, 36575–36583.
- Eischen, C.M. (2001). Bcl-2 is an apoptotic target suppressed by both c-Myc and E2F-1. *Oncogene* 20, 6983–6993.

References

- Eischen, C.M., Roussel, M.F., Korsmeyer, S.J., and Cleveland, J.L. (2001a). Bax loss impairs Myc-induced apoptosis and circumvents the selection of p53 mutations during Myc-mediated lymphomagenesis. *Mol Cell Biol* *21*, 7653–7662.
- Eischen, C.M., Woo, D., Roussel, M.F., and Cleveland, J.L. (2001b). Apoptosis triggered by Myc-induced suppression of Bcl-X(L) or Bcl-2 is bypassed during lymphomagenesis. *Mol. Cell. Biol.* *21*, 5063–5070.
- Eischen CM, Weber JD, Roussel MF, Sherr CJ, and Cleveland JL (1999). Disruption of the ARF-Mdm2-p53 tumor suppressor pathway in Myc-induced lymphomagenesis. *Genes Dev* *13*, 2658–2669.
- Eisenman, R.N., Tachibana, C.Y., Abrams, H.D., and Hann, S.R. (1985). V-myc- and c-myc-encoded proteins are associated with the nuclear matrix. *Mol. Cell. Biol.* *5*, 114–126.
- Evan, G.I. (1992). Induction of apoptosis in fibroblasts by c-myc protein. *Cell* *69*, 119–128.
- Faiola, F., Liu, X., Lo, S., Pan, S., Zhang, K., Lymar, E., Farina, A., and Martinez, E. (2005). Dual regulation of c-Myc by p300 via acetylation-dependent control of Myc protein turnover and coactivation of Myc-induced transcription. *Mol. Cell. Biol.* *25*, 10220–10234.
- Farrell, A.S., and Sears, R.C. (2014). MYC degradation. *Cold Spring Harb. Perspect. Med.* *4*.
- Farrell, A.S., Pelz, C., Wang, X., Daniel, C.J., Wang, Z., Su, Y., Janghorban, M., Zhang, X., Morgan, C., Impey, S., et al. (2013). Pin1 Regulates the Dynamics of c-Myc DNA Binding To Facilitate Target Gene Regulation and Oncogenesis. *Mol. Cell. Biol.* *33*, 2930–2949.
- Farrell, A.S., Allen-Petersen, B., Daniel, C.J., Wang, X., Wang, Z., Rodriguez, S., Impey, S., Oddo, J., Vitek, M.P., Lopez, C., et al. (2014). Targeting Inhibitors of the Tumor Suppressor PP2A for the Treatment of Pancreatic Cancer. *Mol. Cancer Res. MCR* *12*, 924–939.
- Felsher, D.W., and Bishop, J.M. (1999). Transient excess of MYC activity can elicit genomic instability and tumorigenesis. *Proc Natl Acad Sci USA* *96*, 3940–3944.
- Finch, A. (2006). Bcl-xL gain of function and p19 ARF loss of function cooperate oncogenically with Myc in vivo by distinct mechanisms. *Cancer Cell* *10*, 113–120.
- Finlan, L.E. (2008). Recruitment to the nuclear periphery can alter expression of genes in human cells. *PLoS Genet* *4*, e1000039.

References

- Fischer, G., and Aumuller, T. (2003). Regulation of peptide bond cis/transisomerization by enzyme catalysis and its implication in physiological processes. *Rev Physiol Biochem Pharmacol* 148, 105–150.
- Flinn, E.M., Wallberg, A.E., Hermann, S., Grant, P.A., Workman, J.L., and Wright, A.P.H. (2002). Recruitment of Gcn5-containing Complexes during c-Myc-dependent Gene Activation STRUCTURE AND FUNCTION ASPECTS. *J. Biol. Chem.* 277, 23399–23406.
- Forman-Kay, J.D., and Mittag, T. (2013). From sequence and forces to structure, function, and evolution of intrinsically disordered proteins. *Struct. Lond. Engl.* 1993 21, 1492–1499.
- Francastel, C., Schübeler, D., Martin, D.I.K., and Groudine, M. (2000). Nuclear compartmentalization and gene activity. *Nat. Rev. Mol. Cell Biol.* 1, 137–143.
- Frank, S.R. (2003). MYC recruits the TIP60 histone acetyltransferase complex to chromatin. *EMBO Rep* 4, 575–580.
- Frank, S.R., Schroeder, M., Fernandez, P., Taubert, S., and Amati, B. (2001). Binding of c-Myc to chromatin mediates mitogen-induced acetylation of histone H4 and gene activation. *Genes Dev.* 15, 2069–2082.
- Fraser, P., and Bickmore, W. (2007). Nuclear organization of the genome and the potential for gene regulation. *Nature* 447, 413–417.
- Fuchs, M., Gerber, J., Drapkin, R., Sif, S., Ikura, T., Ogryzko, V., Lane, W.S., Nakatani, Y., and Livingston, D.M. (2001). The p400 Complex Is an Essential E1A Transformation Target. *Cell* 106, 297–307.
- Fujimori, F., Takahashi, K., Uchida, C., and Uchida, T. (1999). Mice lacking Pin1 develop normally, but are defective in entering cell cycle from G(0) arrest. *Biochem. Biophys. Res. Commun.* 265, 658–663.
- Fuxreiter, M., and Tompa, P. (2012). Fuzzy complexes: a more stochastic view of protein function. *Adv. Exp. Med. Biol.* 725, 1–14.
- Gao, P., Tchernyshyov, I., Chang, T.-C., Lee, Y.-S., Kita, K., Ochi, T., Zeller, K.I., De Marzo, A.M., Van Eyk, J.E., Mendell, J.T., et al. (2009). c-Myc suppression of miR-23a/b enhances mitochondrial glutaminase expression and glutamine metabolism. *Nature* 458, 762–765.
- Geng, F., Wenzel, S., and Tansey, W.P. (2012). Ubiquitin and Proteasomes in Transcription. *Annu. Rev. Biochem.* 81, 177–201.
- Georges-Labouesse, E., Messaddeq, N., Yehia, G., Cadalbert, L., Dierich, A., and Le Meur, M. (1996). Absence of integrin $\alpha 6$ leads to epidermolysis bullosa and neonatal death in mice. *Nat. Genet.* 13, 370–373.

References

- Geyer, P.K., Vitalini, M.W., and Wallrath, L.L. (2011). Nuclear organization: taking a position on gene expression. *Curr. Opin. Cell Biol.* *23*, 354–359.
- Girardini, J.E., Napoli, M., Piazza, S., Rustighi, A., Marotta, C., Radaelli, E., Capaci, V., Jordan, L., Quinlan, P., Thompson, A., et al. (2011). A Pin1/mutant p53 axis promotes aggressiveness in breast cancer. *Cancer Cell* *20*, 79–91.
- Göthel, S.F., and Marahiel, M.A. (1999). Peptidyl-prolyl cis-trans isomerases, a superfamily of ubiquitous folding catalysts. *Cell. Mol. Life Sci. CMLS* *55*, 423–436.
- Grim, J.E., Gustafson, M.P., Hirata, R.K., Hagar, A.C., Swanger, J., Welcker, M., Hwang, H.C., Ericsson, J., Russell, D.W., and Clurman, B.E. (2008). Isoform- and cell cycle-dependent substrate degradation by the Fbw7 ubiquitin ligase. *J. Cell Biol.* *181*, 913–920.
- Guelen, L., Pagie, L., Brasset, E., Meuleman, W., Faza, M.B., Talhout, W., Eussen, B.H., de Klein, A., Wessels, L., de Laat, W., et al. (2008). Domain organization of human chromosomes revealed by mapping of nuclear lamina interactions. *Nature* *453*, 948–951.
- Guo, J., Pang, X., and Zhou, H.-X. (2015). Two pathways mediate interdomain allosteric regulation in pin1. *Struct. Lond. Engl.* *1993* *23*, 237–247.
- Hanahan, D., and Weinberg, R.A. (2000). The hallmarks of cancer. *Cell* *100*, 57–70.
- Hann, S.R. (2006). Role of post-translational modifications in regulating c-Myc proteolysis, transcriptional activity and biological function. *Semin. Cancer Biol.* *16*, 288–302.
- Hariharan, N., and Sussman, M.A. (2014). Pin1: a molecular orchestrator in the heart. *Trends Cardiovasc. Med.* *24*, 256–262.
- Harris, A.W., Pinkert, C.A., Crawford, M., Langdon, W.Y., Brinster, R.L., and Adams, J.M. (1988). The E mu-myc transgenic mouse. A model for high-incidence spontaneous lymphoma and leukemia of early B cells. *J. Exp. Med.* *167*, 353–371.
- Hase, M.E., and Cordes, V.C. (2003). Direct interaction with nup153 mediates binding of Tpr to the periphery of the nuclear pore complex. *Mol. Biol. Cell* *14*, 1923–1940.
- He, T.C., Sparks, A.B., Rago, C., Hermeking, H., Zawel, L., da Costa, L.T., Morin, P.J., Vogelstein, B., and Kinzler, K.W. (1998). Identification of c-MYC as a target of the APC pathway. *Science* *281*, 1509–1512.
- Heikkila, R., Schwab, G., Wickstrom, E., Loke, S.L., Pluznik, D.H., Watt, R., and Neckers, L.M. (1987). A c-myc antisense oligodeoxynucleotide inhibits entry into S phase but not progress from G0 to G1. *Nature* *328*, 445–449.
- Helander, S., Montecchio, M., Pilstål, R., Su, Y., Kuruvilla, J., Elvén, M., Ziauddin, J.M.E., Anandapadamanaban, M., Cristobal, S., Lundström, P., et al. (2015). Pre-

References

- Anchoring of Pin1 to Unphosphorylated c-Myc in a Fuzzy Complex Regulates c-Myc Activity. *Struct. Lond. Engl.* 1993 *23*, 2267–2279.
- Hermeking, H., Rago, C., Schuhmacher, M., Li, Q., Barrett, J.F., Obaya, A.J., O'Connell, B.C., Mateyak, M.K., Tam, W., Kohlhuber, F., et al. (2000). Identification of CDK4 as a target of c-MYC. *Proc. Natl. Acad. Sci.* *97*, 2229–2234.
- Herold, S. (2002). Negative regulation of the mammalian UV response by Myc through association with Miz-1. *Mol Cell* *10*, 509–521.
- Herrick, D.J., and Ross, J. (1994). The half-life of c-myc mRNA in growing and serum-stimulated cells: influence of the coding and 3' untranslated regions and role of ribosome translocation. *Mol. Cell. Biol.* *14*, 2119–2128.
- Hnisz, D., Abraham, B.J., Lee, T.I., Lau, A., Saint-André, V., Sigova, A.A., Hoke, H.A., and Young, R.A. (2013). Super-enhancers in the control of cell identity and disease. *Cell* *155*, 934–947.
- Huang, J., Marco, E., Pinello, L., and Yuan, G.-C. (2015). Predicting chromatin organization using histone marks. *Genome Biol.* *16*, 162.
- Hurtley, S.M. (2016). Close-up view of the nuclear periphery. *Science* *351*, 929–929.
- Hydbring, P., Bahram, F., Su, Y., Tronnorsjö, S., Högstrand, K., von der Lehr, N., Sharifi, H.R., Lilischkis, R., Hein, N., Wu, S., et al. (2010). Phosphorylation by Cdk2 is required for Myc to repress Ras-induced senescence in cotransformation. *Proc. Natl. Acad. Sci. U. S. A.* *107*, 58–63.
- Ibarra, A., and Hetzer, M.W. (2015). Nuclear pore proteins and the control of genome functions. *Genes Dev.* *29*, 337–349.
- Ishii, K., Arib, G., Lin, C., Van Houwe, G., and Laemmli, U.K. (2002). Chromatin boundaries in budding yeast: the nuclear pore connection. *Cell* *109*, 551–562.
- Jacobs, J.J. (1999). Bmi-1 collaborates with c-Myc in tumorigenesis by inhibiting c-Myc-induced apoptosis via INK4a/ARF. *Genes Dev.* *13*, 2678–2690.
- Jacobs, D.M., Saxena, K., Vogtherr, M., Bernado, P., Pons, M., and Fiebig, K.M. (2003). Peptide binding induces large scale changes in inter-domain mobility in human Pin1. *J. Biol. Chem.* *278*, 26174–26182.
- Jiang X, Tsang YH, and Yu Q (2007). c-Myc overexpression sensitizes Bim-mediated Bax activation for apoptosis induced by histone deacetylase inhibitor suberoylanilide hydroxamic acid (SAHA) through regulating Bcl-2/Bcl-xL expression. *Int J Biochem Cell Biol* *39*, 1016–1025.
- Johnston, L.A., Prober, D.A., Edgar, B.A., Eisenman, R.N., and Gallant, P. (1999). *Drosophila myc* regulates cellular growth during development. *Cell* *98*, 779–790.

References

- Jones, P.H., and Watt, F.M. (1993). Separation of human epidermal stem cells from transit amplifying cells on the basis of differences in integrin function and expression. *Cell* 73, 713–724.
- Jones, T.R., and Cole, M.D. (1987). Rapid cytoplasmic turnover of c-myc mRNA: requirement of the 3[prime] untranslated sequences. *Mol Cell Biol* 7, 4513–4521.
- Kalverda, B., Pickersgill, H., Shloma, V.V., and Fornerod, M. (2010). Nucleoporins directly stimulate expression of developmental and cell-cycle genes inside the nucleoplasm. *Cell* 140, 360–371.
- Kashyap, V., Rezende, N.C., Scotland, K.B., Shaffer, S.M., Persson, J.L., Gudas, L.J., and Mongan, N.P. (2009). Regulation of Stem Cell Pluripotency and Differentiation Involves a Mutual Regulatory Circuit of the Nanog, OCT4, and SOX2 Pluripotency Transcription Factors With Polycomb Repressive Complexes and Stem Cell microRNAs. *Stem Cells Dev.* 18, 1093–1108.
- Kasper, L.H., Brindle, P.K., Schnabel, C.A., Pritchard, C.E.J., Cleary, M.L., and Van, D. (1999). CREB binding protein interacts with nucleoporin-specific FG repeats that activate transcription and mediate NUP98-HOXA9 oncogenicity. *Mol. Cell. Biol.* 19, 764–776.
- Kato, G.J., Barrett, J., Villa-Garcia, M., and Dang, C.V. (1990). An amino-terminal c-myc domain required for neoplastic transformation activates transcription. *Mol Cell Biol* 10, 5914–5920.
- Kelly, K., Cochran, B.H., Stiles, C.D., and Leder, P. (1983a). Cell-specific regulation of the c-myc gene by lymphocyte mitogens and platelet-derived growth factor. *Cell* 35, 603–610.
- Kelly, K., Cochran, B.H., Stiles, C.D., and Leder, P. (1983b). Cell-specific regulation of the c-myc gene by lymphocyte mitogens and platelet-derived growth factor. *Cell* 35, 603–610.
- Kenneth, N.S., Ramsbottom, B.A., Gomez-Roman, N., Marshall, L., Cole, P.A., and White, R.J. (2007). TRRAP and GCN5 are used by c-Myc to activate RNA polymerase III transcription. *Proc. Natl. Acad. Sci. U. S. A.* 104, 14917–14922.
- Khanal, P., Namgoong, G.M., Kang, B.S., Woo, E.-R., and Choi, H.S. (2010). The prolyl isomerase Pin1 enhances HER-2 expression and cellular transformation via its interaction with mitogen-activated protein kinase/extracellular signal-regulated kinase kinase 1. *Mol. Cancer Ther.* 9, 606–616.
- Kim, H.H., Kuwano, Y., Srikantan, S., Lee, E.K., Martindale, J.L., and Gorospe, M. (2009). HuR recruits let-7/RISC to repress c-Myc expression. *Genes Dev.* 23, 1743–1748.

References

- Kim, J.P., Zhang, K., Chen, J.D., Wynn, K.C., Kramer, R.H., and Woodley, D.T. (1992). Mechanism of human keratinocyte migration on fibronectin: Unique roles of RGD site and integrins. *J. Cell. Physiol.* *151*, 443–450.
- Kind, J., Pagie, L., Ortobozkoyun, H., Boyle, S., de Vries, S.S., Janssen, H., Amendola, M., Nolen, L.D., Bickmore, W.A., and van Steensel, B. (2013). Single-cell dynamics of genome-nuclear lamina interactions. *Cell* *153*, 178–192.
- Knoepfler, P.S., Zhang, X., Cheng, P.F., Gafken, P.R., McMahon, S.B., and Eisenman, R.N. (2006). Myc influences global chromatin structure. *EMBO J.* *25*, 2723–2734.
- Kress, T.R., Sabò, A., and Amati, B. (2015). MYC: connecting selective transcriptional control to global RNA production. *Nat. Rev. Cancer* *15*, 593–607.
- Krull, S., Thyberg, J., Björkroth, B., Rackwitz, H.-R., and Cordes, V.C. (2004). Nucleoporins as components of the nuclear pore complex core structure and Tpr as the architectural element of the nuclear basket. *Mol. Biol. Cell* *15*, 4261–4277.
- Krull, S., Dörries, J., Boysen, B., Reidenbach, S., Magnius, L., Norder, H., Thyberg, J., and Cordes, V.C. (2010). Protein Tpr is required for establishing nuclear pore-associated zones of heterochromatin exclusion. *EMBO J.* *29*, 1659–1673.
- Kurshakova, M.M., Krasnov, A.N., Kopytova, D.V., Shidlovskii, Y.V., Nikolenko, J.V., Nabirochkina, E.N., Spehner, D., Schultz, P., Tora, L., and Georgieva, S.G. (2007). SAGA and a novel *Drosophila* export complex anchor efficient transcription and mRNA export to NPC. *EMBO J.* *26*, 4956–4965.
- Lam, P.B., Burga, L.N., Wu, B.P., Hofstatter, E.W., Lu, K.P., and Wulf, G.M. (2008). Prolyl isomerase Pin1 is highly expressed in Her2-positive breast cancer and regulates erbB2 protein stability. *Mol. Cancer* *7*, 91.
- Lanctôt, C., Cheutin, T., Cremer, M., Cavalli, G., and Cremer, T. (2007). Dynamic genome architecture in the nuclear space: regulation of gene expression in three dimensions. *Nat. Rev. Genet.* *8*, 104–115.
- Landschulz, W.H., Johnson, P.F., and McKnight, S.L. (1988). The leucine zipper: a hypothetical structure common to a new class of DNA binding proteins. *Science* *240*, 1759–1764.
- Lannigan, D.A. (2003). Estrogen receptor phosphorylation. *Steroids* *68*, 1–9.
- Larsson, L.G., Pettersson, M., Oberg, F., Nilsson, K., and Lüscher, B. (1994). Expression of mad, mx1, max and c-myc during induced differentiation of hematopoietic cells: opposite regulation of mad and c-myc. *Oncogene* *9*, 1247–1252.
- Lee, T.H., Chen, C.-H., Suizu, F., Huang, P., Schiene-Fischer, C., Daum, S., Zhang, Y.J., Goate, A., Chen, R.-H., Zhou, X.Z., et al. (2011a). Death-Associated Protein Kinase 1

References

- Phosphorylates Pin1 and Inhibits Its Prolyl Isomerase Activity and Cellular Function. *Mol. Cell* 42, 147–159.
- Lee, T.H., Chen, C.-H., Suizu, F., Huang, P., Schiene-Fischer, C., Daum, S., Zhang, Y.J., Goate, A., Chen, R.-H., Zhou, X.Z., et al. (2011b). Death-associated protein kinase 1 phosphorylates Pin1 and inhibits its prolyl isomerase activity and cellular function. *Mol. Cell* 42, 147–159.
- van der Lee, R., Buljan, M., Lang, B., Weatheritt, R.J., Daughdrill, G.W., Dunker, A.K., Fuxreiter, M., Gough, J., Gsponer, J., Jones, D.T., et al. (2014). Classification of Intrinsically Disordered Regions and Proteins. *Chem. Rev.* 114, 6589–6631.
- Legouy, E., DePinho, R., Zimmerman, K., Collum, R., Yancopoulos, G., Mitscock, L., Kriz, R., and Alt, F.W. (1987). Structure and expression of the murine L-myc gene. *EMBO J.* 6, 3359–3366.
- Leung, K.-W., Tsai, C.-H., Hsiao, M., Tseng, C.-J., Ger, L.-P., Lee, K.-H., and Lu, P.-J. (2009). Pin1 overexpression is associated with poor differentiation and survival in oral squamous cell carcinoma. *Oncol. Rep.* 21, 1097–1104.
- Li, Z. (2003). A global transcriptional regulatory role for c-Myc in Burkitt's lymphoma cells. *Proc Natl Acad Sci USA* 100, 8164–8169.
- Liang, Y., Franks, T.M., Marchetto, M.C., Gage, F.H., and Hetzer, M.W. (2013). Dynamic Association of NUP98 with the Human Genome. *PLOS Genet.* 9, e1003308.
- Liao, Y., Wei, Y., Zhou, X., Yang, J.-Y., Dai, C., Chen, Y.-J., Agarwal, N.K., Sarbassov, D., Shi, D., Yu, D., et al. (2009). Peptidyl-prolyl cis/trans isomerase Pin1 is critical for the regulation of PKB/Akt stability and activation phosphorylation. *Oncogene* 28, 2436–2445.
- Light, W.H., and Brickner, J.H. (2013). Nuclear pore proteins regulate chromatin structure and transcriptional memory by a conserved mechanism. *Nucl. Austin Tex* 4, 357–360.
- Lin, C.-H., Li, H.-Y., Lee, Y.-C., Calkins, M.J., Lee, K.-H., Yang, C.-N., and Lu, P.-J. (2015). Landscape of Pin1 in the cell cycle. *Exp. Biol. Med.* 240, 403–408.
- Lin, C.Y., Lovén, J., Rahl, P.B., Paranal, R.M., Burge, C.B., Bradner, J.E., Lee, T.I., and Young, R.A. (2012a). Transcriptional amplification in tumor cells with elevated c-Myc. *Cell* 151, 56–67.
- Lin, C.Y., Lovén, J., Rahl, P.B., Paranal, R.M., Burge, C.B., Bradner, J.E., Lee, T.I., and Young, R.A. (2012b). Transcriptional Amplification in Tumor Cells with Elevated c-Myc. *Cell* 151, 56–67.
- Liou, Y.C. (2002). Loss of Pin1 function in the mouse causes phenotypes resembling cyclin D1-null phenotypes. *Proc Natl Acad Sci USA* 99, 1335–1340.

References

- Liou, Y.-C., Zhou, X.Z., and Lu, K.P. (2011). Prolyl isomerase Pin1 as a molecular switch to determine the fate of phosphoproteins. *Trends Biochem. Sci.* *36*, 501–514.
- Littlewood, T.D., Amati, B., Land, H., and Evan, G.I. (1992). Max and c-Myc/Max DNA-binding activities in cell extracts. *Oncogene* *7*, 1783–1792.
- Lowe, S.W., Cepero, E., and Evan, G. (2004). Intrinsic tumour suppression. *Nature* *432*, 307–315.
- Lu, K.P., and Zhou, X.Z. (2007). The prolyl isomerase PIN1: a pivotal new twist in phosphorylation signalling and disease. *Nat. Rev. Mol. Cell Biol.* *8*, 904–916.
- Lu, Z., and Hunter, T. (2014). Prolyl isomerase Pin1 in cancer. *Cell Res.* *24*, 1033–1049.
- Lu, J., Hu, Z., Wei, S., Wang, L.-E., Liu, Z., El-Naggar, A.K., Sturgis, E.M., and Wei, Q. (2009). A novel functional variant (-842G>C) in the PIN1 promoter contributes to decreased risk of squamous cell carcinoma of the head and neck by diminishing the promoter activity. *Carcinogenesis* *30*, 1717–1721.
- Lu, K.P., Liou, Y.C., and Zhou, X.Z. (2002a). Pinning down proline-directed phosphorylation signaling. *Trends Cell Biol.* *12*, 164–172.
- Lu, K.P., Finn, G., Lee, T.H., and Nicholson, L.K. (2007). Prolyl cis-trans isomerization as a molecular timer. *Nat. Chem. Biol.* *3*, 619–629.
- Lu, P.J., Zhou, X.Z., Shen, M., and Lu, K.P. (1999). Function of WW domains as phosphoserine- or phosphothreonine-binding modules. *Science* *283*, 1325–1328.
- Lu, P.-J., Zhou, X.Z., Liou, Y.-C., Noel, J.P., and Lu, K.P. (2002b). Critical role of WW domain phosphorylation in regulating phosphoserine binding activity and Pin1 function. *J. Biol. Chem.* *277*, 2381–2384.
- Lucchetti, C., Caligiuri, I., Toffoli, G., Giordano, A., and Rizzolio, F. (2013). The prolyl isomerase Pin1 acts synergistically with CDK2 to regulate the basal activity of estrogen receptor α in breast cancer. *PLoS One* *8*, e55355.
- Lukhele, S., Bah, A., Lin, H., Sonenberg, N., and Forman-Kay, J.D. (2013). Interaction of the eukaryotic initiation factor 4E with 4E-BP2 at a dynamic bipartite interface. *Struct. Lond. Engl.* *1993* *21*, 2186–2196.
- Luo, M.-L., Gong, C., Chen, C.-H., Hu, H., Huang, P., Zheng, M., Yao, Y., Wei, S., Wulf, G., Lieberman, J., et al. (2015). The Rab2A GTPase promotes breast cancer stem cells and tumorigenesis via Erk signaling activation. *Cell Rep.* *11*, 111–124.
- Luscher, B., and Eisenman, R.N. (1990). New light on Myc and Myb. Part I. *Myc. Genes Dev* *4*, 2025–2035.

References

- Lüscher, B., and Vervoorts, J. (2012). Regulation of gene transcription by the oncoprotein MYC. *Gene* 494, 145–160.
- Luthra, R., Kerr, S.C., Harreman, M.T., Apponi, L.H., Fasken, M.B., Ramineni, S., Chaurasia, S., Valentini, S.R., and Corbett, A.H. (2007). Actively Transcribed GAL Genes Can Be Physically Linked to the Nuclear Pore by the SAGA Chromatin Modifying Complex. *J. Biol. Chem.* 282, 3042–3049.
- Lutterbach, B., and Hann, S.R. (1994). Hierarchical phosphorylation at N-terminal transformation-sensitive sites in c-Myc protein is regulated by mitogens and in mitosis. *Mol. Cell. Biol.* 14, 5510–5522.
- Ma, L., Young, J., Prabhala, H., Pan, E., Mestdagh, P., Muth, D., Teruya-Feldstein, J., Reinhardt, F., Onder, T.T., Valastyan, S., et al. (2010). miR-9, a MYC/MYCN-activated microRNA, regulates E-cadherin and cancer metastasis. *Nat. Cell Biol.* 12, 247–256.
- Maclean, K.H., Keller, U.B., Rodriguez-Galindo, C., Nilsson, J.A., and Cleveland, J.L. (2003). c-Myc augments gamma irradiation-induced apoptosis by suppressing Bcl-XL. *Mol. Cell. Biol.* 23, 7256–7270.
- Magri, L., Gacias, M., Wu, M., Swiss, V.A., Janssen, W.G., and Casaccia, P. (2014). c-Myc-dependent transcriptional regulation of cell cycle and nucleosomal histones during oligodendrocyte differentiation. *Neuroscience* 276, 72–86.
- Malhas, A., Lee, C.F., Sanders, R., Saunders, N.J., and Vaux, D.J. (2007). Defects in lamin B1 expression or processing affect interphase chromosome position and gene expression. *J. Cell Biol.* 176, 593–603.
- Martinez, C., Churchman, M., Freeman, T., and Ilyas, M. (2010). Osteopontin provides early proliferative drive and may be dependent upon aberrant c-myc signalling in murine intestinal tumours. *Exp. Mol. Pathol.* 88, 272–277.
- Martínez-Cerdeño, V., Lemen, J.M., Chan, V., Wey, A., Lin, W., Dent, S.R., and Knoepfler, P.S. (2012). N-Myc and GCN5 Regulate Significantly Overlapping Transcriptional Programs in Neural Stem Cells. *PLOS ONE* 7, e39456.
- Marval, P.L.M. de, Macias, E., Rounbehler, R., Sicinski, P., Kiyokawa, H., Johnson, D.G., Conti, C.J., and Rodriguez-Puebla, M.L. (2004). Lack of Cyclin-Dependent Kinase 4 Inhibits c-myc Tumorigenic Activities in Epithelial Tissues. *Mol. Cell. Biol.* 24, 7538–7547.
- Matena, A., Sinnen, C., van den Boom, J., Wilms, C., Dybowski, J.N., Maltaner, R., Mueller, J.W., Link, N.M., Hoffmann, D., and Bayer, P. (2013). Transient domain interactions enhance the affinity of the mitotic regulator Pin1 toward phosphorylated peptide ligands. *Struct. Lond. Engl.* 1993 21, 1769–1777.

References

- Mateyak, M.K., Obaya, A.J., and Sedivy, J.M. (1999). c-Myc regulates cyclin D-Cdk4 and -Cdk6 activity but affects cell cycle progression at multiple independent points. *Mol. Cell Biol.* *19*, 4672–4683.
- McMahon, S.B., Van Buskirk, H.A., Dugan, K.A., Copeland, T.D., and Cole, M.D. (1998). The novel ATM-related protein TRRAP is an essential cofactor for the c-Myc and E2F oncoproteins. *Cell* *94*, 363–374.
- McMahon, S.B., Wood, M.A., and Cole, M.D. (2000). The essential cofactor TRRAP recruits the histone acetyltransferase hGCN5 to c-Myc. *Mol Cell Biol* *20*, 556–562.
- Mekhail, K., and Moazed, D. (2010). The nuclear envelope in genome organization, expression and stability. *Nat. Rev. Mol. Cell Biol.* *11*, 317–328.
- Mendjan, S., Taipale, M., Kind, J., Holz, H., Gebhardt, P., Schelder, M., Vermeulen, M., Buscaino, A., Duncan, K., Mueller, J., et al. (2006). Nuclear pore components are involved in the transcriptional regulation of dosage compensation in *Drosophila*. *Mol. Cell* *21*, 811–823.
- Meyer, N., and Penn, L.Z. (2008). Reflecting on 25 years with MYC. *Nat. Rev. Cancer* *8*, 976–990.
- Min, S.-H., Lau, A.W., Lee, T.H., Inuzuka, H., Wei, S., Huang, P., Shaik, S., Lee, D.Y., Finn, G., Balastik, M., et al. (2012). Negative regulation of the stability and tumor suppressor function of Fbw7 by the Pin1 prolyl isomerase. *Mol. Cell* *46*, 771–783.
- Mittag, T., Orlicky, S., Choy, W.-Y., Tang, X., Lin, H., Sicheri, F., Kay, L.E., Tyers, M., and Forman-Kay, J.D. (2008). Dynamic equilibrium engagement of a polyvalent ligand with a single-site receptor. *Proc. Natl. Acad. Sci. U. S. A.* *105*, 17772–17777.
- Miyashita, H., Uchida, T., Mori, S., Echigo, S., and Motegi, K. (2003a). Expression status of Pin1 and cyclins in oral squamous cell carcinoma: Pin1 correlates with Cyclin D1 mRNA expression and clinical significance of cyclins. *Oncol Rep* *10*, 1045–1048.
- Miyashita, H., Mori, S., Motegi, K., Fukumoto, M., and Uchida, T. (2003b). Pin1 is overexpressed in oral squamous cell carcinoma and its levels correlate with cyclin D1 overexpression. *Oncol Rep* *10*, 455–461.
- Monje, P., Hernandez-Losa, J., Lyons, R.J., Castellone, M.D., and Gutkind, J.S. (2005). Regulation of the transcriptional activity of c-Fos by ERK. A novel role for the prolyl isomerase PIN1. *J Biol Chem* *280*, 35081–35084.
- Moretto-Zita, M., Jin, H., Shen, Z., Zhao, T., Briggs, S.P., and Xu, Y. (2010). Phosphorylation stabilizes Nanog by promoting its interaction with Pin1. *Proc. Natl. Acad. Sci. U. S. A.* *107*, 13312–13317.
- Morgan, D.O. (1997). Cyclin-dependent kinases: engines, clocks, and microprocessors. *Annu. Rev. Cell Dev. Biol.* *13*, 261–291.

References

- Morse, R.H. (2000). RAP, RAP, open up! New wrinkles for RAP1 in yeast. *Trends Genet.* *16*, 51–53.
- Myant, K., Qiao, X., Halonen, T., Come, C., Laine, A., Janghorban, M., Partanen, J.I., Cassidy, J., Ogg, E.-L., Cammareri, P., et al. (2015). Serine 62-Phosphorylated MYC Associates with Nuclear Lamins and Its Regulation by CIP2A Is Essential for Regenerative Proliferation. *Cell Rep.* *12*, 1019–1031.
- Nair, S.K., and Burley, S.K. (2003). X-Ray Structures of Myc-Max and Mad-Max Recognizing DNA: Molecular Bases of Regulation by Proto-Oncogenic Transcription Factors. *Cell* *112*, 193–205.
- Nakashima, M. (2004). Cyclin D1 overexpression in thyroid tumours from a radio-contaminated area and its correlation with Pin1 and aberrant [beta]-catenin expression. *J Pathol* *202*, 446–455.
- Namanja, A.T., Wang, X.J., Xu, B., Mercedes-Camacho, A.Y., Wilson, K.A., Etkorn, F.A., and Peng, J.W. (2011). Stereospecific gating of functional motions in Pin1. *Proc. Natl. Acad. Sci. U. S. A.* *108*, 12289–12294.
- Nau, M.M. (1985). L-myc, a new myc-related gene amplified and expressed in human small cell lung cancer. *Nature* *318*, 69–73.
- Nguyen, H.Q., and Bosco, G. (2015). Gene Positioning Effects on Expression in Eukaryotes. *Annu. Rev. Genet.* *49*, 627–646.
- Nickerson, A., Huang, T., Lin, L.-J., and Nan, X. (2014). Photoactivated Localization Microscopy with Bimolecular Fluorescence Complementation (BiFC-PALM) for Nanoscale Imaging of Protein-Protein Interactions in Cells. *PLOS ONE* *9*, e100589.
- Nie, Z., Hu, G., Wei, G., Cui, K., Yamane, A., Resch, W., Wang, R., Green, D.R., Tessarollo, L., Casellas, R., et al. (2012). c-Myc is a universal amplifier of expressed genes in lymphocytes and embryonic stem cells. *Cell* *151*, 68–79.
- Nishi, M., Akutsu, H., Masui, S., Kondo, A., Nagashima, Y., Kimura, H., Perrem, K., Shigeri, Y., Toyoda, M., Okayama, A., et al. (2011). A distinct role for Pin1 in the induction and maintenance of pluripotency. *J. Biol. Chem.* *286*, 11593–11603.
- Nishi, M., Sakai, Y., Akutsu, H., Nagashima, Y., Quinn, G., Masui, S., Kimura, H., Perrem, K., Umezawa, A., Yamamoto, N., et al. (2014). Induction of cells with cancer stem cell properties from nontumorigenic human mammary epithelial cells by defined reprogramming factors. *Oncogene* *33*, 643–652.
- Okamoto, K., and Sagata, N. (2007). Mechanism for inactivation of the mitotic inhibitory kinase Wee1 at M phase. *Proc Natl Acad Sci* *104*, 3753–3758.
- Palomero, T., Lim, W.K., Odom, D.T., Sulis, M.L., Real, P.J., Margolin, A., Barnes, K.C., O’Neil, J., Neuberg, D., Weng, A.P., et al. (2006). NOTCH1 directly regulates c-

References

- MYC and activates a feed-forward-loop transcriptional network promoting leukemic cell growth. *Proc. Natl. Acad. Sci. U. S. A.* *103*, 18261–18266.
- Pang, R. (2004). PIN1 overexpression and [beta]-catenin gene mutations are distinct oncogenic events in human hepatocellular carcinoma. *Oncogene* *23*, 4182–4186.
- Pastorino, L. (2006). The prolyl isomerase Pin1 regulates amyloid precursor protein processing and amyloid-b production. *Nature* *440*, 528–534.
- Pauklin S, Kristjuhan A, maimets T, and Jaks V (2005). ART and ATM//ATR cooperate in p53-mediated apoptosis upon oncogenic stress. *Biochem Biophys Res Commun* *334*, 386–394.
- Pawson, T., and Scott, J.D. (2005). Protein phosphorylation in signaling--50 years and counting. *Trends Biochem. Sci.* *30*, 286–290.
- Pearson, G., Robinson, F., Beers Gibson, T., Xu, B.E., Karandikar, M., Berman, K., and Cobb, M.H. (2001). Mitogen-activated protein (MAP) kinase pathways: regulation and physiological functions. *Endocr. Rev.* *22*, 153–183.
- Pelengaris, S., Littlewood, T., Khan, M., Elia, G., and Evan, G. (1999). Reversible activation of c-Myc in skin: induction of a complex neoplastic phenotype by a single oncogenic lesion. *Mol Cell* *3*, 565–577.
- Peng, J.W. (2015). Investigating Dynamic Interdomain Allostery in Pin1. *Biophys. Rev.* *7*, 239–249.
- Peric-Hupkes, D., Meuleman, W., Pagie, L., Bruggeman, S.W.M., Solovei, I., Brugman, W., Gräf, S., Flicek, P., Kerkhoven, R.M., van Lohuizen, M., et al. (2010). Molecular maps of the reorganization of genome-nuclear lamina interactions during differentiation. *Mol. Cell* *38*, 603–613.
- Pickersgill, H. (2006). Characterization of the *Drosophila melanogaster* genome at the nuclear lamina. *Nat. Genet* *38*, 1005–1014.
- Podsypanina, K., Politi, K., Beverly, L.J., and Varmus, H.E. (2008). Oncogene cooperation in tumor maintenance and tumor recurrence in mouse mammary tumors induced by Myc and mutant Kras. *Proc. Natl. Acad. Sci. U. S. A.* *105*, 5242–5247.
- Pombo, A., and Dillon, N. (2015). Three-dimensional genome architecture: players and mechanisms. *Nat. Rev. Mol. Cell Biol.* *16*, 245–257.
- Poole, C.J., and van Riggelen, J. (2017). MYC—Master Regulator of the Cancer Epigenome and Transcriptome. *Genes* *8*, 142.
- Proestling, K., Birner, P., Gamperl, S., Nirtl, N., Marton, E., Yerlikaya, G., Wenzl, R., Streubel, B., and Husslein, H. (2015). Enhanced epithelial to mesenchymal transition

References

- (EMT) and upregulated MYC in ectopic lesions contribute independently to endometriosis. *Reprod. Biol. Endocrinol.* *13*, 75.
- Pulverer, B.J., Fisher, C., Vousden, K., Littlewood, T., Evan, G., and Woodgett, J.R. (1994). Site-specific modulation of c-Myc cotransformation by residues phosphorylated in vivo. *Oncogene* *9*, 59–70.
- Pusapati RV, Rounbehler RJ, Hong S, Powers JT, Yan M, and Kiguchi K (2006). ATM promotes apoptosis and suppresses tumorigenesis in response to Myc. *Proc Natl Acad Sci USA* *103*, 1446–1451.
- Qi, Y., Tu, Y., Yang, D., Chen, Q., Xiao, J., Chen, Y., Fu, J., Xiao, X., and Zhou, Z. (2007). Cyclin a but not cyclin D1 is essential for c-myc-modulated cell-cycle progression. *J. Cell. Physiol.* *210*, 63–71.
- Qing, G., Skuli, N., Mayes, P.A., Pawel, B., Martinez, D., Maris, J.M., and Simon, M.C. (2010). Combinatorial Regulation of Neuroblastoma Tumor Progression by N-Myc and Hypoxia Inducible Factor HIF-1 α . *Cancer Res.* *70*, 10351–10361.
- Rahl, P.B., Lin, C.Y., Seila, A.C., Flynn, R.A., McCuine, S., Burge, C.B., Sharp, P.A., and Young, R.A. (2010). c-Myc regulates transcriptional pause release. *Cell* *141*, 432–445.
- Rajanala, K., and Nandicoori, V.K. (2012). Localization of Nucleoporin Tpr to the Nuclear Pore Complex Is Essential for Tpr Mediated Regulation of the Export of Unspliced RNA. *PLOS ONE* *7*, e29921.
- Rajbhandari, P., Finn, G., Solodin, N.M., Singarapu, K.K., Sahu, S.C., Markley, J.L., Kadunc, K.J., Ellison-Zelski, S.J., Kariagina, A., Haslam, S.Z., et al. (2012). Regulation of estrogen receptor α N-terminus conformation and function by peptidyl prolyl isomerase Pin1. *Mol. Cell. Biol.* *32*, 445–457.
- Rajbhandari, P., Schalper, K.A., Solodin, N.M., Ellison-Zelski, S.J., Ping Lu, K., Rimm, D.L., and Alarid, E.T. (2014). Pin1 modulates ER α levels in breast cancer through inhibition of phosphorylation-dependent ubiquitination and degradation. *Oncogene* *33*, 1438–1447.
- Ranganathan, R., Lu, K.P., Hunter, T., and Noel, J.P. (1997). Structural and functional analysis of the mitotic rotamase Pin1 suggests substrate recognition is phosphorylation dependent. *Cell* *89*, 875–886.
- Rangasamy, V., Mishra, R., Sondarva, G., Das, S., Lee, T.H., Bakowska, J.C., Tzivion, G., Malter, J.S., Rana, B., Lu, K.P., et al. (2012). Mixed-lineage kinase 3 phosphorylates prolyl-isomerase Pin1 to regulate its nuclear translocation and cellular function. *Proc. Natl. Acad. Sci. U. S. A.* *109*, 8149–8154.

References

- Rapp, U.R., Korn, C., Ceteci, F., Karreman, C., Luetkenhaus, K., Serafin, V., Zanucco, E., Castro, I., and Potapenko, T. (2009). MYC is a metastasis gene for non-small-cell lung cancer. *PloS One* 4, e6029.
- Reddy, K.L., Zullo, J.M., Bertolino, E., and Singh, H. (2008). Transcriptional repression mediated by repositioning of genes to the nuclear lamina. *Nature* 452, 243–247.
- Reimann, M. (2007). The Myc-evoked DNA damage response accounts for treatment resistance in primary lymphomas in vivo. *Blood* 110, 2996–3004.
- Rizzolio, F., Lucchetti, C., Caligiuri, I., Marchesi, I., Caputo, M., Klein-Szanto, A.J., Bagella, L., Castronovo, M., and Giordano, A. (2012). Retinoblastoma tumor-suppressor protein phosphorylation and inactivation depend on direct interaction with Pin1. *Cell Death Differ.* 19, 1152–1161.
- Rodríguez-Navarro, S., Fischer, T., Luo, M.-J., Antúnez, O., Brettschneider, S., Lechner, J., Pérez-Ortín, J.E., Reed, R., and Hurt, E. (2004). Sus1, a Functional Component of the SAGA Histone Acetylase Complex and the Nuclear Pore-Associated mRNA Export Machinery. *Cell* 116, 75–86.
- Royds, J.A., Sharrard, R.M., Wagner, B., and Polaczar, S.V. (1992). Cellular localisation of c-myc product in human colorectal epithelial neoplasia. *J. Pathol.* 166, 225–233.
- Rustighi, A., Tiberi, L., Soldano, A., Napoli, M., Nuciforo, P., Rosato, A., Kaplan, F., Capobianco, A., Pece, S., Di Fiore, P.P., et al. (2009). The prolyl-isomerase Pin1 is a Notch1 target that enhances Notch1 activation in cancer. *Nat. Cell Biol.* 11, 133–142.
- Rustighi, A., Zannini, A., Tiberi, L., Sommaggio, R., Piazza, S., Sorrentino, G., Nuzzo, S., Tuscano, A., Eterno, V., Benvenuti, F., et al. (2014a). Prolyl-isomerase Pin1 controls normal and cancer stem cells of the breast. *EMBO Mol. Med.* 6, 99–119.
- Rustighi, A., Zannini, A., Tiberi, L., Sommaggio, R., Piazza, S., Sorrentino, G., Nuzzo, S., Tuscano, A., Eterno, V., Benvenuti, F., et al. (2014b). Prolyl-isomerase Pin1 controls normal and cancer stem cells of the breast. *EMBO Mol. Med.* 6, 99–119.
- Ryo, A. (2002). Pin1 is an E2F target gene essential for the Neu/Ras-induced transformation of mammary epithelial cells. *Mol Cell Biol* 22, 5281–5295.
- Ryo, A. (2003). Regulation of NF- κ B signaling by Pin1-dependent prolyl isomerization and ubiquitin-mediated proteolysis of p65/RelA. *Mol Cell* 12, 1413–1426.
- Ryo, A., Nakamura, N., Wulf, G., Liou, Y.C., and Lu, K.P. (2001). Pin1 regulates turnover and subcellular localization of β -catenin by inhibiting its interaction with APC. *Nat. Cell Biol* 3, 793–801.
- Sabò, A., Kress, T.R., Pelizzola, M., de Pretis, S., Gorski, M.M., Tesi, A., Morelli, M.J., Bora, P., Doni, M., Verrecchia, A., et al. (2014). Selective transcriptional regulation by Myc in cellular growth control and lymphomagenesis. *Nature* 511, 488–492.

References

- Salghetti, S.E., Kim, S.Y., and Tansey, W.P. (1999). Destruction of Myc by ubiquitin-mediated proteolysis: cancer-associated and transforming mutations stabilize Myc. *EMBO J.* *18*, 717–726.
- Sampson, V.B., Rong, N.H., Han, J., Yang, Q., Aris, V., Soteropoulos, P., Petrelli, N.J., Dunn, S.P., and Krueger, L.J. (2007). MicroRNA let-7a down-regulates MYC and reverts MYC-induced growth in Burkitt lymphoma cells. *Cancer Res.* *67*, 9762–9770.
- Schelhorn, C., Martín-Malpartida, P., Suñol, D., and Macias, M.J. (2015). Structural Analysis of the Pin1-CPEB1 interaction and its potential role in CPEB1 degradation. *Sci. Rep.* *5*, srep14990.
- Schermelleh, L., Carlton, P.M., Haase, S., Shao, L., Winoto, L., Kner, P., Burke, B., Cardoso, M.C., Agard, D.A., Gustafsson, M.G.L., et al. (2008). Subdiffraction Multicolor Imaging of the Nuclear Periphery with 3D Structured Illumination Microscopy. *Science* *320*, 1332–1336.
- Scheuermann, M.O., Tajbakhsh, J., Kurz, A., Saracoglu, K., Eils, R., and Lichter, P. (2004). Topology of genes and nontranscribed sequences in human interphase nuclei. *Exp. Cell Res.* *301*, 266–279.
- Schmitt, A.D., Hu, M., and Ren, B. (2016). Genome-wide mapping and analysis of chromosome architecture. *Nat. Rev. Mol. Cell Biol.* *17*, 743–755.
- Schmitt CA, McCurrach ME, De Stanchina E, Wallace-Brodeur RR, and Lowe SW (1999). INK4a//ARF mutations accelerate lymphomagenesis and promote chemoresistance by disabling p53. *Genes Dev* *13*, 2670–2677.
- Schuhmacher, M. (1999). Control of cell growth by c-Myc in the absence of cell division. *Curr Biol* *9*, 1255–1258.
- Schweizer, N., Ferrás, C., Kern, D.M., Logarinho, E., Cheeseman, I.M., and Maiato, H. (2013). Spindle assembly checkpoint robustness requires Tpr-mediated regulation of Mad1/Mad2 proteostasis. *J. Cell Biol.* *203*, 883–893.
- Sears, R.C. (2004). The life cycle of C-myc: from synthesis to degradation. *Cell Cycle Georget. Tex* *3*, 1133–1137.
- Sears, R., Leone, G., DeGregori, J., and Nevins, J.R. (1999). Ras enhances Myc protein stability. *Mol Cell* *3*, 169–179.
- Sears, R., Nuckolls, F., Haura, E., Taya, Y., Tamai, K., and Nevins, J.R. (2000). Multiple Ras-dependent phosphorylation pathways regulate Myc protein stability. *Genes Dev.* *14*, 2501–2514.
- Shachar, S., Voss, T.C., Pegoraro, G., Sciascia, N., and Misteli, T. (2015). Identification of Gene Positioning Factors Using High-Throughput Imaging Mapping. *Cell* *162*, 911–923.

References

- Sharma, V.M., Calvo, J.A., Draheim, K.M., Cunningham, L.A., Hermance, N., Beverly, L., Krishnamoorthy, V., Bhasin, M., Capobianco, A.J., and Kelliher, M.A. (2006). Notch1 contributes to mouse T-cell leukemia by directly inducing the expression of c-myc. *Mol. Cell. Biol.* *26*, 8022–8031.
- Shim, H., Dolde, C., Lewis, B.C., Wu, C.-S., Dang, G., Jungmann, R.A., Dalla-Favera, R., and Dang, C.V. (1997). c-Myc transactivation of LDH-A: Implications for tumor metabolism and growth. *Proc. Natl. Acad. Sci.* *94*, 6658–6663.
- Shou, Y., Martelli, M.L., Gabrea, A., Qi, Y., Brents, L.A., Roschke, A., Dewald, G., Kirsch, I.R., Bergsagel, P.L., and Kuehl, W.M. (2000). Diverse karyotypic abnormalities of the c-myc locus associated with c-myc dysregulation and tumor progression in multiple myeloma. *Proc. Natl. Acad. Sci. U. S. A.* *97*, 228–233.
- Smith, A.P., Verrecchia, A., Fagà, G., Doni, M., Perna, D., Martinato, F., Guccione, E., and Amati, B. (2008). A positive role for Myc in TGF β -induced Snail transcription and epithelial-to-mesenchymal transition. *Oncogene* *28*, 422–430.
- Staller, P. (2001). Repression of p15INK4b expression by Myc through association with Miz-1. *Nat. Cell Biol* *3*, 392–399.
- Stoneley, M., Paulin, F.E., Le Quesne, J.P., Chappell, S.A., and Willis, A.E. (1998). C-Myc 5' untranslated region contains an internal ribosome entry segment. *Oncogene* *16*, 423–428.
- Strambio-De-Castillia, C., Niepel, M., and Rout, M.P. (2010). The nuclear pore complex: bridging nuclear transport and gene regulation. *Nat. Rev. Mol. Cell Biol.* *11*, 490–501.
- Strickfaden, H., Zunhammer, A., van Koningsbruggen, S., Köhler, D., and Cremer, T. (2010). 4D chromatin dynamics in cycling cells: Theodor Boveri's hypotheses revisited. *Nucl. Austin Tex* *1*, 284–297.
- Stukenberg, P.T., and Kirschner, M.W. (2001). Pin1 acts catalytically to promote a conformational change in Cdc25. *Mol Cell* *7*, 1071–1083.
- Suizu, F., Ryo, A., Wulf, G., Lim, J., and Lu, K.P. (2006). Pin1 regulates centrosome duplication and its overexpression induces centrosome amplification, chromosome instability and oncogenesis. *Mol Cell Biol* *26*, 1463–1479.
- Sun, X.-X., He, X., Yin, L., Komada, M., Sears, R.C., and Dai, M.-S. (2015). The nucleolar ubiquitin-specific protease USP36 deubiquitinates and stabilizes c-Myc. *Proc. Natl. Acad. Sci.* *112*, 3734–3739.
- Taddei, A. (2006). Nuclear pore association confers optimal expression levels for an inducible yeast gene. *Nature* *441*, 774–778.

References

- Taddei, A., Van Houwe, G., Hediger, F., Kalck, V., Cubizolles, F., Schober, H., and Gasser, S.M. (2006). Nuclear pore association confers optimal expression levels for an inducible yeast gene. *Nature* *441*, 774–778.
- Takahashi, K. (2007). Ablation of a peptidyl prolyl isomerase Pin1 from p53-null mice accelerated thymic hyperplasia by increasing the level of the intracellular form of Notch1. *Oncogene* *26*, 3835–3845.
- Takahashi, K., and Yamanaka, S. (2006). Induction of pluripotent stem cells from mouse embryonic and adult fibroblast cultures by defined factors. *Cell* *126*, 663–676.
- Takizawa, T., Meaburn, K.J., and Misteli, T. (2008). The meaning of gene positioning. *Cell* *135*, 9–13.
- Tanabe, H., Müller, S., Neusser, M., Hase, J. von, Calcagno, E., Cremer, M., Solovei, I., Cremer, C., and Cremer, T. (2002a). Evolutionary conservation of chromosome territory arrangements in cell nuclei from higher primates. *Proc. Natl. Acad. Sci.* *99*, 4424–4429.
- Tanabe, H., Habermann, F.A., Solovei, I., Cremer, M., and Cremer, T. (2002b). Non-random radial arrangements of interphase chromosome territories: evolutionary considerations and functional implications. *Mutat. Res. Mol. Mech. Mutagen.* *504*, 37–45.
- Tan-Wong, S.M., Wijayatilake, H.D., and Proudfoot, N.J. (2009). Gene loops function to maintain transcriptional memory through interaction with the nuclear pore complex. *Genes Dev.* *23*, 2610–2624.
- Taub, R., Kirsch, I., Morton, C., Lenoir, G., Swan, D., Tronick, S., Aaronson, S., and Leder, P. (1982). Translocation of the c-myc gene into the immunoglobulin heavy chain locus in human Burkitt lymphoma and murine plasmacytoma cells. *Proc. Natl. Acad. Sci. U. S. A.* *79*, 7837–7841.
- Tong, Y., Ying, H., Liu, R., Li, L., Bergholz, J., and Xiao, Z.-X. (2015). Pin1 inhibits PP2A-mediated Rb dephosphorylation in regulation of cell cycle and S-phase DNA damage. *Cell Death Dis.* *6*, e1640.
- Tu, W.B., Helander, S., Pilstål, R., Hickman, K.A., Lourenco, C., Jurisica, I., Raught, B., Wallner, B., Sunnerhagen, M., and Penn, L.Z. (2015). Myc and its interactors take shape. *Biochim. Biophys. Acta* *1849*, 469–483.
- Twoorkowski, K.A., Salghetti, S.E., and Tansey, W.P. (2002). Stable and unstable pools of Myc protein exist in human cells. *Oncogene* *21*, 8515–8520.
- Ubersax, J.A., and Ferrell, J.E. (2007). Mechanisms of specificity in protein phosphorylation. *Nat. Rev. Mol. Cell Biol.* *8*, 530–541.
- Vaquerizas, J.M. (2010). Nuclear pore proteins Nup153 and Megator define transcriptionally active regions in the *Drosophila* genome. *PLoS Genet* *6*, e1000846.

References

- Vazquez, J., Belmont, A.S., and Sedat, J.W. (2001). Multiple regimes of constrained chromosome motion are regulated in the interphase *Drosophila* nucleus. *Curr. Biol.* *11*, 1227–1239.
- Vennstrom, B., Sheiness, D., Zabielski, J., and Bishop, J.M. (1982). Isolation and characterization of c-myc, a cellular homolog of the oncogene (v-myc) of avian myelocytomatosis virus strain 29. *J. Virol.* *42*, 773–779.
- Verdecia, M.A., Bowman, M.E., Lu, K.P., Hunter, T., and Noel, J.P. (2000). Structural basis for phosphoserine-proline recognition by group IV WW domains. *Nat. Struct. Biol.* *7*, 639–643.
- Vervoorts, J., Lüscher-Firzlaff, J.M., Rottmann, S., Lilischkis, R., Walsemann, G., Dohmann, K., Austen, M., and Lüscher, B. (2003). Stimulation of c-MYC transcriptional activity and acetylation by recruitment of the cofactor CBP. *EMBO Rep.* *4*, 484–490.
- Vervoorts, J., Lüscher-Firzlaff, J., and Lüscher, B. (2006). The Ins and Outs of MYC Regulation by Posttranslational Mechanisms. *J. Biol. Chem.* *281*, 34725–34729.
- Vomastek, T., Iwanicki, M.P., Burack, W.R., Tiwari, D., Kumar, D., Parsons, J.T., Weber, M.J., and Nandicoori, V.K. (2008). Extracellular Signal-Regulated Kinase 2 (ERK2) Phosphorylation Sites and Docking Domain on the Nuclear Pore Complex Protein Tpr Cooperatively Regulate ERK2-Tpr Interaction. *Mol. Cell. Biol.* *28*, 6954–6966.
- Vriz, S., Lemaitre, J.M., Leibovici, M., Thierry, N., and Méchali, M. (1992). Comparative analysis of the intracellular localization of c-Myc, c-Fos, and replicative proteins during cell cycle progression. *Mol. Cell. Biol.* *12*, 3548–3555.
- Waikel, R.L., Kawachi, Y., Waikel, P.A., Wang, X.J., and Roop, D.R. (2001). Deregulated expression of c-Myc depletes epidermal stem cells. *Nat. Genet.* *28*, 165–168.
- Walz, S., Lorenzin, F., Morton, J., Wiese, K.E., von Eyss, B., Herold, S., Rycak, L., Dumay-Odelot, H., Karim, S., Bartkuhn, M., et al. (2014). Activation and repression by oncogenic MYC shape tumour-specific gene expression profiles. *Nature* *511*, 483–487.
- Wang, R., Dillon, C.P., Shi, L.Z., Milasta, S., Carter, R., Finkelstein, D., McCormick, L.L., Fitzgerald, P., Chi, H., Munger, J., et al. (2011a). The Transcription Factor Myc Controls Metabolic Reprogramming upon T Lymphocyte Activation. *Immunity* *35*, 871–882.
- Wang, X., Cunningham, M., Zhang, X., Tokarz, S., Laraway, B., Troxell, M., and Sears, R.C. (2011b). Phosphorylation regulates c-Myc's oncogenic activity in the mammary gland. *Cancer Res.* *71*, 925–936.
- Wanzel, M. (2008). A ribosomal protein L23-nucleophosmin circuit coordinates Miz1 function with cell growth. *Nat. Cell Biol.* *10*, 1051–1061.

References

- Welcker, M., Orian, A., Jin, J., Grim, J.E., Grim, J.A., Harper, J.W., Eisenman, R.N., and Clurman, B.E. (2004). The Fbw7 tumor suppressor regulates glycogen synthase kinase 3 phosphorylation-dependent c-Myc protein degradation. *Proc. Natl. Acad. Sci. U. S. A.* *101*, 9085–9090.
- Weng, A.P., Millholland, J.M., Yashiro-Ohtani, Y., Arcangeli, M.L., Lau, A., Wai, C., Del Bianco, C., Rodriguez, C.G., Sai, H., Tobias, J., et al. (2006). c-Myc is an important direct target of Notch1 in T-cell acute lymphoblastic leukemia/lymphoma. *Genes Dev.* *20*, 2096–2109.
- Werner-Allen, J.W., Lee, C.-J., Liu, P., Nicely, N.I., Wang, S., Greenleaf, A.L., and Zhou, P. (2011). cis-Proline-mediated Ser(P)5 dephosphorylation by the RNA polymerase II C-terminal domain phosphatase Ssu72. *J. Biol. Chem.* *286*, 5717–5726.
- Wickstrom, E.L., Bacon, T.A., Gonzalez, A., Freeman, D.L., Lyman, G.H., and Wickstrom, E. (1988). Human promyelocytic leukemia HL-60 cell proliferation and c-myc protein expression are inhibited by an antisense pentadecadeoxynucleotide targeted against c-myc mRNA. *Proc. Natl. Acad. Sci.* *85*, 1028–1032.
- Wilson, K.A., Bouchard, J.J., and Peng, J.W. (2013). Interdomain interactions support interdomain communication in human Pin1. *Biochemistry (Mosc.)* *52*, 6968–6981.
- Winqvist, R., Saksela, K., and Alitalo, K. (1984). The myc proteins are not associated with chromatin in mitotic cells. *EMBO J.* *3*, 2947–2950.
- Wintjens, R., Wieruszkeski, J.M., Drobecq, H., Rousselot-Pailley, P., Buée, L., Lippens, G., and Landrieu, I. (2001). 1H NMR study on the binding of Pin1 Trp-Trp domain with phosphothreonine peptides. *J. Biol. Chem.* *276*, 25150–25156.
- Wise, D.R., DeBerardinis, R.J., Mancuso, A., Sayed, N., Zhang, X.-Y., Pfeiffer, H.K., Nissim, I., Daikhin, E., Yudkoff, M., McMahon, S.B., et al. (2008). Myc regulates a transcriptional program that stimulates mitochondrial glutaminolysis and leads to glutamine addiction. *Proc. Natl. Acad. Sci.* *105*, 18782–18787.
- Wolfer, A., Wittner, B.S., Irimia, D., Flavin, R.J., Lupien, M., Gunawardane, R.N., Meyer, C.A., Lightcap, E.S., Tamayo, P., Mesirov, J.P., et al. (2010). MYC regulation of a “poor-prognosis” metastatic cancer cell state. *Proc. Natl. Acad. Sci. U. S. A.* *107*, 3698–3703.
- Wu, S. (2003). Myc represses differentiation-induced p21^{CIP1} expression via Miz-1-dependent interaction with the p21 core promoter. *Oncogene* *22*, 351–360.
- Wu, F., and Yao, J. (2013). Spatial compartmentalization at the nuclear periphery characterized by genome-wide mapping. *Epigenetics Chromatin* *6*, P126.
- Wulf, G.M. (2001). Pin1 is overexpressed in breast cancer and potentiates the transcriptional activity of phosphorylated c-Jun towards the cyclin D1 gene. *EMBO J* *20*, 3459–3472.

References

- Wulf, G., Garg, P., Liou, Y.C., Iglehart, D., and Lu, K.P. (2004). Modeling breast cancer in vivo and ex vivo reveals an essential role of Pin1 in tumorigenesis. *EMBO J* 23, 3397–3407.
- Wulf, G., Finn, G., Suizu, F., and Lu, K.P. (2005). Phosphorylation-specific prolyl isomerization: is there an underlying theme? *Nat. Cell Biol* 7, 435–441.
- Xie, L., Pelz, C., Wang, W., Bashar, A., Varlamova, O., Shadle, S., and Impey, S. (2011). KDM5B regulates embryonic stem cell self-renewal and represses cryptic intragenic transcription. *EMBO J.* 30, 1473–1484.
- Xu, Y.-X., and Manley, J.L. (2007a). Pin1 modulates RNA polymerase II activity during the transcription cycle. *Genes Dev.* 21, 2950–2962.
- Xu, Y.X., and Manley, J.L. (2007b). The prolyl isomerase pin1 functions in mitotic chromosome condensation. *Mol Cell* 26, 287–300.
- Yada, M., Hatakeyama, S., Kamura, T., Nishiyama, M., Tsunematsu, R., Imaki, H., Ishida, N., Okumura, F., Nakayama, K., and Nakayama, K.I. (2004). Phosphorylation-dependent degradation of c-Myc is mediated by the F-box protein Fbw7. *Embo J* 23, 2116–2125.
- Yaffe, M.B. (1997). Sequence-specific and phosphorylation-dependent proline isomerization: a potential mitotic regulatory mechanism. *Science* 278, 1957–1960.
- Yang, J., Altahan, A.M., Hu, D., Wang, Y., Cheng, P.-H., Morton, C.L., Qu, C., Nathwani, A.C., Shohet, J.M., Fotsis, T., et al. (2015). The role of histone demethylase KDM4B in Myc signaling in neuroblastoma. *J. Natl. Cancer Inst.* 107, djv080.
- Yap, C.-S., Peterson, A.L., Castellani, G., Sedivy, J.M., and Neretti, N. (2011). Kinetic profiling of the c-Myc transcriptome and bioinformatic analysis of repressed gene promoters. *Cell Cycle* 10, 2184–2196.
- Yeh, E., Cunningham, M., Arnold, H., Chasse, D., Monteith, T., Ivaldi, G., Hahn, W.C., Stukenberg, P.T., Shenolikar, S., Uchida, T., et al. (2004a). A signalling pathway controlling c-Myc degradation that impacts oncogenic transformation of human cells. *Nat. Cell Biol.* 6, 308–318.
- Yeh, E., Cunningham, M., Arnold, H., Chasse, D., Monteith, T., Ivaldi, G., Hahn, W.C., Stukenberg, P.T., Shenolikar, S., Uchida, T., et al. (2004b). A signalling pathway controlling c-Myc degradation that impacts oncogenic transformation of human cells. *Nat. Cell Biol.* 6, 308–318.
- Young, R.A. (2011). Control of Embryonic Stem Cell State. *Cell* 144, 940–954.
- Zhang, K., Faiola, F., and Martinez, E. (2005). Six lysine residues on c-Myc are direct substrates for acetylation by p300. *Biochem. Biophys. Res. Commun.* 336, 274–280.

References

- Zhang, X., Farrell, A.S., Daniel, C.J., Arnold, H., Scanlan, C., Laraway, B.J., Janghorban, M., Lum, L., Chen, D., Troxell, M., et al. (2012). Mechanistic insight into Myc stabilization in breast cancer involving aberrant Axin1 expression. *Proc. Natl. Acad. Sci. U. S. A.* *109*, 2790–2795.
- Zhou, X.Z., and Lu, K.P. (2016). The isomerase PIN1 controls numerous cancer-driving pathways and is a unique drug target. *Nat. Rev. Cancer* *16*, 463–478.
- Zhou, V.W., Goren, A., and Bernstein, B.E. (2011). Charting histone modifications and the functional organization of mammalian genomes. *Nat. Rev. Genet.* *12*, 7–18.
- Zhou, X.Z., Kops, O., Werner, A., Lu, P.J., Shen, M., Stoller, G., Küllertz, G., Stark, M., Fischer, G., and Lu, K.P. (2000). Pin1-dependent prolyl isomerization regulates dephosphorylation of Cdc25C and tau proteins. *Mol. Cell* *6*, 873–883.
- Zullo, J.M., Demarco, I.A., Piqué-Regi, R., Gaffney, D.J., Epstein, C.B., Spooner, C.J., Luperchio, T.R., Bernstein, B.E., Pritchard, J.K., Reddy, K.L., et al. (2012). DNA sequence-dependent compartmentalization and silencing of chromatin at the nuclear lamina. *Cell* *149*, 1474–1487.